A study on the development of chemically modified *acyclic* nucleic acids for next generation oligonucleotide therapeutics

（次世代型核酸医薬基盤の構築に向けた修飾型非環状型人工核酸の開発に関する研究）

Fuminori SATO

2024

Contents

Chapter 1. General Introduction

1-1 Nucleic acids

  DNA, deoxyribonucleic acid, is the biopolymer which store our genetic code as duplexes. DNA translate genetic information to RNA, messenger RNAs(mRNAs). Based on RNA sequence, proteins synthesized by ribosome. These transmission of information from DNA to proteins is called the central dogma. A point of DNA and RNA function is realized by base-pairing thorough Watson-click rule, Adenine(A) with Thymine(T) or Uracil(U), or Guanine(G) with Cytosine(C), as shown Figure 1.[1, 2, 3] On the other hand, about 60% of all RNA do not code protein information and regulate gene expressions at various steps of central dogma. MicroRNA(miRNA), long non-coding RNA(lnc RNA) are most important non-coding RNAs in term of regulation protein expression levels.
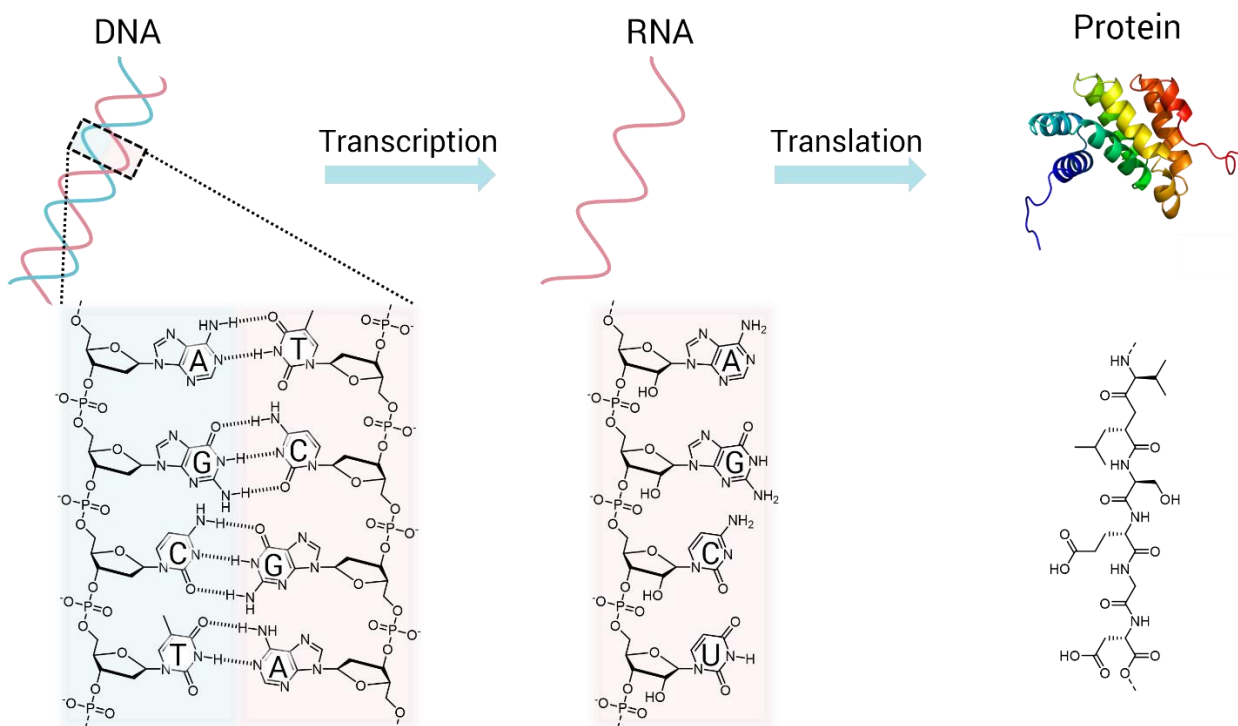
Figure 1-1 Central dogma, from DNA to protein expressions

1-2 Nucleic acid Therapeutics

Nucleic acid drugs are basically composed of chemically synthesized DNA or RNA and regulate disease-related proteins through hybridization with the sequence which are associated diseases.[4, 5, 6, 7] Until 2022, 18 nucleic acid drugs including mRNA vaccine for COVID-19 approved, as shown Figure 1-2.[7] Recently, research about nucleic acid drugs is done actively because they can treat intractable genetic diseases. DNA and RNA, most basic scaffold of Nucleic acid drugs, are easily degraded by enzymes in cells and don't show treat efficacy. So artificial nucleic acids are often utilized for improving nuclease-resistance and activities.

Figure 1-2 Currently approved oligonucleotide drugs and mRNA vaccines, year of approval (between 1998 and 2022), and indication[7]

So far, as shown Figure 1-3, many chemical modifications are developed and applied to nucleic acid drugs. Phosphorothioate modification[8] is most basic and common because PS modification easily improve nuclease-resistance and half-life time of drugs *via* non-specific protein interaction.[9] Like PS modification, chemical modifications applied to a various site of DNA and RNA for

improving DNA/RNA affinity, nuclease-resistance, and retention in blood *in vivo*, as shown figure 1-3.

Figure 1-3 Structures and properties of several key modifications which have been used in clinical trials and/or approved products

PS modification, 2'-Fluoro,[12] 2'-O-methyl,[13] are used into nucleic acid drugs on market. These are proved safety and effectiveness on almost scene, especially siRNA drugs. 2'-MOE[14] and PMO[15] are used for antisense drugs.[16~20] LNA[21] and cEt,[22] a series of locked nucleic acids, which are locked to ribose pakaring like in A-type duplex formation have high RNA affinity. However LNA and cEt potencially improve drugs efficacy, they are sometimes toxic due to off-target effect and non-specific protein interaction. [23] PMO is proved its safety, non-toxicity, for duchenne muscular dystrophy treatment. But, the cost of PMO oligomers is very high due to its difficulty of oligomer synthesis and low yield. The point is that great artificial nucleic acid with high RNA affinity, non-toxicity, and low cost for manufacturing drugs have not developed until now.

1-3 Serinol nucleic acid and L-threoninol *acyclic* nucleic acids, as *acyclic* artificial nucleic acids

Acyclic artificial nucleic acids are easily synthesized. The ease of synthesis is superior to ribose-modified nucleic acids for decrease costs of drug manufucturing. The first report of synthesis of *acyclic* artificial nucleic acid, flexible nucleoside analogs is on 1990.[24] From the rerport, a various arificial are developed however, only few nucleic acids can form stable duplexes with RNA or DNA.[25~31] PNA is most famous *acyclic* artificial nucleic acids.[27] PNA have no electric charge, and have high DNA/RNA affinity with electrostatic repulsion.
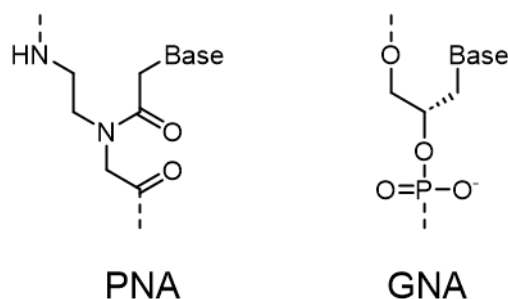
Figure. 1-4 Chemical structures of representative *acyclic* XNAs.

In our laboratory, a series of *acyclic* artificial nucleic acids D-threoninol *acyclic* nucleic acids(D-*a*TNA),[32] serinol nucleic acids(SNA),[33] and L-threoninol *acyclic* nucleic acids(L-*a*TNA)[34] were developed. They have each interesting property. D-*a*TNA is L-*a*TNA enantiomer, while D-*a*TNA can form left-handed homoduplex, L-*a*TNA can form right-handed homoduplex. SNA can form homo duplexes with sequence-dependent turns due to its meso property. D-*a*TNA can be used scafold for support Dyes into DNA,[35, 36] but never can form hetero duplexes with natural nucleic acids, so D-*a*TNA is utilized Color-Changing Fluorescent Barcode etc. because D-*a*TNA form orthogonal homo hybridization reaction to DNA/RNA.[37, 38] On the other hand, SNA and L-*a*TNA can form L-*a*TNA can stable hetero duplex with DNA and RNA that can form right-handed duplexes. SNA and L-

*a*TNA are utilized probes for DNA and RNA, materials which can be regulated by light, and nucleic acids drugs.[39~43]

  SNA and L-*a*TNA have some merits for nucleic acid drugs. First, They have stronger nuclease-resistance than any other artificial nucleic acids.[43] Nuclease-resistance is important for extended duration of drugs. Second, they are synthesized easily which is important point for decreasing of manufacturing costs. In the term of RNA affinity, they have about equal or greater affinity than that of RNA. As mentioned above, we thought SNA and L-*a*TNA are definitely useful for nucleic acid drugs.
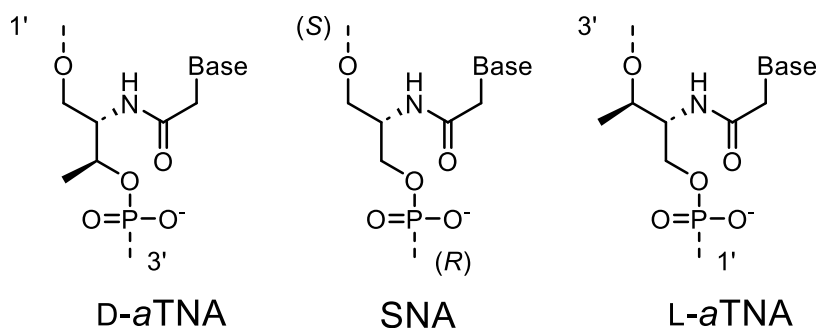
Figure. 1-5 Chemical structures of D-*a*TNA, SNA, and L-*a*TNA.

1-4 Anti miRNA oligonucleotide

  Anti miRNA oligonucleotide is a kind of nucleic acid drugs. They can block miRNA function, regulating translation of mRNA through hybridization to complementary sequence.

  miRNAs, classified as non-coding RNA, is 20~23 mer length RNA.[44, 45] Pri-miRNAs are transcribed by RNA polymerase II from DNA sequence and converted to pre-miRNAs, about 70 base-pair length hairpin with a stem-loop, by Drosha. Then, pre-miRNAs are brought, removed the stem-loop part by Dicer and converted to miRNAs, about 22 base-pair length RNA duplexes, sense strand and passenger strand, with overhang compartment. miRNAs are interacted Argonaute 2 protein and released the passenger strand. The argonaute 2-miRNA complexes are called as

miRISC.[46, 47] Based on the sense strand sequence, miRISC recognized the Fully or partially complenetary mRNA, and cuts mRNA or block access of translation-related proteins by remaining hybridization with mRNA. MicroRNAs strictly control mRNA translation in each stage of a various cell. In the disease-related cell, abnormal expressions of miRNAs are reported.[48-52]

  Anti miRNA oligonucleotide, or AMO, hybridize miRNA depending on the sequence and block miRNA access to mRNA.[53-60] AMOs aim to treat diseases by restoring expressions of protein associated diseases. So far, while 18 nucleic acid drugs are on the market, there are no AMOs on the market. While Some AMOs are in clinical trial and have been tried developing, the development of some AMOs were stopped for insufficient activities, toxicity, and/or change in management policy. Miravirsen, anti miR-122 oligonucleotide for treating hepatitis C virus is famous as the first AMO been in clinical trials. As shown table 1-1, 2'-O-MOE and LNA as artificial nucleic acids are used for AMO. Spinraza®, Nusinersen, is based on 2'-O-MOE for spinal muscular atrophy without toxicity, however 2'-O-MOE sometimes induce toxicity. In term of LNA, TGC and TCC motifs induce hepatotoxicity, and the hydrophobicity induces non-specific toxicity based on nonspecific interactions. To break through this current situation, using a completely different type of artificial nucleic acids from existing artificial nucleic acids is necessary. We thought the development of innovative AMO would be realized by SNA and L-*a*TNA.

Drug	Target	Indication	Chemical modification	Phase	Reference
RG-012	miR-21	Alport syndrome	2'-O-MOE, PS	I/II	(Gomez et al., 2015)
Miravirsen (SPC3649)	miR-122	Hepatitis C virus	LNA, PS	II	(Lanford et al., 2010; Gebert et al., 2014)
RG-101	miR-122	Hepatitis C virus	GalNAc	Terminated, metabolic/ hepatic toxicity	(van der Ree et al., 2017)
Cobomarsen (MRG-106)	miR-155	CTCL (MF subtype)	LNA	I/II	(Seto et al., 2018)
S95010 (MRG-110)	miR-92	Accelerate wound healing	LNA	I	(Gallant-Behm et al., 2018)

CTCL, cutaneous T-cell lymphoma; MF, mycosis fungoides

Table 1-1 published studies employing antisense to mir-21 to block disease.[61]

1-5 The purpose of this study

  We believe the artificial nucleic acids, SNA and L-*a*TNA, realize the AMO drugs. In this study, we tried to develop AMOs based on SNA and/or L-*a*TNA. We choose miR-21 for the target gene because miR-21 is famous as the microRNA associated most cancer cells, cardiovascular disease, autoimmune disease, renal dysfunction, and so on, and anti miR-21 oligonucleotide can treat many diseases.[61-64] For treating those diseases, anti miR-21 oligonucleotides, Antagomir, Tiny-LNA, and 2'-Fluoro/MOE are used *in vivo* study. Each of them also has problems with the miR-21 inhibitory activity or toxicity. We expect SNA/L-*a*TNA based Anti miR-21 oligonucleotide has high miR-21 inhibitory activity and no toxicity. In chapter 2, we referred the problems of SNA based Anti miR-21 and solution for the problems. In chapter 3, for solving the probrems of SNA based anti miR-21 oligonucleotide, we developed the method to introduce artificial nucleobases into SNA and L-*a*TNA. In chapter 4, we designed SNA and L-*a*TNA based anti miR-21 with artificial nucleobases and perform the evaluation miR-21 inhibitory activity in syngeneic mice.

1-6 References

[1] J. D. Watson, F. H. C. Crick, *Nature* **1953**, *171*, 737-738.

[2] Rich A., Davies D.R., *J. Am. Chem. Soc.*, **1956**, **78**, 3548-3549.

[3] Rich A., *Proc. Natl. Acad. Sci. U.S.A.*, **1960**, *46*, 1044-1053.

[4] Stephenson M.L., Zamecnik P.C., *Proc. Natl. Acad. Sci. U.S.A.*, **1978**, *75*, 285-288.

[5] Zamecnik P.C., Stephenson M.L., Proc. Natl. Acad. Sci. U.S.A., **1978**, *75*,280-284.

[6] Stanley T. Crooke, Xue-Hai Liang, Brenda F. Baker, and Rosanne M. Crooke, *J Biol Chem.*, **2021**, *296*, 100416.

[7] Martin Egli, Muthiah Manoharan, *Nucleic Acids Research,* **2023**, *51*, 2529–2573.

[8] Eckstein F., *J. Am. Chem. Soc.*, **1966**, *88*, 4292-4294.

[9] Stec W.J., Zon G., Egan W., *J. Am. Chem. Soc.*, **1984**, *106*, 6077.

[10] Hans J Gaus, Ruchi Gupta, Alfred E Chappell, Michael E Østergaard, Eric E Swayze, Punit P Seth, *Nucleic Acids Research,* **2019**, *47*, 1110-1122.

[11] Codington J.F., Doerr I., Van Praag D., Bendich A., Fox J.J., *J. Am. Chem. Soc.*, **1961**, *83*, 5030-5031.

[12] Furukawa Y., Kobayashi K., Kanai Y., Honjo M. *Chem.*, **1965**, *13,* 1273-1278.

[13] Hideo Inoue, Yoji Hayase, Akihiro Imura, Shigenori Iwai, Kazunobu Miura, Eiko Ohtsuka,

Nucleic Acids Research, **1987**, *15*, 6131–6148

[14] Martin P., *Helv. Chim. Acta.*, **1995**, *78*, 486-504.

[15] Summerton J.E., *Methods Mol. Biol.*, **2017**, *1565*, 1-15.

[16] Geary R.S., Watanabe T.A., Truong L., Freier S., Lesnik E.A., Sioufi N.B., Sasmor H.,

Manoharan M., Levin A.A., *J. Pharmacol. Exp. Ther.*, **2001**, *296*, 890-897.

[17] Gales L., *Pharmaceuticals*, **2019**, *12*, 78.

[18] Mathew V., Wang A.K., *Drug Des. Dev. Ther.*, **2019**, *13*, 1515-1525.

[19] Paik J., Duggan S., *first approval. Drugs*, **2019**, *79*, 1349-1354

[20] Heo Y.-A., *first approval. Drugs*, **2020**, *80*, 329-333

[21] (a) S. Obika, *et al.*, *Tetrahedron Lett.*, **1997**, *38*, 8735. (b) A.A. Koshkin, *et al.*, *Tetrahedron*, **1998**, *54*, 3607

[22] Pallan P.S., Allerson C.R., Berdeja A., Seth P.P., Swayze E.E., Prakash T.P., Egli M.,

Chem. Commun., **2012**, *48*, 8195-197.

[23] Crooke S.T., Witztum J.L., Bennett C.F., Baker B.F., **2018**, *Cell Metab.*, *27*, 714-739.

[24] K. Christian Schneider, Steven A. Benner, *J. Am. Chem. Soc.*, **1990**, *112*, *1*, 453-455

[25] Y. Merle, E. Bonneil, L. Merle, J. Saggi and A. Szemzo, *Int. J. Biol. Macromol.*, **1995**, *17*, 239-246.

[26] F. Vandendriessche, K. Augustyns, A. Vanaerschot, R. Busson, J. Hoogmartens and P. Herdewijn, *Tetrahedron*, **1993**,
49, 7223-7238

[27] P. E. Nielsen , M. Egholm , R. H. Berg and O. Buchardt, *Science*, **1991**, *254*, 1497-1500.

[28] J. Kehler, U. Henriksen, H. Vejbjerg and O. Dahl, *Bioorg. Med. Chem.*, **1998**, *6*, 315-322.

[29] V. A. Efimov, O. G. Chakhmakhcheva and E. Wickstrom,

Nucleosides, Nucleotides Nucleic Acids, **2005**, *24*, 1853-1874.

[30] P. Srivastava, R. A. El Asrar, C. Knies, M. Abramov, M. Froeyen, J. Rozenski, H. Rosemeyer and P. Herdewijn,

Org. Biomol. Chem., **2015**, *13*, 9249-9260.

[31] L. Zhang , A. Peritz and E. Meggers , J. Am. Chem. Soc., 2005, 127 , 4174-4175.

[32] H. Asanuma, T. Toda, K. Murayama, X. G. Liang, and H. Kashida, *J. Am. Chem. Soc.*, **2010**, *132*, 14702-14703.

[33] H. Kashida, K. Murayama, T. Toda, and H. Asanuma, *Angew. Chem., Int. Ed.*, **2011**, *50*, 1285-1288.

[34] K. Murayama, H. Kashida, and H. Asanuma, *Chem. Commun.*, **2015**, *51*, 6500-6503.

[35] H. Asanuma, H. Kashida, and Y. Kamiya, *Chem. Rec.*, **2014**, *14*, 1055-1069.

[36] Y. Kamiya and H. Asanuma , *Acc. Chem. Res.*, **2014**, *47*, 1663-1672.

[37] Y. Chen, R. Nagao, K. Murayama, H. Asanuma, *J. Am. Chem. Soc.*, **2022**, *144*, 5887-5892.

[38] K. Makino, E. Susaki, M. Endo, H. Asanuma, and H. Kashida, *J. Am. Chem. Soc.*, **2022**, *144*, 1572-1579.

[39] K. Murayama, Y. Yamano, and H. Asanuma, *J. Am. Chem. Soc.*, **2019**, *141*, 9485-9489.

[40] K. Murayama and H. Asanuma, *ChemBioChem*, **2020**, *21*, 120-128.

[41] Y. Chen, K. Murayama, and H. Asanuma, *Chem. Lett.*, **2022**, *51*, 330-333.

[42] B. T. Le, K. Murayama, F. Shabanpoor, H. Asanuma, and R. N. Veedu, *RSC Advances*, **2017**, *7*, 34049-34052.

[43] Y. Kamiya, Y. Donoshita, H. Kamimoto, K. Murayama, J. Ariyoshi, and H. Asanuma, *ChemBioChem*, **2017**, *18*, 1917-1922.

[44] V. Ambros, *Nature* **2004**, *431*, 350-355.

[45] N. Bushati, S. M. Cohen, *Annu. Rev. Cell Dev. Biol.*, **2007**, *23*, 175-205.

[46] M. Ha, V. N. Kim, *Nat. Rev. Mol. Cell Biol.*, **2014**, *15*, 509-524.

[47] A. K. Leung, *Trends Cell Biol.*, **2015**, *25*, 601-610.

[48] A. Esquela-Kerscher, F. J. Slack, *Nat. Rev. Cancer*, **2006**, *6*, 259-269.

[49] B. D. Adams, A. L. Kasinski, F. J. Slack, *Curr. Biol.*, **2014**, *24*, R762-R776.

[50] M. Ohtsuka, H. Ling, Y. Doki, M. Mori, G. A. Calin, *J. Clin. Med.*, **2015**, *4*, 1651-1667.

[51] S. Lin, R. I. Gregory, *Nat. Rev. Cancer*, **2015**, *15*, 321-333.

[52] A. Hata, J. Lieberman, *Sci. Signaling*, **2015**, *8*, re 3.

[53] Jan Krützfeldt, *et al.*, *Nature*, **2005**, *438*, 685-689.

[54] Scott Davis, Bridget Lollo, Susan Freier, Christine Esau, *Nucleic Acids Research*, **2006**, *34*,   2294-2304,

[55] Scott Davis, *et al.*, *Nucleic Acids Research*, **2009**, *37*, 70-77.

[56] Kim A. Lennox and Mark A. Behlke, *Pharmaceutical Research*, **2010**, *27*, 1788-1799.

[57] Susanna Obad, *et al.*,   *Nature Genetics*, **2011***, 43*, 371-378.

[58] Luca F. R. Gebert, Mario A. E. Rebhan, Silvia E. M. Crivelli, Rémy Denzler, Markus Stoffel, and Jonathan Hall, *Nucleic Acids Research*, **2014**, *42*, 609-621.

[59] Kotaro Yoshioka, *et al.*, *Nucleic Acids Research*, **2019**, *47*, 7321-7332.

[60] Tomo Takegawa-Araki*, Shinji Kumagai, Kai Yasukawa, Masataka Kuroda, Takashi Sasaki, and Satoshi Obika*, *J. Med. Chem.*, **2022**, *65*, 2139-2148

[61] Frederick J. Sheedy*, Frontiers in Immunology, **2015**, *6*, 19.

[62] Cheng-Kai Huang, Christian Bär,* Thomas Thum,* *Frontiers in Pharmacology*, **2020**, *11*, 726

[63] P. P. Medina, M. Nolde, F. J. Slack, *Nature*, **2010**, *467*, 86-90.

[64] Diana Bautista-Sánchez, *et al*, *Molecular Therapy - Nucleic Acids*, **2020**, *20*, 409-420.

Chapter 2. The problem of SNA and L-*a*TNA based AMO

2-1 Abstract

We prepared SNA or L-*a*TNA based anti miR-21 oligonucleotides and measured them miR-21 inhibitory activities by dual luciferase assay system. Unfortunately, they have no activity. However SNA based anti miR-122 oligonucleotide have as active as Tiny-LNA. So, in this chapter, we considered the reason why activity varies between target miRNAs. We revealed that formation of higher-order structures of SNA or L-*a*TNA based anti miR-21 decreased them activity relating T_m values of them homo-duplexes with them miR-21 inhibitory activities.

2-2 Introduction

Anti miRNA oligonucleotides have basically the complementary sequence to target microRNA including partially complementary one.[1-8] Especially, tiny-LNAs is composed of only LNA and complement to only seed region, which is the most important site for mRNA recognition of miRNA.[5] The point of this design is what can inhibit miRNA family. But this design is realized by consisting only of LNAs with high RNA affinity. In the case that AMOs not composed of consecutive LNA, AMOs probably need fully complementary sequence to the target miRNA due to slightly lower RNA affinity than LNA. The most used AMO is 15 ~ 20 mer length mixed DNA and LNA, whose LNA locations are optimized for high activity. As shown in chapter 1, AMOs including LNA are often used *in vivo* study but not in clinical trials because LNA has risks in toxicity.[9] So new-type AMOs are desired for drugs used in humans.

In this chapter, we tried designing SNA[9] or L-*a*TNA[10] based AMO *in vitro* study for starters. In addition, we referred the problem of SNA and L-*a*TNA based AMOs and the solution.

2-3 Results and Discussion

2-3-1 The activity of SNA or L-*a*TNA based anti-miRNA oligonucleotide

We prepared SNA based anti miR-21 oligonucleotides and evaluated miR-21 inhibitory activities by Dual luciferase assay. The Firefly luciferase and Renilla luciferase expression vector pmirGLO, which has the miRNA binding sequence in multi cloning site of Firefly luciferase. When we transfected the vector plasmid into miRNA expression cells, internal miRNAs cut the mRNA transcribed from miRNA binding site and Firefly luciferase expression is suppressed. Transfecting AMO, depending on the AMO activity, Firefly Luciferase expression restored. So we can know the AMO activity by measuring the amount of light emitted of oxyluciferin after adding D-Luciferin to cell lysate. We can use the amount of Renilla Luciferase to calibrate the amount of vector Plasmid introduced into cells. Using dual luciferase assay, we measured the SNA based AMO activities against miR-21(Fig. 2-1 A). As shown the figure, unfortunately, there AMOs have no activities. On the other hand, when we measured the SNA based Anti miR-122 oligonucleotide, we knew the AMO had a relatively high activity(Fig. 2-1 B). In the case that target miRNA is miR-21, SNA based AMO does not show miRNA inhibitory activity. In addition, L-*a*TNA based anti miR-21 oligonucleotides show no activity(2-1 C).
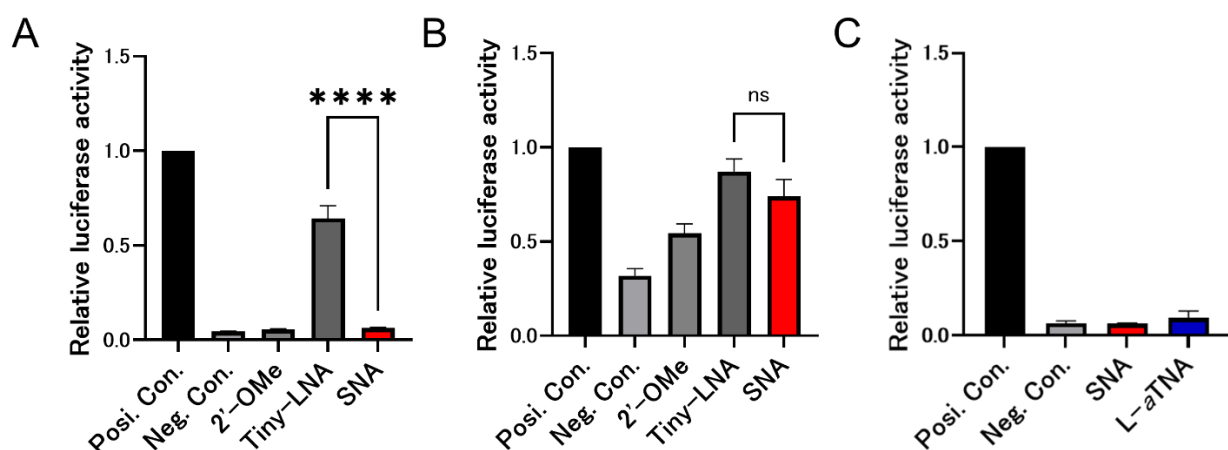
2-3-2 The reason why SNA or L-*a*TNA based Anti miR-21 oligonucleotides have no activities.

We considered that SNA or L-*a*TNA based Anti miR-21 oligonucleotides and we revealed the

reason. The reason is the homo duplex formation of SNA based Anti miR-21.

We focused on the difference of miR-21 and miR-122 sequences, and we reveal that while miR-122

doesn't have any self-complementary sequence, miR-21 has the self-complementary sequence as

shown figure 2-2. Here, we treated 4 mer or more complementary sequence as a self-complementary

sequence. Then, also AMOs against miR-21 have the self-complementary sequence corresponding

miR-21.

Figure 2-2 Sequences of miR-21 and miR-122. miR-21 has two 5 mer self-complementary sequence.

In ASO design, to select target sequence for avoiding sequences that form higher-order structures is

important, because the formation of ASO's higher-order structures disturb to hybridization with

target RNA and decrease the activities. According to this prevailing theory, it is not surprising that

SNA based anti miR-21oligonucleotide had no activity and SNA based anti miR-122 oligonucleotide

had good activity. Moreover, compared to other ribose-modified nucleic acids, homo-duplexes is

much more stable than hetero-duplex with RNA(Table 2-1).

Table 2-1 Melting temperature (ºC) of SNA and L-*a*TNA homo-duplexes and hetero-duplexes with RNA

Duplexes	T_m(°C)
SNA/RNA	35.0
SNA/RNA	51.1
L-aTNA/RNA	41.0
L-aTNA/L-aTNA	58.0

Sequence: -GCATCAGT-/-CGTAGTCA-, 100 mM NaCl, 10 mM phosphate buffer,

pH 7.0, [ONs]= 2.0 μM

So, we guessed that SNA or L-aTNA based anti miR-21 can form stable homo-duplexes or hairpin structures and cannot hybridize with miR-21.

Then, we examined the effects of self-association of anti mioR-21 to its activity. Actually, our laboratory reported 2,6-diaminopurine(D), Adenine derivative, improved SNA based anti miR-21 oligonucleotides. In the report, the position of D greatly influences anti miR-21 activities. Also, we guess that the influence is from stabilization of homo-duplexes by introduction of D. Whenever Ds were introduced into self-complementary region of SNA based anti miR-21 oligonucleotides, there T_ms of homo-duplexes became higher and the activities became lower than those without D in the region. Then, we measured T_ms of there mono-duplexes and hetero-duplexes, and associated there activities reported in the paper as shown table 2-2.

Table 2-2 association of D introduction, stability of homo-duplex, and miR-21 inhibitory activities

AMO	Sequence, Violet box: self-complementary region	T_m(°C) of without RNA[a]	T_m(°C) of with miR-21[a]	miR-21 inhibitory activity[b]
SNA	ATC GAA TAG TCT GAC TAC AAC	62.3	67.3	0.06 ± 0.004
S-SD2RD2	ATC GDD TAG TCT GAC TAC DDC	63.6	72.0	0.61 ± 0.03
S-D7	ATC GDD TDG TCT GDC TDC DDC	79.6	76.0	0.34 ± 0.02
S-RD2	ATC GDD TAG TCT GAC TAC AAC	65.4	70.0	0.26 ± 0.02
S-RD3	ATC GDD TDG TCT GAC TAC AAC	69.3	70.3	0.21 ± 0.02
S-SD2	ATC GAA TAG TCT GAC TAC DDC	65.8	68.7	0.39 ± 0.04
S-SD4	ATC GAA TAG TCT GDC TDC DDC	71.6	70.6	0.22 ± 0.03
S-D4	ATC GDA TDG TCT GDC TDC AAC	75.0	71.4	0.07 ± 0.002

We know S-SD2RD2 which has the highest miR-21 inhibitory activity in the report avoids stabilizing its homo-duplex. According there data, When we develop more functional SNA or L-aTNA based anti miR-21 oligonucleotides, techniques to avoid to stabilize there homo-duplexes and to increase RNA affinity specifically, not self-affinity. While S-SD2RD2 show high activity, its activity is lower than Tiny-LNA(Figure 2-3). We aimed to develop SNA or L-aTNA based anti miR-21 oligonucleotides which have higher activity than Tiny-LNA. In chapter 3, we tried to the develop techniques to improve RNA affinity of SNA and L-aTNA specifically and to suppress the self-association.

2-4 Conclusions

In this chapter, we referred to the problem of SNA or L-aTNA based Anti miR-21 oligonucleotides. When we targeted miR-21, SNA or L-aTNA based AMOs had no activities, however in the case of miR-122, SNA based AMO had good activity. SNA or L-aTNA based anti miR-21 oligonucleotides easily form homo-duplexes, which occurred to decrease of them activities. From T_m measurements of SNA based anti miR-21 oligonucleotides bearing some D residues used in the previous study. Also, there are other miRNAs having self-complementary regions. SNA or L-aTNA based AMOs targeting any miRNAs are largely influenced by the miRNA's sequences. So, for designing highly activated SNA or L-aTNA based AMOs, which is not affected by target miRNA's sequence, novel techniques to suppress self-association and to increase RNA affinity especially is needed. In chapter 3, we report the development of the techniques.

2-5 Experimental Section

Materials

For Luciferase assay, Anti miR-21 oligonucleotides composed of 2'-OMe or LNA were purchased from FASMAC or Genedesign, Inc. SNA or L-aTNA oligomers synthesized following reported procedures, except that oligomers were synthesized using an NTS M-8-SE DNA/RNA synthesizer (NIHON TECHNO SERVICE CO., Ltd.) using SNA and L-aTNA phosphoramidite monomers bearing [Bz]A, [iBu]G, [Bz]C, and T. Vector plasmid having no target binding site was purchased from Promega Corporation. We prepared the pmirGLO-miR21, by inserting the miR-21 binding sequence (5′-CAACA TCAGT CTGAT AAGCT A-3′) between the XhoI and SalI sites in the 3′-UTR region of the gene encoding the firefly luciferase.

Dual luciferase assay

Cotransfections of HeLa cells or HuH-7 cells with AMO and 100 ng/well vector plasmids (100 ng) were performed by using Lipofectamine® 2000 (Invitrogen) in 96-well plates according to the manufacturer's instructions. After 24 h incubation, we removed 75 µl culture medium and added Dual-Glo regent (75 µL, Promega) to the medium of HeLa cells in 96 well-plates. We measured Firefly luciferase luminescence by using Multi-label Plate Reader (EnSpire, PerkinElmer). Subsequently, we adeed Dual-Glo Stop & Glo reagent (75 µL, Promega), and measured Renilla luciferase luminescence.

Melting-temperature measurements

  Oligonucleotides of SNA or L-aTNA with or without RNA (2 µM) were dissolved in 10 mM sodium phosphate buffer (pH 7.0) with 100 mM NaCl. The melting curves were obtained with a Shimazu UV-1800 by measuring the change in absorbance at 260 nm versus temperature. Temperature ramp was 0.5 °C min^{-1}. T_m values were determined from the maximum in the first derivative of the melting curve.

2-6 References

[1] Jan Krützfeldt, *et al.*, *Nature*, **2005**, *438*, 685-689.

[2] Scott Davis, Bridget Lollo, Susan Freier, Christine Esau, *Nucleic Acids Research*, **2006**, *34*, 2294-2304,

[3] Scott Davis, *et al.*, *Nucleic Acids Research*, **2009**, *37*, 70-77.

[4] Kim A. Lennox and Mark A. Behlke, *Pharmaceutical Research*, **2010**, *27*, 1788-1799.

[5] Susanna Obad, *et al.*, *Nature Genetics*, **2011***, 43*, 371-378.

[6] Luca F. R. Gebert, Mario A. E. Rebhan, Silvia E. M. Crivelli, Rémy Denzler, Markus Stoffel, and Jonathan Hall, *Nucleic Acids Research*, **2014**, *42*, 609-621.

[7] Kotaro Yoshioka, *et al.*, *Nucleic Acids Research*, **2019**, *47*, 7321-7332.

[8] Tomo Takegawa-Araki*, Shinji Kumagai, Kai Yasukawa, Masataka Kuroda, Takashi Sasaki, and Satoshi Obika*, *J. Med. Chem.*, **2022**, *65*, 2139-2148

[9] Crooke S.T., Witztum J.L., Bennett C.F., Baker B.F., **2018**, *Cell Metab.*, *27*, 714-739.

[10] H. Kashida, K. Murayama, T. Toda, and H. Asanuma, *Angew. Chem., Int. Ed.*, **2011**, *50*, 1285-1288.

[11] K. Murayama, H. Kashida, and H. Asanuma, *Chem. Commun.*, **2015**, *51*, 6500-6503.

Chapter 3.   Development of a method to suppress self-affinity of SNA and L-*a*TNA, and to increase them RNA affinity.

3-1 Abstract

  Our group reported *acyclic* nucleic acids, SNA and L-*a*TNA. They can be synthesized more easily than ribose modified nucleic acids like a LNA, and they can form stable duplexes with natural nucleic acids, DNA or RNA. Moreover, they have much stronger enzyme-resistance then ribose modified nucleic acids. For these characters, they are very useful for biological applications. However, they sometimes form self-association preferentially despite in the presence of perfectly complementary DNA or RNA because they have higher self-affinity than affinity to DNA or RNA, which causes inactive function of applications based on SNA and L-*a*TNA.

  In this study, we tried developing a method to decrease self-affinity of SNA and L-*a*TNA for suppression of them self-association. For the purpose, we introduced 2,6-Diaminopurine(D) and 2-Thiouracil(sU), which are nucleobase analogs of Adenine(A) and Thymine(T) or Uracil(U). instead of A and T in SNA or L-*a*TNA. For introduction of D and sU into SNA or L-*a*TNA, I designed and synthesized phosphoroamidite monomers of SNA and L-*a*TNA bearing D and sU. Then, we investigated effect of D-sU introduction to self-association and RNA affinity of SNA and L-*a*TNA.

3-2 Introduction

  As reported in chapter 2, for developing more functional SNA[1] or L-*a*TNA[2] based anti miR-21 oligonucleotides, we need to techniques to suppress them self-association and increase them RNA affinity beforehand. So far, for suppress formation of secondary-structures, 2,6-diaminopurine(D)[3, 4] and 2-thiouracil(sU)/2-thiothymine(sT) base pair,[5, 6, 7] 7-deazaguanine,[8-12] Inosine,[13, 14] 7-methyl-guanine[15] are introduced to any-type oligonucleotides. D and sU/sT, known as pseudo

complementary base pairs, often used for decrease PNA association for improving invasion efficiency into DNA duplexes. D and sU/sT cannot form base pair due to the steric hindrance between 2-amino group on D and 2-thiocarbonyl group on sU. Sometimes only sU for suppress formation of secondary structures because sU suppress to hybridize guanine residues through Hoogsteen base pair rule. In PNA invasions, also 7-methyl-guanine is utilized. The Cation of 7-methylguanine on uncharged PNA induced electrostatic repulsion between PNA to PNA, resulting in decreasing self-affinity of PNA strands and increase RNA affinity by electrostatic interaction. 7-deaza-guanine Inosine are used for avoiding G-G hoogsteen interaction, but its RNA affinity is slightly lower than guanine.

2,6-Diaminopurine   Steric hindrance   2-Thiouracil (R = H) / 2-Thiothymine (R = Me)

7-deaza-Guanine   Inosine   7-Methyl-Guanine

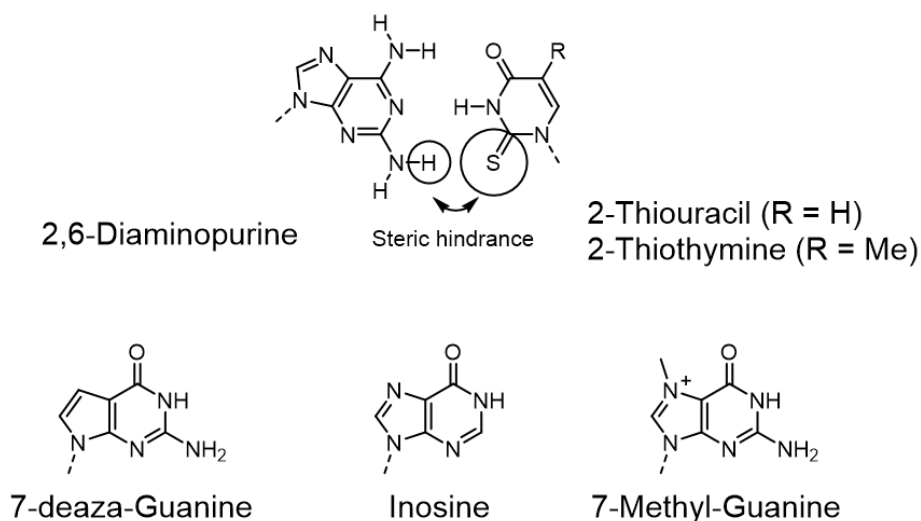Figure 3-1 The chemical structures of artificial nucleobases for suppressing undesired interactions

Then, we focused on D-sU/sT base pair. As the same of PNA, we guessed D-sU/sT introduction suppress self-interactions of SNA or L-*a*TNA oligomers and improve them RNA affinity especially. So, introducing D-sU/sT base pairs into SNA or L-*a*TNA based anti miR-21, increase of them activity is expected.
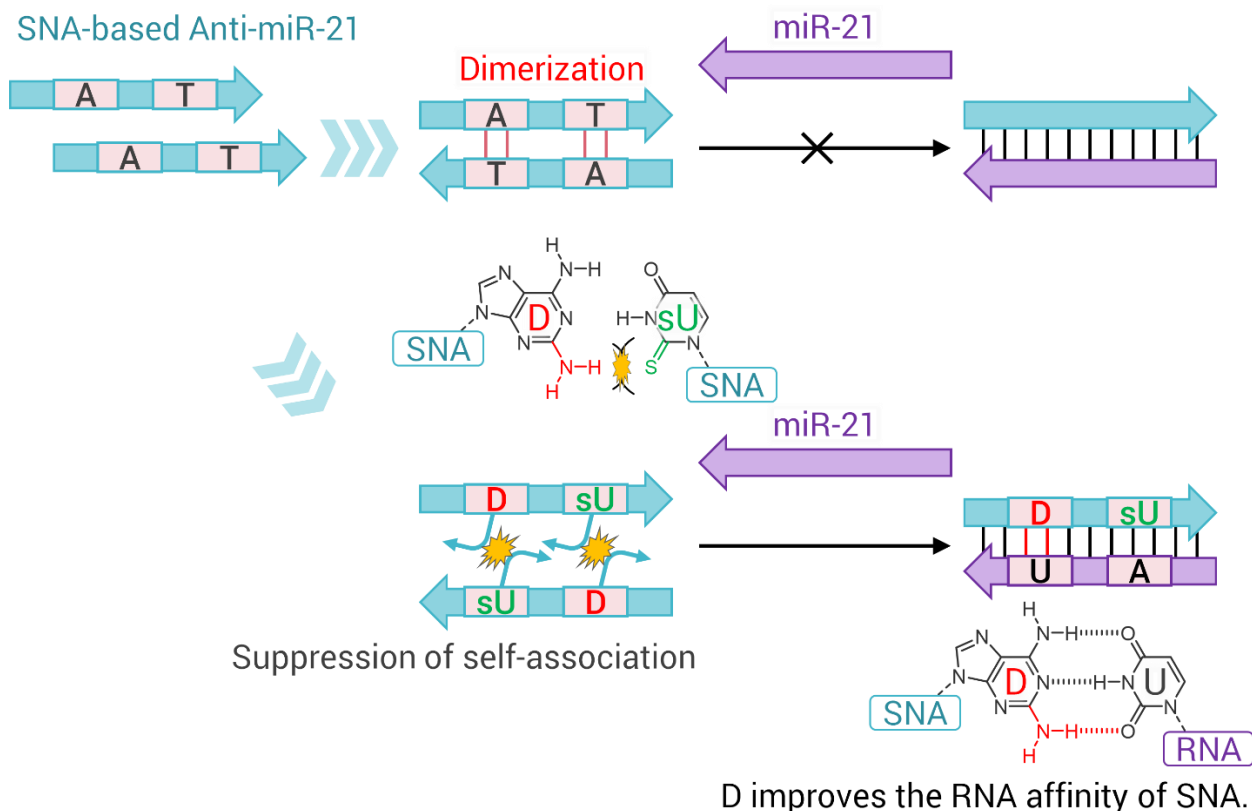
Figure 3-2 The schematic illustration: incorporation of D and sU suppresses self-hybridization of XNA and facilitates formation of

hybrid DNA/XNA or RNA/XNA duplexes.

In this chapter, we tried developing the method how to introduce D and residues into SNA and L-*a*TNA oligomers. According to solid-phase synthesis by phosphoramidite method on DNA synthesizer, we started synthesizing phosphoramidite monomers bearing D or sU whose reactive functional groups are protected with appropriate protecting groups. Our groups succeeded D introduction into SNA based anti mIR-21 oligonucleotides by using phosphoramidite monomer bearing D protected by *N*, *N*-diisopropylformamidine group. Actually, when we use the monomer, we change oxidizing reagent in solid-phase synthesis for suppressing to produce truncated product. Then we optimized D monomer design as the same time of sU/sT monomer design.

In general, 2-type sU/sT amidite monomer, which is unprotected or toluoyl-protected, are used.[5, 7] The unprotected sT DNA phosphoramidite monomer is commercially available from Gren Research.

When coupling this monomer on DNA synthesis, t-BuOOH/MeCN/H_2O solution should be used at the oxidation step to prevent the desulfurization of 2-thiothymine caused by iodine/puridine/H_2O solution which is used in general, and longer reaction time is required.[16, 17] Moreover, most nucleic acid-based drugs have phosphorothioate linkages; incorporation of this linkage requires sulfurizing reagents such as N,N-dimethyl-N'-(3-thioxo-3H-1,2,4-dithiazol-5-yl)methanimidamide.[18] To avoid unfavorable reaction of sT and sU with sulfurizing reagents or byproducts such as thiocarbamoyl isothiocyanate derivatives, we thought the thiocarbonyl group of sT and sU phosphoroamidite monomers on SNA or L-aTNA should be protected. On the other hand, as another type phosphoramidite monomer of sU/sT, the thiocarbonyl group on sT has been protected with an $N3/O4$ toluoyl adduct to avoid desulfurization by iodine during solid-phase synthesis.[7] However, the long incubation with NH_3 solution necessary for removal of the protecting group resulted in ammonolysis of sT and sU.[5, 7] Then, we tried synthesizing toluoyl-protected-sU SNA amidite monomer. Although either sU or sT could have been used, we selected sU because sU is cheaper than sT and it is reported that sU have slightly higher RNA affinity on PNA. While we planned to synthesize toluoyl-protected sU amidite monomer (Scheme 3-1), we could not synthesize the monomer because toluoyl group was removed on the step of TBDMS deprotection. We guess primary alcohol of SNA caused a nucleophilic reaction to $C2$ under basic conditions (data not shown). Then, we decided synthesizing sU-SNA amidite monomer protected acid-labile protecting groups. Usually, acid-labile protecting groups cannot be used for DNA synthesis due to depurination induced during deprotection step of acid-labile-protecting groups. And only protecting groups which are deprotected by strong acid can be used because 3% Trichloroacetic acid in CH_2Cl_2 solution is used for deprotection of 4,4'-dimethoxytrityl groups on DNA synthesis. So, for phosphoramidite monomers of DNA and other ribose modified nucleic acids, acid-labile protecting groups on nucleobases are never used. On the other hand, we thought acid-labile protecting groups can be utilized to only SNA and L-aTNA synthesis because SNA and L-aTNA don't have ribose-scaffold and don't occur depuration under

strong acid conditions. 4-Methoxy-2-methylbenzyl (MMPM) group was used sU-PNA monomer on Fmoc-based solid-phase synthesis.[20] This protecting group was deprotected Trifluoroacetic acid (TFA) solution after solid-phase synthesis. So, we tried applying MMPM group to sU-SNA amidite monomer firstly. As the same of PNA, we would deprotected MMPM on sU after SNA solid-phase synthesis under TFA solution. Then, we applied acid-labile protecting group to D-SNA amidite monomer. We tried synthesizing Boc-protected D-SNA amidite monomer because the synthesis of Boc-protected D-PNA monomer for Fmoc-based solid-phase synthesis was reported and our group reported Boc groups could be used for phosphoramidite monomer of D-*a*TNA.[21] In this chapter, we tried to synthesize MMPM-protected sU-SNA amidite monomer and Boc-protected D-SNA amidite monomer. In addition, we examined whether we can synthesis SNA oligomers bearing D and sU through phosphoramidite method by using these monomers.

3-3 Results and Discussions

Synthesis of Boc-protected D-SNA phosphoramidite

Briefly, amino groups on D were fully protected by Boc groups and then Boc on *N*9 position was removed under $NaHCO_3$/MeOH conditions. The *N*9 was reacted with ethyl bromoacetate to yield the ethyl ester derivative, which was hydrolyzed under basic conditions to give carboxylic acid derivative of Boc-protected D. Compound 6 was synthesized through the reported procedure. Then, compound 7 was obtained by condensation of 4,4'-dimethoxytritylated SNA with compound 5 and was further converted to the corresponding phosphoramidite monomer according to the conventional procedure. [1, 2]
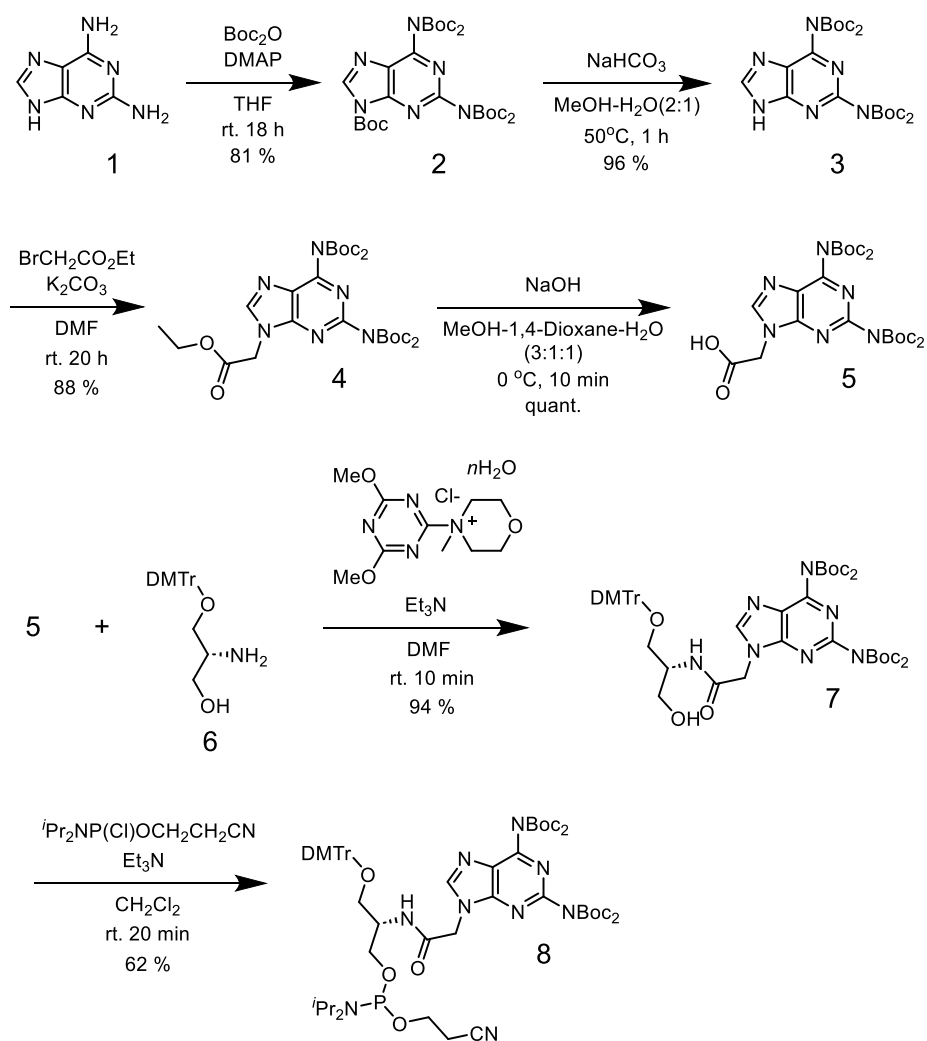
Scheme 3-1 The synthetic route to the phosphoramidite monomer of Boc-protected D-SNA. Boc: *tert*-butoxycarbonyl, DMTr: 4,4'-dimethoxytrityl group.

Synthesis of MMPM-protected sU-SNA phosphoramidite

Briefly, we synthesized halogenated MMPM group, compound 11, then, using compound 11 we protected 2-thiouracil. Next, we synthesized compound 14, carboxylic acid derivative of compound 12, through the either of compound 12. Then, compound 15 was obtained by condensation of 4,4'-dimethoxytritylated SNA with compound 14 and was further converted to the corresponding phosphoramidite monomer.
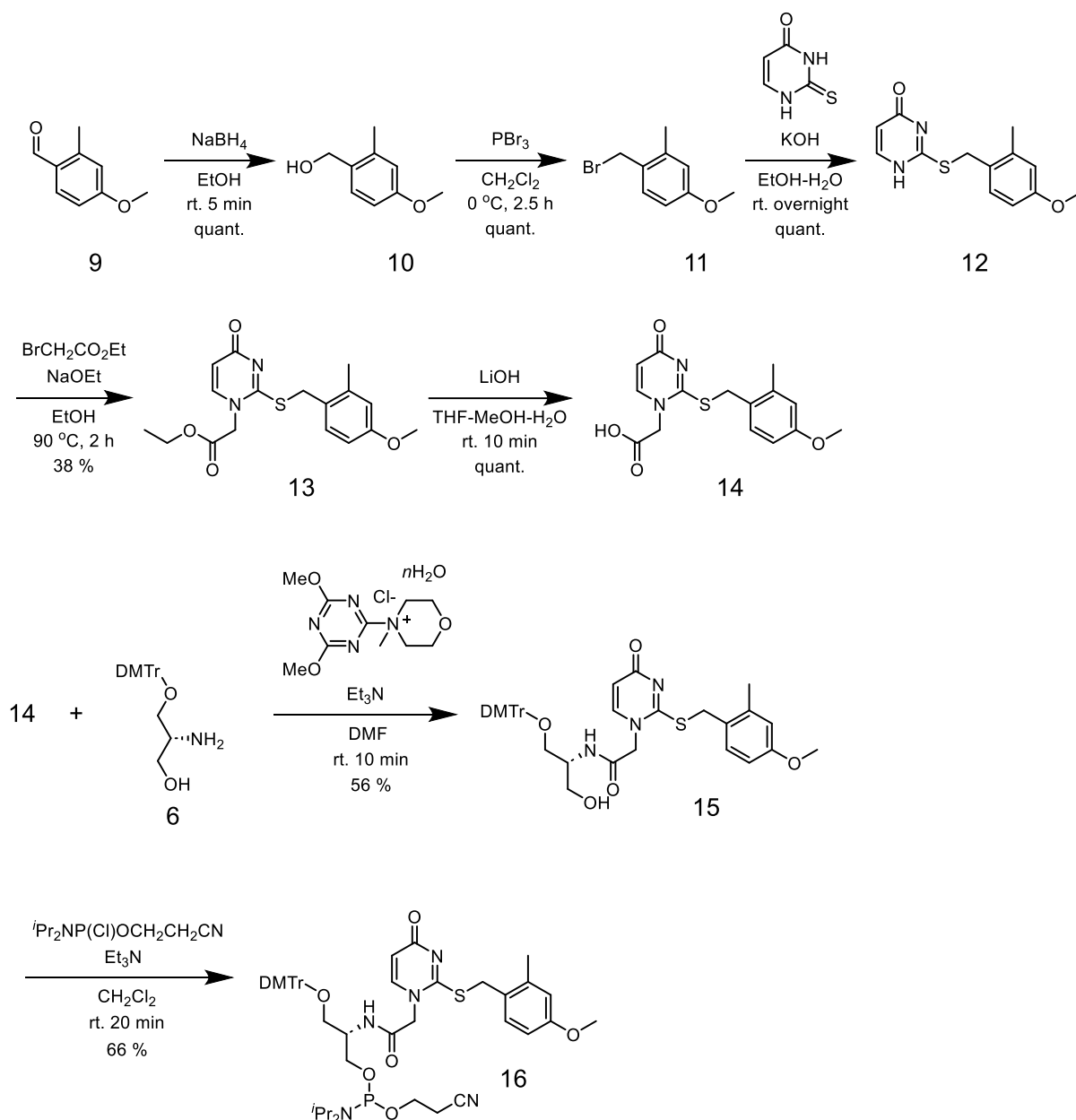
Scheme 3-2. The synthetic route to the phosphoramidite monomer of MMPM-protected sU-SNA. DMTr: 4,4'-dimethoxytrityl group.

Synthesis of SNA oligomer bearing D and sU

First, we checked we could synthesize SNA oligonucleotide involving [Boc]D (SNA-1D: (*S*)-C[Boc]DGAGACA-(*R*)) or [MMPM]sU (SNA-1sU: (*S*)-TGCAGC[MMPM]sUA-(*R*)) by the standard phosphoramidite scheme and following deprotection steps (trifluoroacetic acid (TFA) containing 13.9 % m-cresol and 2.8 % H_2O and 28 % NH_3 aq. at 55 °C. The TFA treatment was carried out

before cleavage of SNA oligonucleotide from controlled pore glass (CPG) support by NH_3 aq.. We

analyzed crude products involving D or sU by MALDI-TOF-MS analysis. In terms of SNA-1D, MS

peak of the object was clearly observed without Boc-groups and significant side products (Figure 3-

3).
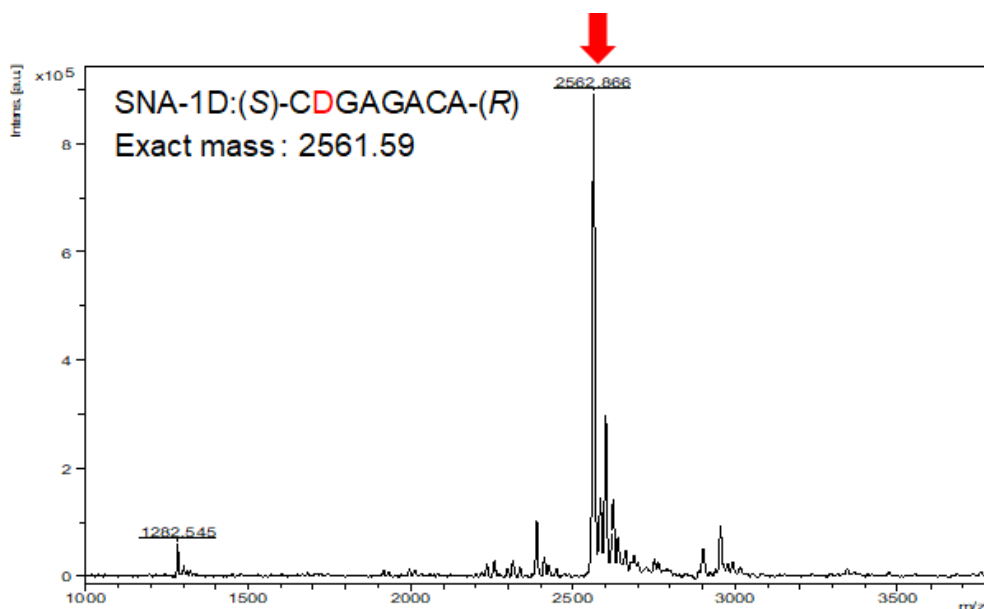
Fig. 3-3. MALDI-TOF-MS analysis of crude SNA-1D: (S)-CDGAGACA-(R)), exact mass: 2561.59. Boc-protected SNA-1D was

synthesized using standard protocols and then Boc was deprotected by treatment with TFA containing 13.9% m-cresol and 2.8% H_2O

for 3 h. The crude product was obtained after incubation with 28% aqueous ammonia for deprotection of natural bases and removal of

oligonucleotide from CPG. Red arrow shows completely deprotected product.

In the case of SNA-1sU, we synthesized the one, changing oxidizing reagent to milder oxidizer, (1S)-

(+)-10-camphorsulfonyl)-oxaziridine (CSO) for oligomerization of phosphoramidite scheme because

sulfur atom is known to be oxidized and desulfured under normal oxidative conditions.[22] As shown

in figure 3-4A, S converted product to O and desulfured product were observed. This is mean that the

MMPM group on sU is deprotected during deblocking reaction on DNA synthesizer. So, we

attempted to synthesize SNA-1sU by standard phosphoramidite scheme with t-BuOOH in CH_2Cl-

$_2$/decane as an oxidation reagent for suppressing desulfurization. [16, 19] Without TFA treatment (figure

28

3-4B), or with TFA treatment (figure 3-4C) deprotection and cleavage of SNA-1sU by NH_3 aq. were done. Therefore, we changed oxidizer to *t*-BuOOH for synthesis of SNA-1sU. With or without TFA treatment crude product after deprotection by 28% aqueous ammonia treatment exhibited MS peak corresponding to SNA-1sU as a major peak in MALDI-TOF-MS profile (Fig. 3-4 B and C). In short, MMPM-protecting group was deprotected during deblocking step, and when Iodine/pyridine/H_2O or CSO were used, sU residue on SNA is desulfured. When we used *t*-BuOOH solution as an oxidizing reagent, we obtained SNA-1sU without noticeable impurities.
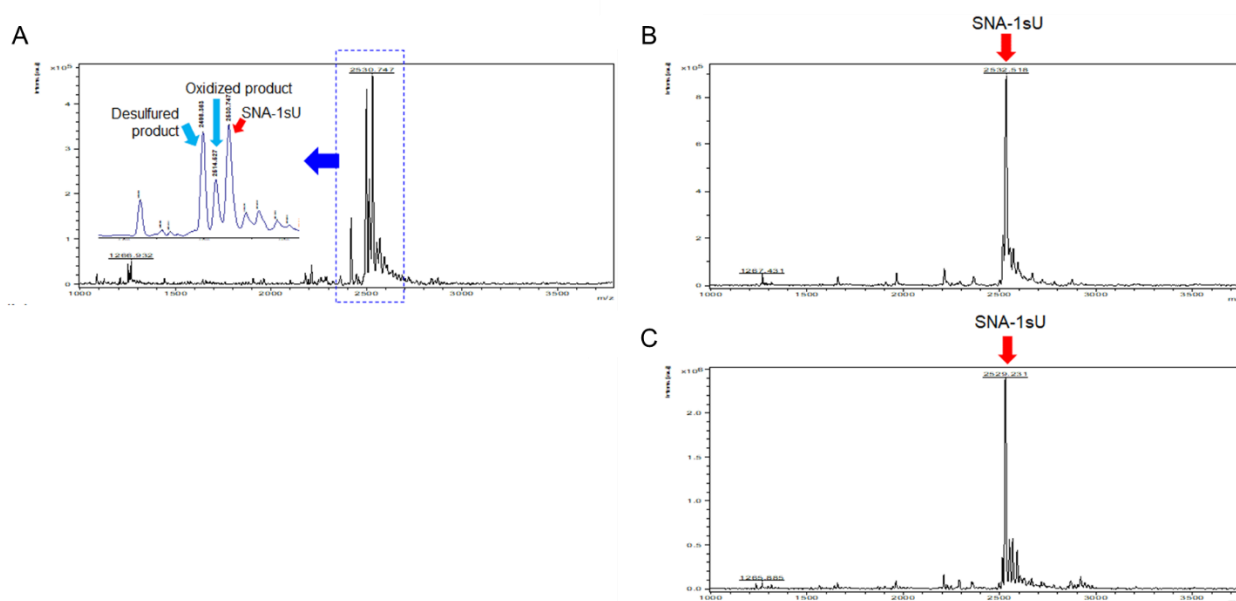
Figure 3-4. MALDI-TOF-MS analysis of crude SNA-1sU: (*S*)-TGCAGCsUA-(*R*), exact mass: 2530.32). (A) MMPM-protected SNA-1sU was synthesized using standard protocols with CSO as oxidizer. The crude SNA oligonucleotides were obtained after incubation with 28% aqueous ammonia. (B, C) MMPM-protected SNA-1sU was synthesized using standard protocols with *t*-BuOOH as oxidizer. The crude products were incubated (B) without (C) with TFA containing 13.9% *m*-cresol and 2.8% H_2O and then with 28% aqueous ammonia. obtained after incubation with 28% aqueous ammonia.

Then, we tried to optimize the protecting group of sU, and we synthesized 2-methoxybenzyl-protected sU-SNA phosphoramidite through the same scheme of scheme 3-2 and unprotected sU-SNA phosphoramidite through the same scheme inserted TFA treatment after synthesis of compound

13. When we used 2-methoxybenzyl-protected sU phosphoramidite and iodine/pyridine/H_2O as an oxidizer, the MS peak of M - 16 was observed more strongly, as the number of synthesis cycles after sU increased (figure 3-5 A). This data means 2-methoxybenzyl group on sU is slightly deprotected per synthesis cycle and desulfurization was induced by the oxidizer. Therefore, we used 3% dichloroacetic acid as a milder acidic deblocking reagent than 3% Trichloroacetic acid. By using DCA reagent, deprotection of 2-methoxybenzyl group were suppressed, but MS peak of M - 16 was still observed (figure 3-5 B and C).

Figure 3-5. (A) MALDI-TOF-MS analysis of crude (S)-AAAAAAsUT-(R), (S)-AAAAsUAAT-(R), and (S)-AsUAAAAAT-(R), exact mass: 2546.560. The SNA oligomer was synth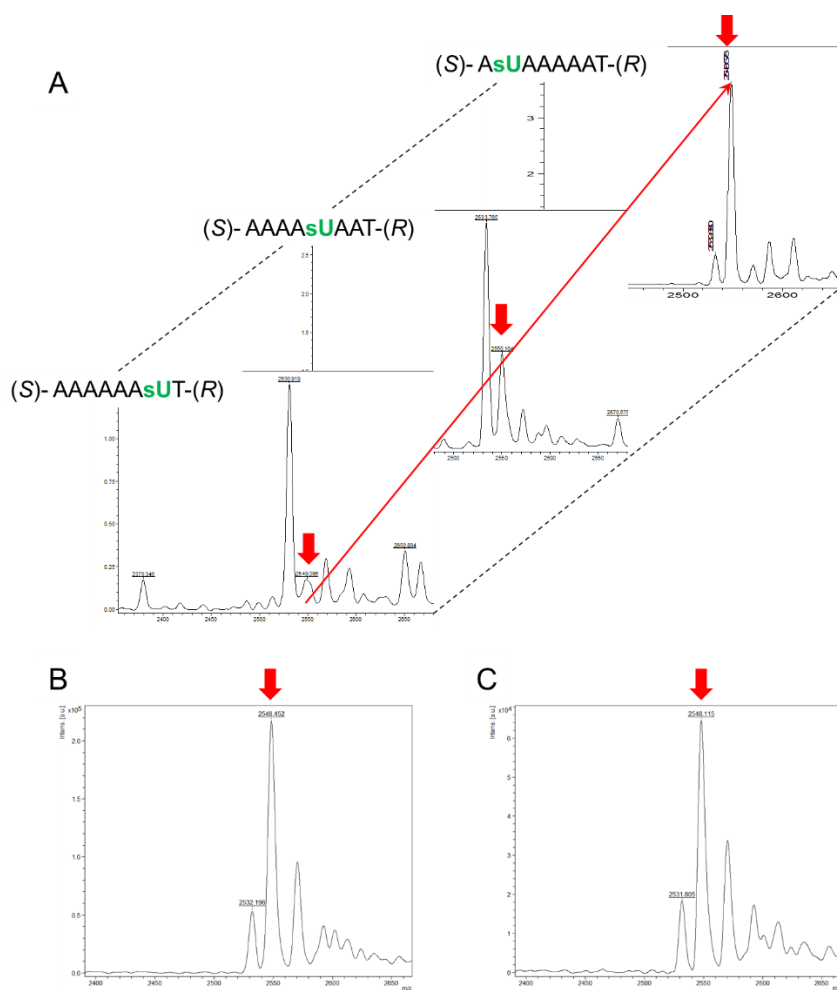esized using standard protocols with iodine/pyridine/H_2O as an oxidizing reagent. The crude SNA oligonucleotides incubated TFA treatment for 2 h. Red arrow means the product.

(B, C) MALDI-TOF-MS analysis of crude (*S*)-AAAAsUAAT-(*R*). The SNA oligomer was synthesized using standard protocols with

3% DCA as a deblocking reagent and (B) iodine/pyridine/H$_2$O (C) 1.0 M *t*-BuOOH in decane/CH$_2$Cl$_2$ as an oxidizing reagent. The

crude SNA oligonucleotides incubated TFA treatment for 2 h. Red arrow means the product.

When we used unprotected-sU phosphoramidite, we obtained the product with side product, obs.

MS: M-16.
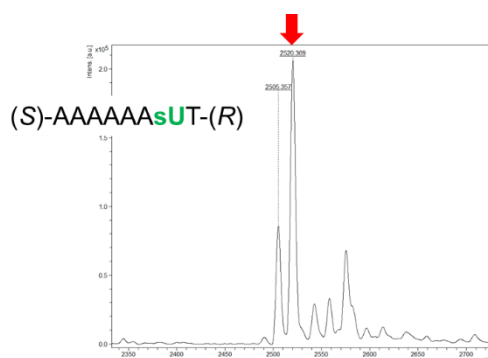
(*S*)-AAAAAAsUT-(*R*)

Figure 3-6 MALDI-TOF-MS analysis of crude (*S*)-AAAAAAsUT-(*R*), exact mass: 2546.560. The SNA oligomer was synthesized

using standard protocols with 1.0 M *t*-BuOOH in decane/CH$_2$Cl$_2$ as an oxidizing reagent without TFA treatment. Red arrow means the

product.

We couldn't suppress procedure of M-16 perfectly by any method, we decided to prepare SNA

oligomers bearing D and sU residues, using Boc-protected D phosphoramidite, MMPM-sU

phosphoramidite and 1.0 M *t*-BuOOH solution as an oxidizing reagent.

Thus, we successfully established synthetic and deprotection scheme of SNA oligonucleotide

involving Boc-D and/or MMPM-sU.

Evaluation of D-sU pairs on self-association and RNA recognition

We designed 8-nt long palindromic SNA oligonucleotides (Figure 3-7 A) to evaluate hybridization

properties of SNA homo-duplexes and hetero-duplexes with RNA. SNA oligonucleotides were

purified by reversed phase HPLC and were characterized by MALDI-TOF-MS (Figure 3-7 B and C).
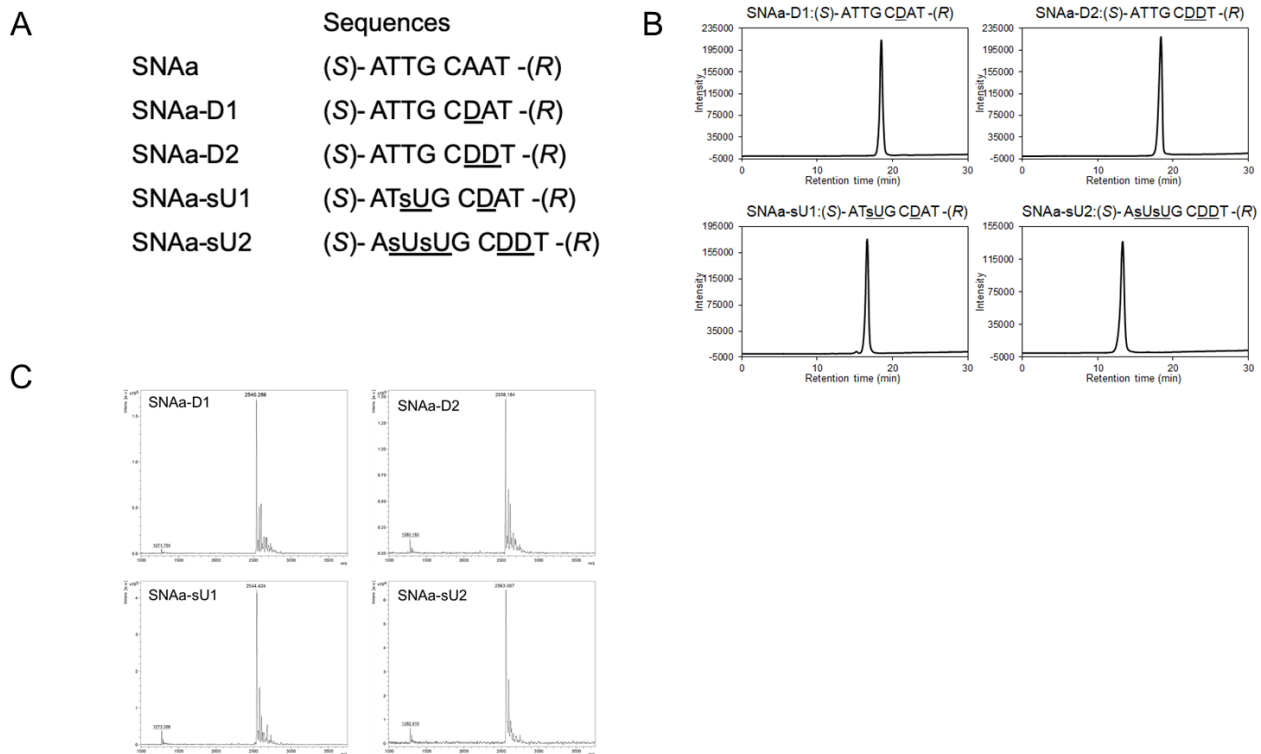
Figure 3-7 (A) Sequences (B) HPLC profiles (C) MALDI-TOF-MS analyses of D and/or sU incorporated SNA. Calculated masses are

[SNAa-D1+H]$^+$: 2543.57; [SNAa-D2+H]$^+$: 2558.58; [SNAa-sU1+H]$^+$: 2545.53; and [SNAa-sU2+H]$^+$: 2562.50.

First, we measured T_ms of SNA oligonucleotides without complementary RNA, RNAb. As shown in Figure 3-8 B, melting temperature of SNA increased remarkably by D introduction, which means D introduction increased the stability of SNA homo-duplex. On the other hand, the melting temperature of SNA decreased dramatically by D-sU base pair introduction, which means D-sU base pair introduction decreased SNA self-association. These melting profiles clearly show that only D residues introduction promote self-association of SNA oligonucleotides, but D-sU base pair, pseudo-complementary bases, can inhibit it.

Next, we measured T_ms of SNA oligonucleotides with RNAb. The melting profile of the mixture of SNA not involving sU residues with RNAb had two sigmoidal transition regions (Figure 3-8 C and Table 3-1). Each T_m values correspond to the profiles of the homo duplexes of SNAs and RNAb (Table 3-1), which means that SNA/RNA hybridization was disturbed by self-association and only D

32

introduction enhanced the inhibition. In contrast, the melting profile of the mixture of SNA involving D-sU base pairs with RNAb had only one sigmoidal transition regions (Figure 3-8 D and Table 3-1) and T_m values increased depending on the number of D-sU base pairs, which indicates that D-sU introduction increased RNA recognition ability of SNA oligonucleotides.
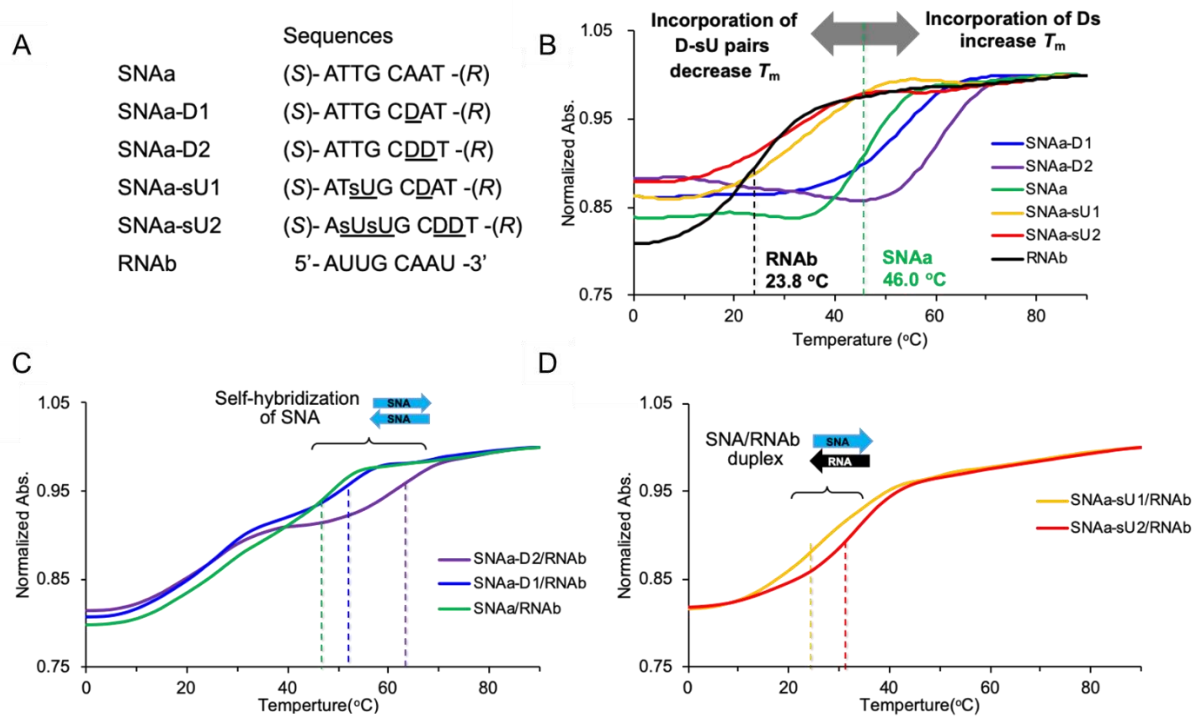
Figure 3-8 (A) Sequences of SNAs and target RNA. (B) Melting curves of self-complementary SNAs and RNAb. (C) Melting curves of mixtures of SNAa, SNAa-D1, or SNAa-D2 with RNAb. (D) Melting curves of mixtures of SNAa-sU1 or SNAa-sU2 with RNAb. T_m measurements were performed under 100 mM NaCl, 10 mM sodium phosphate buffer (pH 7.0), 2.0 μM oligonucleotide.

Table 3-1 T_ms of SNA oligonucleotides in the presence or absence of RNAb.[a]

	T_m (°C) without RNAb	T_m (°C) with RNAb[b]	
		Higher	Lower
SNAa-D2	61.0	62.3	25.4
SNAa-D1	53.2	51.6	25.9
SNAa	46.0	47.9	27.0
SNAa-sU1	36.4	-	26.0
SNAa-sU2	30.6	-	32.7

[a] T_m measurements were under 100 mM NaCl, 10 mM phosphate buffer (pH 7.0), 2.0 μM oligonucleotide.

[b] T_m of homo-duplex of RNAb is 23.8 °C

Then, we confirmed hetero-duplex formation of SNAa-sU2 and RNAb by MS analysis under non-denaturing condition (Native MS) and Native-PAGE analysis. Native-MS can be used to analyze assembly of biomolecules such as protein complexes and interactions of oligonucleotides when ionization and desolvation conditions are optimized to avoid disruption of the noncovalent interaction.[21, 23, 24] In Native-MS analysis, although single strands of SNAa-sU2 and RNAb were observed, MS signals corresponding of -3 charge and -2 charge state of duplex of SNAa-sU2 and RNAb were clearly observed with sufficiently high intensity (Figure 3-9). Native-PAGE analysis revealed that the extent of SNAa-sU2/RNAb was roughly ten times higher than homo duplex of SNAa-sU2 in the mixture (Figure 3-10). Thus, we could unambiguously conclude that incorporation of D and sU pairs in SNA oligonucleotides promotes hybridization with complementary RNA by suppressing self-pairing.
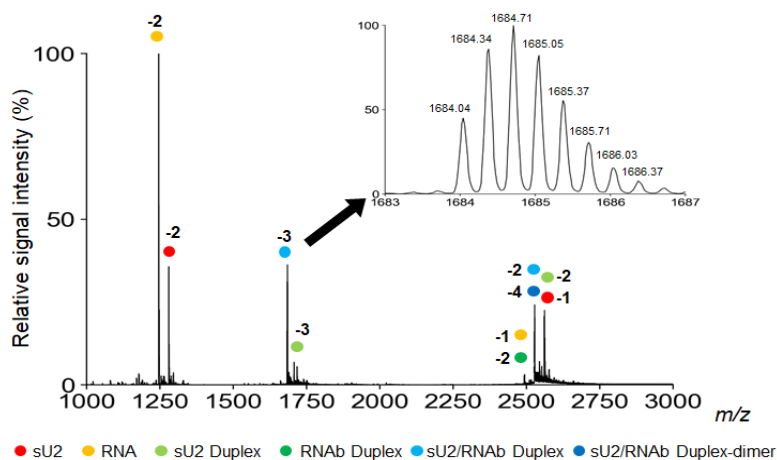
Figure 3-9 Native-MS profile of mixture of SNAa-sU2 and RNAb performed under native condition with negative ionization mode.

Exact mass of sU2: 2561.48605, RNAb: 2493.36642, sU2 duplex: 5122.91210, RNAb duplex: 4986.73284, sU2-RNAb duplex:

5054.85247, sU2-RNAb duplex-dimer: 10109.70494
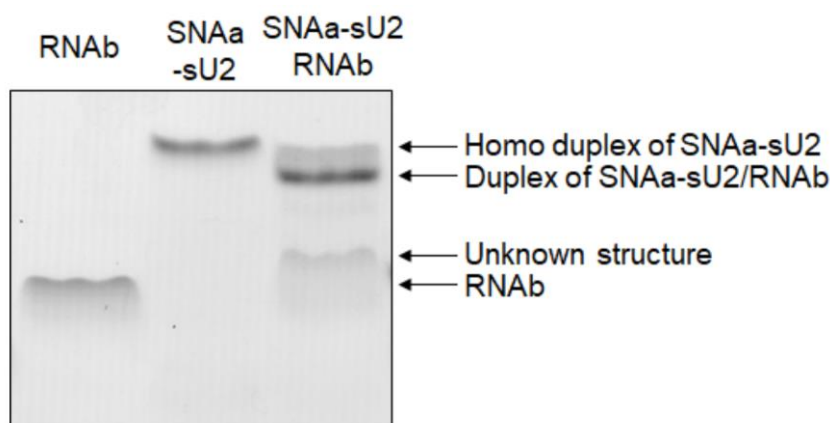
Figure 3-10 Native-PAGE analysis of duplex formation of SNA-sU2 and RNAb.

Redesign of D and sU-SNA and L-*a*TNA phosphoramidite monomer.

As mentioned above, we succeeded to synthesize D/sU-SNA phosphoramidite and introduce D-sU base pairs into SNA. However, there are the big problem. In the future, we aimed to utilize D-sU for SNA or L-*a*TNA based antisense drugs. For the purpose, compatibility to large-scale synthesis is required. For example, there are high yields of phosphoramidite synthesis and oligomer synthesis, easy purification, and no additional steps from common oligomer synthesis methods. Now, in our method of D-sU introduction, the yield of sU phosphoramidite was low, the additional step and changing oxidizing reagent were required, and oligomer purification is very difficult because pre-purification by C18 cartridge is not available due to deprotection of DMTr group in TFA treatment step. So, we concluded that Boc-protected D-SNA phosphoramidite and MMPM-protected sU-SNA phosphoramidite and oligomer synthetic method are not compatible with large scale synthesis. Therefore, we need the new method which is not required additional steps and can be through pre-purification. We decided to redesign D and sU phosphoramidite monomers. The protecting groups which are used for D and sU must be easily deprotected under mild condition due to possibility of sU's side reaction, ammonolysis.[5, 7] For suppressing ammonolysis of sU perfectly, we thought protecting groups should be deprotected after oligomer synthesis under mild basic condition, aqueous

35

ammonia at room temperature for any times or at about 55 $^{\circ}$C for short hour. We attempted to utilize a various protecting group which is easily deprotected under mild basic conditions. We tried to synthesize cyanoethyl, trifluoroacetyl, benzoyl, acetyl, and so on, but it ended in failure (data is not shown). Then, Ackermann and Famulok previously used the *p*-acetoxybenzyl(Aob) group for the protection of sT to suppress unfavorable nucleosidation at both *S*2 and *N*3 positions.[19] In the route they reported, the Aob group was removed simultaneously with deprotection of hydroxyl groups on the ribose scaffold under basic conditions. This prompted us to use the Aob group to protect the thiocarbonyl from desulfurization at the oxidization step during the solid-phase synthesis. This protecting group is base-labile,[25, 26] so deprotection should be rapid and ammonolysis of sU should be suppressed. We decided to synthesize Aob-protected sU-SNA and L-*a*TNA phosphoramidites. In the case of D phosphoramidites, we utilized phenoxyacetyl (Pac) group which is the most base-labile in acyl protecting groups.[27] Both of Pac and Aob protecting groups would be deprotected under mild basic conditions, so we expected to synthesize SNA and L-*a*TNA oligomer bearing D and sU with pre-purification based on DMTr without additional steps.

Scheme 3-3 Preparation of pseudo-complementary SNA or L-*a*TNA
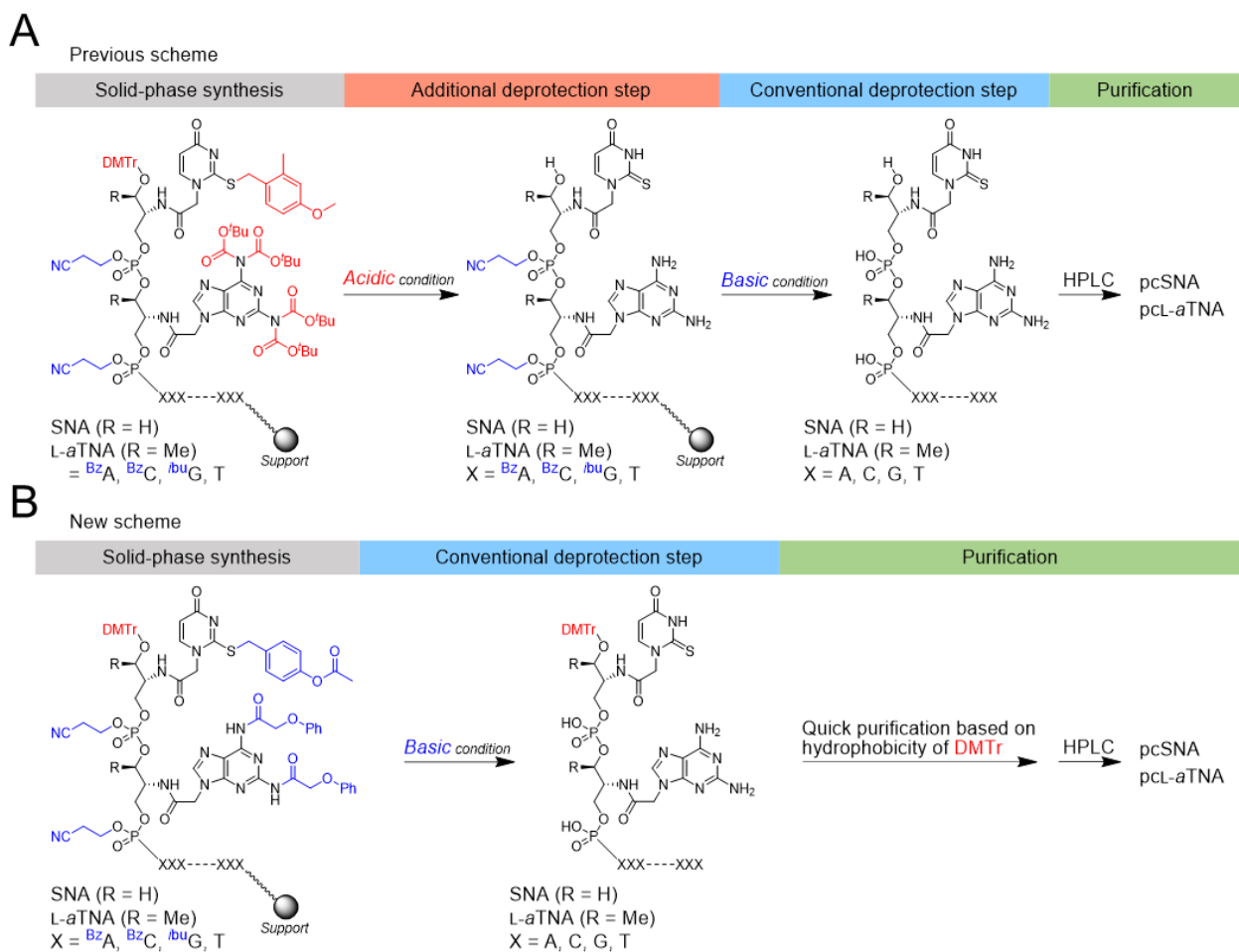
(a) our previous method with acid-labile D and sU phosphoramidite monomers. (b) the method reported here with base-labile D and

sU phosphoramidite monomers. Pc means pseudo-complementary

Syntheses of bisPac-protected D SNA and L-*a*TNA phosphoramidite monomers

The syntheses of SNA and L-*a*TNA phosphoramidite monomers (23 and 24) of bisPac-protected D

began from compound 1 (Scheme 3-4). Briefly, the two amino groups were phenoxyacetylated to

afford 17. The *N*9 was then alkylated using *t*-butyl bromoacetate in the presence of K_2CO_3, followed

by removal of the *t*-butyl ester group to yield 18. Compounds 21 and 22 were obtained by

condensation of compound 19 with either compound 6 or compound 20, respectively. Finally,

compounds 21 and 22 were converted to phosphoramidites 23 and 24, respectively, as previously

described.

Scheme 3-4. Syntheses of bisPac-protected D-SNA and L-*a*TNA phosphoramidites
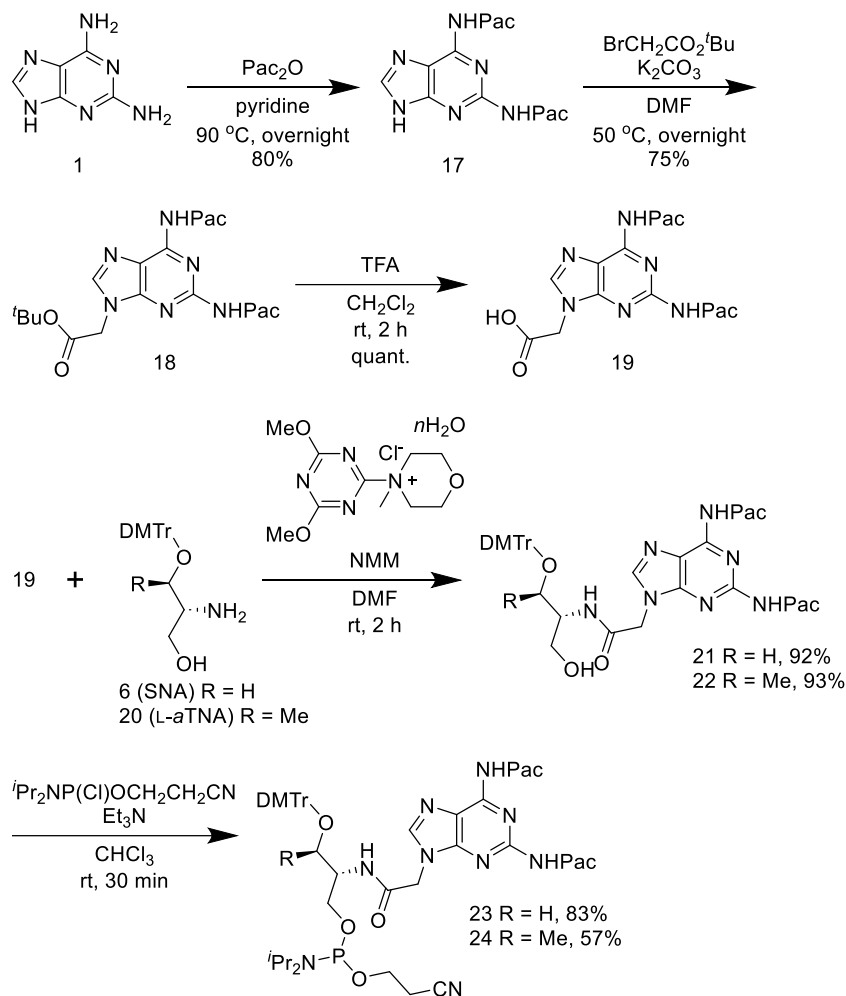
Syntheses of Aob-sU SNA and L-*a*TNA phosphoramidite monomers

We synthesized Aob-sU SNA and L-*a*TNA phosphoramidite monomers according to scheme 3-4.

Briefly, the thiocarbonyl group of sU was protected with 4-(chloromethyl)phenyl acetate (28)

synthesized from 4-hydroxybenzaldehyde (25) to afford compound 16. The compound 29 was

alkylated with *t*-butyl bromoacetate in the presence of Et₃N to yield compound 30, followed by

deprotection to yield the carboxylic acid 31. Compounds 32 and 33 were obtained by condensing

compound 31 with compound 6 or with compound 20, respectively. Compounds 32 and 33 were then

converted to phosphoramidites respectively.

Scheme 3-4. Syntheses of Aob-protected sU-SNA and L-*a*TNA phosphoramidites
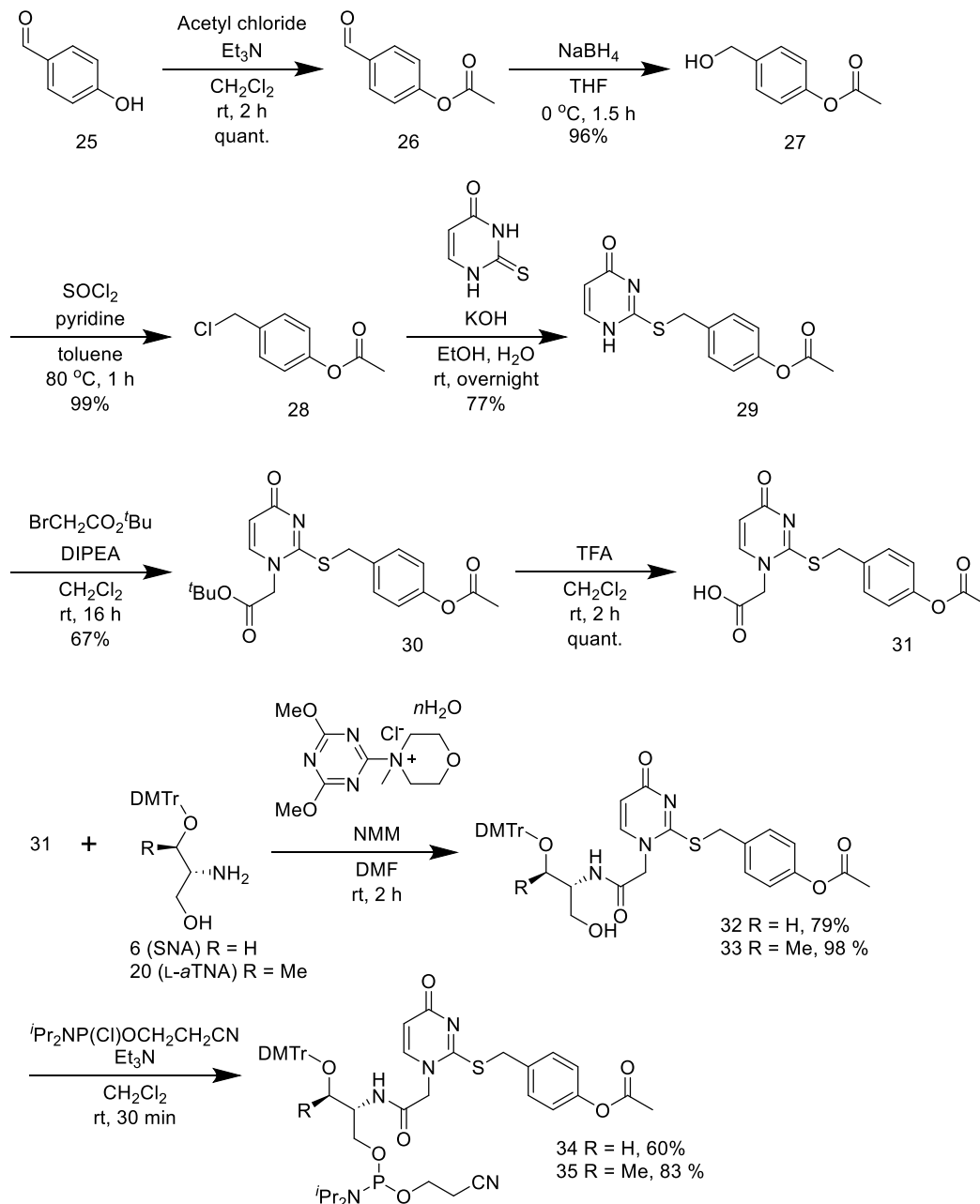
Syntheses of SNA and L-*a*TNA with D and sU monomers

First, we checked the compatibility of new D and sU monomers with solid-phase synthesis through

conventional phosphoramidite-based oligonucleotide synthesis. We synthesized oligomers

incorporated a D or sU into poly-dT strand, 5'-d(TTTTTTTTTTT)-(SNA-D)-d(TT)-3' and 5'-DMTr-d(TTTTTTTTTTT)-(SNA-sU)-d(TT)-3'. Then, we analyzed MS profiles of their crude products. The standard capping reagent, 20% acetic anhydride in acetonitrile and 16% 1-methylimidazole in tetrahydrofuran, replaced slightly the either of the Pac groups on D with an acetyl group (Figure 3-11). For suppressing this replacement, we decided to use phenoxyacetic anhydride in THF/pyridine as the capping reagent instead of 20% acetic anhydride in acetonitrile. Pac groups on D were deprotected perfectly under 28% aqueous ammonia at 55 °C for 3 h, which showed sufficient deprotection efficiency.
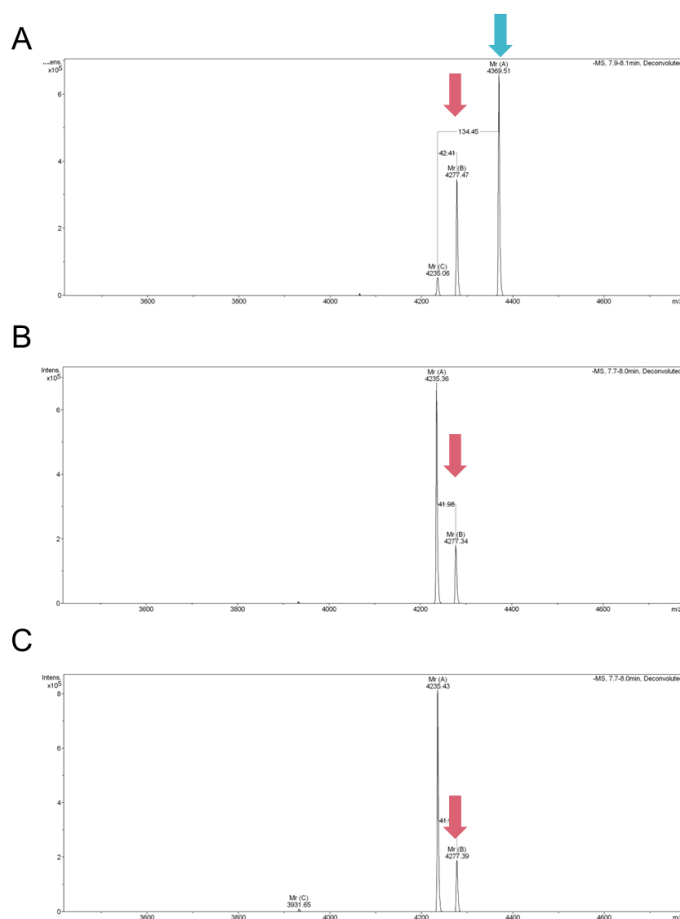
Figure 3-11. ESI-MS profiles of crude product 5'-d(TTTTTTTTTTT)-(SNA-D)-d(TT)-3'. Calculated masses are [M-H]-: 4232.71.

Acetyl anhydrous in THF/pyridine was used as capping reagent. The crude product was obtained after incubation with 28% aqueous

ammonia (A) at room temperature for 20 min, (B) at 55 °C for 3 h, or (C) at 55 °C for 5 h. Red arrow shows product with acetyl group.

Blue arrow shows product with phenoxyacetyl group.

Incubation of the DNA oligonucleotide containing Aob-protected sU-SNA in 28% ammonium

hydroxide, the standard deprotection solution, resulted in some impurities (Figure 3-12 A). The

impurities were presumed to be acrylonitrile and/or *p*-quinone methide adducts. To suppress the

generation of these adducts, we decided to add sodium hydrosulfide (NaSH) to 28% ammonium

hydroxide solution as a scavenger of acrylonitrile and *p*-quinone methide. As a results, NaSH

addition suppressed generation of impurities (Figure 3-12 B).
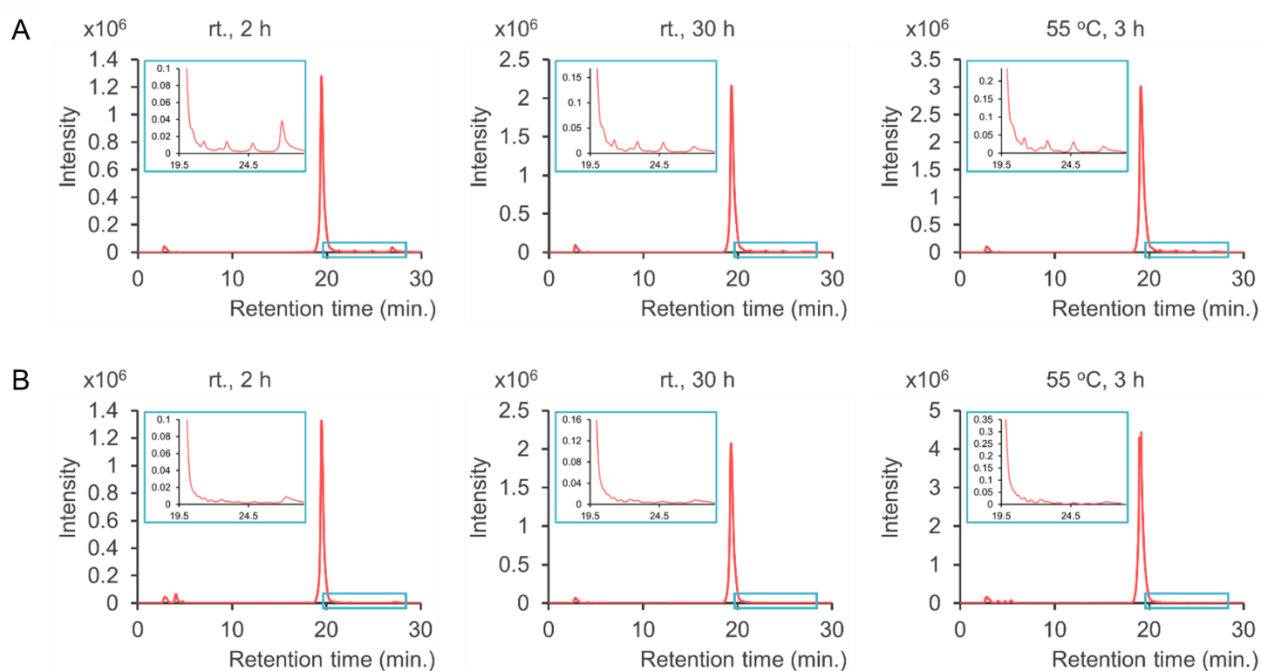
Figure 3-12. HPLC profiles of crude products 5'-DMTr-d(TTTTTTTTTTT)-(SNA-sU)-d(TT)-3'. The samples were obtained after

incubation in (a) 28% aqueous ammonia or (b) 28% aqueous ammonia containing 50 mM NaSH for 2 h at room temperature, for 30 h

at room temperature, or for 3 h at 55 oC. Blue boxes indicate products with acrylonitrile or p-quinone methide.

In short, as describing to scheme 3-5, for syntheses of SNA and L-*a*TNA oligomer bearing only D

residues, capping reagent, 20% acetic anhydride in acetonitrile must be replaced with 5%

phenoxyacetic anhydride in THF/puridine. And for syntheses of SNA and L-*a*TNA oligomer bearing

only sU residues, NaSH addition is recommended for improving yields of oligomer and difficulty of

purification, and conventional capping reagent can be used. For syntheses of SNA and L-*a*TNA oligomer bearing both D and sU residues, modification to capping reagent and deprotection solution is need. As mentioned above, using modified phosphoramidite synthesis method, we could obtain SNA and L-*a*TNA oligomers bearing D and sU with good yield comparable to one without D and sU (Table 3-2).

Scheme 3-5. Preparation of pseudo-complementary SNA or L-*a*TNA using bisPac-D-SNA or bisPac-D-L-*a*TNA phosphoramidite monomers and Aob-sU-SNA or Aob-sU-L-*a*TNA phosphoramidite monomers.
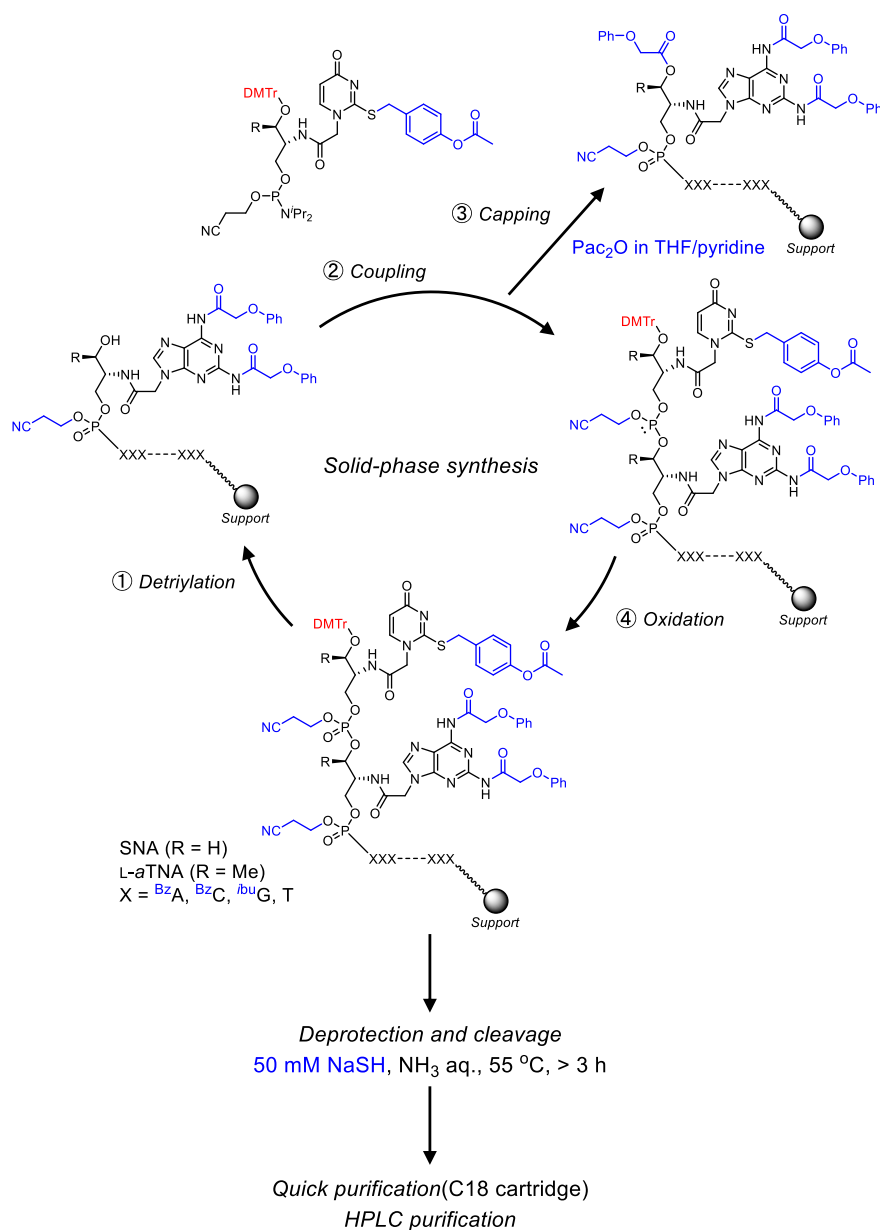
Table 3-2 Yields of SNA and L-*a*TNA oligomers

	Sequence	Yield(%)
SNA	(*S*)-TACTGCAGTA-(*R*)	20
	(*S*)-TDCsUGCDGsUA-(*R*)	17
L-*a*TNA	3'-TACTGCAGTA-1'	26
	3'-TDCsUGCDGsUA-1'	18

Moreover, as shown HPLC profiles of the crude products after pre-purification by C18 cartridge and purified products, the crude products have few impurities, which mean purification dramatically became easier than one synthesized by previous scheme (figure 3-13).
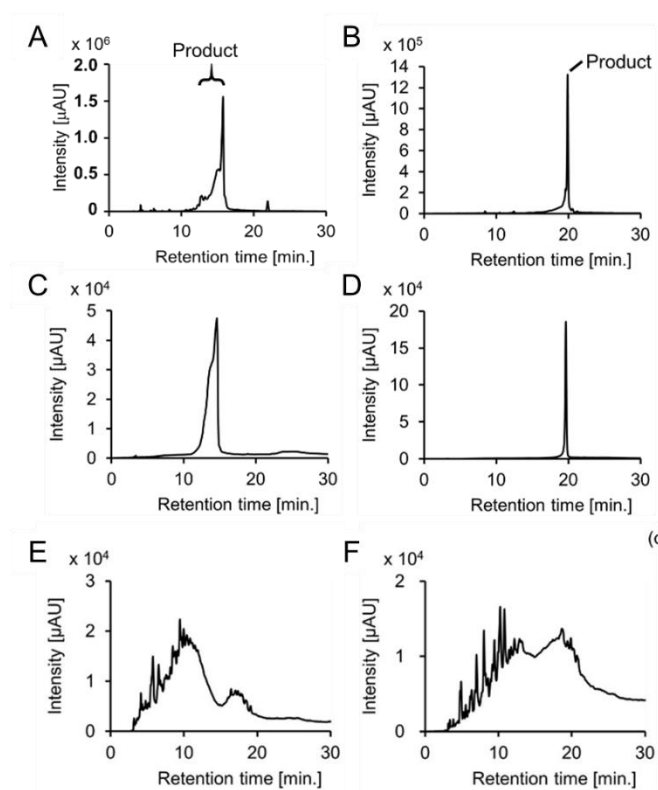
Figure 3-13. (A, B) HPLC trace of detritylated crude (A) SNA, (*S*)-TDCsUGCDGsUA-(*R*), and (B) L-*a*TNA, 3'-TDCsUGCDGsUA-1'. (C, D) HPLC traces of purified (C) SNA and (D) L-*a*TNA. (E, F) Crude HPLC profiles of (E) SNA and (F) L-*a*TNA oligonucleotides synthesized by the acid-labile protecting scheme.

Finally, we measured T_m values to conform D-sU base-pairs could decrease self-association in both cases SNA and L-*a*TNA (figure 3-14). Synthesized SNA and L-*a*TNA oligomer are palindromic sequences.
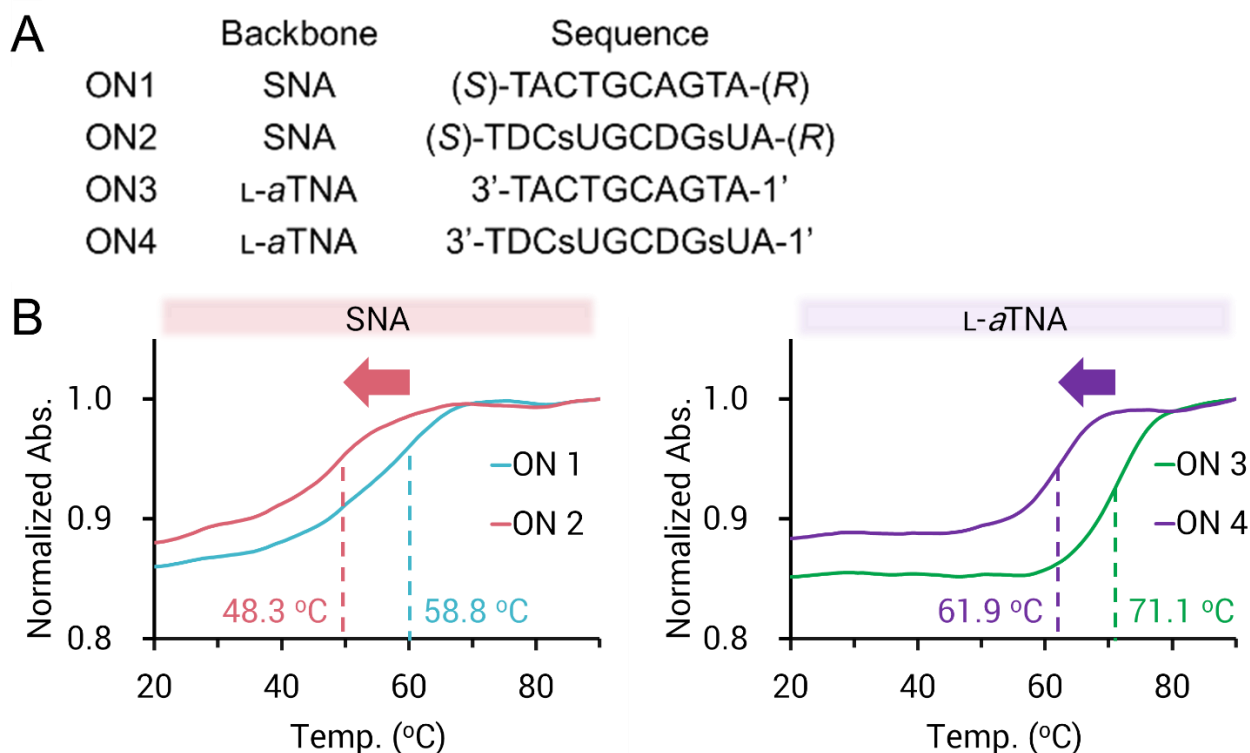
Figure 3-14 (A) Sequences of SNA and L-*a*TNA. (B) Melting curves of ONs in absence of the complementary RNA. Solution conditions for T_m measurements were 100 mM NaCl, 10 mM phosphate buffer (pH 7.0), 2.0 μM oligonucleotide.

As shown in figure 3-14, by D-sU introduction, 10 mer length palindromic SNA and L-*a*TNA decrease them T_ms for about 10 °C, which means D-sU introduction into SNA and L-*a*TNA can also decrease self-affinity.

Finally, we concluded we successfully synthesized novel D and sU SNA and L-*a*TNA phosphoramidite monomers which are compatible with standard phosphoramidite modified slightly.

3-4 Conclusions

We carried out optimization of D and sU phosphoramidite design. We succeeded synthesized bisPac-protected D-SNA and L-*a*TNA phosphoramidites, and Aob-protected sU-SNA and L-*a*TNA phosphoramidites which are compatible with conventional phosphoramidite-based solid-phase synthesis slightly modified. In addition, we proved that introduction D and sU into palindromic oligonucleotide of SNA and L-*a*TNA inhibit them self-hybridization and promote hybridization with the complementary RNA from T_m measurements of SNA and L-*a*TNA oligomers bearing D and sU residues.

3-5 Experimental Section

Materials

Materials for general synthetic procedures. All chemicals were obtained from Combi-Blocks Inc., Kishida Chemical Co., Ltd., Tokyo Kasei Co., Ltd., and Wako Pure Chemical Industries, Ltd. and were used without further purification. Reagents for oligonucleotide synthesis and Poly Pak II cartridges were purchased from Glen Research. Anhydrous and HPLC-grade solvents for SNA and L-*a*TNA synthesis and chromatography were purchased from Kanto Chemical Co., Ltd.. In all cases, silica gel column chromatography was performed with silica gel 60, spherical, particle size 63-210 μm purchased from Kanto Chemical Co., Ltd.. Reactions performed at elevated temperature were performed using a temperature-controlled oil bath. ^{1}H, ^{13}C, and ^{31}P NMR spectra were recorded on a BRUKER Ascend™ 500. Chemical shift values are expressed in values (ppm) relative to internal tetramethylsilane (0.00 ppm), residual CHCl$_3$ (7.26 ppm), or DMSO (2.50 ppm) for ^{1}H NMR and chloroform-*d*1 (77.16 ppm) or DMSO-*d*6 (39.52 ppm) for ^{13}C{^{1}H} NMR. ^{31}P NMR, values (ppm) were not standardized. Multiplicities are described as s (singlet), d (doublet), t (triplet), q (quartet), m (multiplet), and br s (broad singlet). HRMS of compounds were measured on a JMS-700 MStation.

Syntheses and purification of SNA and L-*a*TNA oligonucleotides bearing D and sU

RNAb and SNAa are obtained from Fasmac and Hokkaido System Science Co. Ltd.. SNA and L-*a*TNA were synthesized using an ABI-3400 DNA synthesizer (Applied Biosystems) or NTS M-8-SE DNA/RNA synthesizer (NIHON TECHNO SERVICE CO., Ltd.) using SNA and L-*a*TNA phosphoramidites bearing ^{Bz}A, ^{Bz}C, ^{iBu}G, T, and corresponding D or sU phosphoramidites. Amino lcaa CPG, 500 Å (ChemGenes), tethering T-SNA, ^{Bz}A-SNA, or ^{Bz}A-L-*a*TNA were used as solid supports for oligonucleotide synthesis. The coupling time was changed to 6 min and the step was repeated. As an activator, 0.25 M 5-[3,5-bis(trifluoromethyl)-phenyl]-1*H*-tetrazole in MeCN was used. For detritylation, 3% trichloroacetic acid in CH_2Cl_2, 3% dichloroacetic acid in CH_2Cl_2 were used (detritylation time: 60 s). For capping, 20% acetic anhydride in acetonitrile or 5% phenoxyacetic anhydride in THF/pyridine and 16% 1*H*-methylimidazole in THF were used (capping time: 65 s). As an oxidant, we used 0.02 M iodine in THF/pyridine/water, CSO oxidizer, or 1.0 M *t*-BuOOH in CH_2Cl_2 (oxidation wait time: 60 s). ^{Bz}A, ^{Bz}C, and T SNA and L-*a*TNA phosphoramidites were used as a 0.075 M solution in MeCN. ^{iBu}G, Boc-potected D-SNA, MMPM-protected sU-SNA, Aob-sU SNA, and Aob-sU L-*a*TNA phosphoramidites were used as 0.1 M solutions in acetonitrile. The bisPac-D SNA and L-*a*TNA phosphoramidites were used as 0.1 M solutions in CH_2Cl_2.

For deprotection of Boc group and MMPM group on SNA oligomers, after solid-phase synthesis, CPG-conjugated SNA oligonucleotides were incubated with TFA (13.9 % *m*-cresol and 2.8 % H_2O) at rt for 3 h before aqueous ammonia treatment solution. After TFA treatment CPG-conjugated SNA oligonucleotides were washed. After drying up, cleavage and deprotection were conducted under 28 % aqueous ammonia solution at 55 °C for 4 h.

  For deprotection of all other protecting groups on SNA and L-*a*TNA oligomer bearing no Boc-protected D-SNA and MMPM-protected sU, cleavage from supports and deprotection were conducted under 28 % aqueous ammonia solution at 55 °C for 4 to 6 h. In the case of oligomers having Aob-sU, NaSH was added to ammonia solution. Then, pre-putification was done by Poly Pak

II cartridges according to manufacturer's protocol (trityl-off on the cartridge). Then, all synthesized oligomers were purified by reversed phase HPLC (Kanto Chemical, Mightysil RP 18 GP II column), and characterized by MALDI-TOF MS or ESI-MS.

Measurements of T_m.

Oligonucleotides of SNA or L-*a*TNA with or without RNA (2 µM) were dissolved in 10 mM sodium phosphate buffer (pH 7.0) with 100 mM NaCl. The melting curves were obtained with a Shimazu UV-1800 by measuring the change in absorbance at 260 nm versus temperature. T_m curves were measured with a temperature ramp of 1.0 $^\circ$C min^{-1}. T_m values were determined from the maximum in the first derivative of the melting curve.

Native-MS measurement

The SNAa-sU2 and RNAb oligonucleotides were buffer-exchanged into 100 mM Triethylammonium acetate, pH 7.0 by passing the oligonucleotides through Bio-Rad Micro Bio-Spin 6 columns. The buffer-exchanged oligonucleotides were immediately analyzed by nanoflow electrospray ionization mass spectrometry using gold-coated glass capillaries made in house (approximately 3 µL sample loaded per analysis). Spectra were recorded on a Waters SYNAPT G2-Si HDMS mass spectrometer in negative ionization mode at 1.13 kV with 150 V sampling cone voltage and source offset voltage, 4 V trap and 2 V transfer collision energies, and 5 mL/min trap gas flow. The spectra were calibrated using 2 mg/mL cesium iodide dissolved in 50% 2-propanol and analyzed using MassLynx software (Waters).

Native-PAGE analysis

25 µM of RNAb, SNAa-sU2, and mixture of RNAb and SNAa-sU2 in 10 mM phosphate buffer (pH 7.0) containing 100 mM NaCl was heated to 80 °C and then cooled to 4 °C. Loading buffer without

47

bromophenol blue was mixed with the sample and the mixture was analyzed using 20 %

polyacrylamide gel containing 10% glycerol at 750 CV for 2 h. The temperature of electrophoresis

apparatus was kept at 4 °C during the electrophoresis. The gels were stained with Fast BlastTM DNA

stain (Biorad). The gel image was captured by FLA9500 (GE healthcare). In the lane of mixture

of SNAa-sU2 and RNAb, the band corresponding to the unknown complex was observed.

Synthesis of phosphoramidite monomer of Boc-protected 2,6-diaminopurine SNA

Synthesis of compound 2: 2,6-Diaminopurine (compound **1**) (5 g, 33.3 mmol) and DMAP (0.61g, 5

mmol) was dissolved in THF (150 mL) under nitrogen atmosphere. Boc_2O (61.2 g, 64.4 mL) was

added to this solution at 0 °C. After 5 min of stirring at 0 °C, the mixture was stirring at room

temperature for 18 h. Then, the solvent was removed by evaporation. Subsequently the residue was

dissolved with $CHCl_3$, then mixed with H_2O. Organic layer was dried over $MgSO_4$. The solvent was

removed, and the residue was subjected to silica gel column chromatography (hexane/EtOAc, 10:3)

to afford 17.6 g, 27 mmol compound **2** (yield 81%).

^1H NMR [$CDCl_3$, 500 MHz] δ= 8.55 (s, 1H), 1.70 (s, 9H), 1.45 (s, 18H), 1.43 (s, 18H). $^{13}C\{^1H\}$

NMR [$CDCl_3$, 125 MHz] δ= 153.92, 153.06, 151.78, 150.80, 149.90, 145.77, 144.01, 128.02, 87.43,

84.06, 83.40, 28.01, 27.91, 27.76. HRMS (FAB): Calcd for compound **2** $[M + H]^+$, 651.3348; found

651.3371.

Synthesis of compound 3: Compound **2** (17.6g, 27 mmol) was dissolved in AcOEt (400 mL) and

then washed with 1 N HCl (30 mL) and saturated solution of NaCl. The organic layer was dried over

$MgSO_4$, and the solvent was removed by evaporation and dried *in vacuo.* The mixture was dissolved

in MeOH (200 mL), and $NaHCO_3$ solution (90 mL) was added. The reaction mixture was placed in

an oil bath at 50 °C and stirred for 1 h. After the reaction was complete, MeOH was removed by

evaporation and H_2O (100 mL) was added. $CHCl_3$ (50 mL) was added, and the organic layer was

collected; the extraction was repeated three times. The organic layers were pooled and dried over

MgSO$_4$, and the residual solvent was removed *in vacuo*. The residue was subjected to silica gel column chromatography (hexane/EtOAc, 2:1 to 100% EtOAc) to afford 14.3 g, 26.0 mmol compound **3** (yield 96%).

^{1}H NMR [CDCl$_3$, 500 MHz] δ= 8.38 (s, 1H), 1.49 (s, 18H), 1.44 (s, 18H). ^{13}C{^{1}H} NMR [CDCl$_3$, 125 MHz] δ= 151.54, 151.13, 150.95, 150.03, 84.22, 83.45, 27.86, 27.70. HRMS (FAB) Calcd for compound **3** [M + H]$^+$, 551.2824; found 551.2829.

Synthesis of compound 4: Compound **3** (14.3 g, 26.0 mmol) and K$_2$CO$_3$ (1.15 eq, 4.0 g, 29.9 mmol) was suspended in dry DMF (60 mL) under nitrogen atmosphere. Ethyl bromoacetate (1.1 eq, 3.16 mL, 28.6 mmol) was added stepwise into the mixture at 0 ºC and stirred for 10 min. Then mixture was stirred at room temperature for 20 h. The reaction solution was co-evaporated with toluene and then H$_2$O (150 mL) was added. CHCl$_3$ (100 mL) was added, and the organic layer collected; the extraction was repeated three times. The collected organic layers were washed with H$_2$O and dried over MgSO$_4$, and the solvent was dried *in vacuo*. The residue was subjected to silica gel column chromatography (CHCl$_3$/MeOH, 40:1) to afford 14.6 g, 22.9 mmol compound **4** (yield 88%).

^{1}H NMR [CDCl$_3$, 500 MHz] δ= 8.18 (s, 1H), 5.04 (s, 2H,), 4.29-4.24 (dd, 2H), 1.42 (s, 18H), 1.41 (s, 18H), 1.32-1.28 (t, 3H). ^{13}C{^{1}H} NMR [CDCl$_3$, 125 MHz] δ= 166.69, 154.38, 152.35, 151.18, 150.85, 150.00, 145.92, 126.94, 83.84, 83.36, 62.49, 44.47, 27.88, 27.75, 14.16. HRMS (FAB): Calcd for compound **4** [M + H]$^+$, 637.3192; found 637.3197.

Synthesis of compound 5: Compound **4** (14.6 g, 23 mmol) was dissolved in MeOH (120 mL), 1,4-dioxane (40 mL). Then 2 N NaOH solution (40 mL) was added, and the solution was stirred for 10 min on ice. After the reaction was complete, the pH of the solution was adjusted to 3 by addition of 2 N HCl, and the solvent was removed by evaporation. After extraction with AcOEt three times, the organic layer was washed with H$_2$O, then dried over MgSO$_4$, and the solvent was removed *in vacuo*. The crude product (compound **5**) was used in the next step without further purification (quantitative yield).

^{1}H NMR [CDCl$_3$, 500 MHz] δ= 8.46 (s, 1H), 5.07 (s, 2H), 1.41 (s, 18H), 1.40 (s, 18H). ^{13}C{^{1}H} NMR [CDCl$_3$, 125 MHz] δ= 168.76, 154.31, 152.28, 150.94, 150.59, 149.97, 147.20, 126.28, 84.08, 83.61, 44.54, 27.85, 27.74. HRMS (FAB): Calcd for compound **5** [M + H]$^+$, 609.2879; found 609.2900.

Synthesis of compound 7: Compound **5** (5.4 g, 8.8 mmol) was dissolved in DMF and then coupled with 3.15 g (8.0 mmol) of compound 6 in the presence of Et$_3$N (3.0 eq) and DMT-MM (1.2 eq). After the reaction, the mixture was diluted with CHCl$_3$, and the organic layer was washed with saturated NaHCO$_3$. The mixture was dried over MgSO$_4$. The solvent was removed, and the residue was subjected to silica gel column chromatography (CHCl$_3$/MeOH, 30:1 to 10:1 including 3% Et$_3$N) to afford 7.44g (7.6 mmol) of compound **7** (yield 94%).

^{1}H NMR [CDCl$_3$, 500 MHz] δ=8.19 (s, 1H), 7.40-7.20 (m, 9H), 6.84-6.81 (m, 4H), 6.58-6.55 (d, 1H), 4.87-4.80 (dd, 2H), 4.20-4.10 (m, 1H), 3.85-3.80 (m, 1H), 3.78 (s, 6H), 3.70-3.65 (m, 1H), 3.33-3.30 (m, 1H), 3.28-3.21 (m, 1H), 1.40 (s, 18H), 1.39 (s, 18H). ^{13}C{^{1}H} NMR [CDCl$_3$, 125 MHz] δ=165.28, 162.69, 158.69, 154.38, 152.11, 151.13, 151.09, 150.09, 146.44, 144.62, 135.79, 130.08, 130.03, 128.12, 128.05, 127.07, 113.35, 86.58, 83.98, 83.67, 62.53, 62.41, 55.31, 51.55, 46.16, 27.91, 27.77. HRMS (FAB): Calcd for compound **7** [M + H]$^+$, 984.473; found 984.4686.

Synthesis of compound 8: Compound **7** (6.46 g, 6.56 mmol) was dissolved in dry CH$_2$Cl$_2$ (7 mL) and Et$_3$N (4.55 mL) and cooled on ice under nitrogen. Then 2.2 mL (7.84 mmol) of 2-cyanoethyl *N,N*-diisopropylchlorophosphoramidite was added dropwise. After a 20-min incubation at room temperature, the reaction mixture was diluted with CHCl$_3$. The crude mixture was subjected to silica gel column chromatography (hexane/AcOEt, 4:1 to 1:1 including 3% Et$_3$N) to afford 4.81 g (4.06 mmol) of compound **8** (yield 62%).

^{1}H NMR [CDCl$_3$, 500 MHz] δ=8.23-8.19 (d, 1H), 7.43-7.20 (m, 9H), 6.85-6.82 (m, 4H), 6.37, (m, 1H), 4.93-4.73 (m, 2H), 4.40-4.20 (m, 1H), 4.00-3.80 (m, 2H), 3.79(s, 6H), 3.70-3.60 (m, 1H), 3.61-

3.52 (m, 2H), 3.42-3.35 (m, 1H), 3.21-3.15 (m, 1H), 2.70-2.40 (m, 2H), 1.41 (s, 18H), 1.39 (s, 18H), 1.20-1.10 (m, 12H). $^{13}C\{^1H\}$ NMR [CDCl$_3$, 125 MHz] δ=164.77, 158.58, 154.41, 152.05, 150.84, 150.03, 146.58, 146.48, 144.73, 144.63, 135.91, 135.83, 135.75, 130.13, 130.09, 130.07, 130.04, 128.16, 128.11, 127.93, 126.94, 126.80, 118.59, 118.48, 113.23, 113.20, 86.29, 86.27, 83.73, 83.72, 83.28, 83.24, 65.86, 61.45, 58.54, 58.44, 58.40, 58.29, 55.26, 50.43, 50.37, 45.55, 45.46, 43.18, 43.08, 30.95, 27.82, 27.71, 24.68, 24.62, 20.62, 20.60, 20.60, 20.56, 15.31. ^{31}P NMR [CDCl3, 202 MHz] δ= 148.15, 147.71. HRMS (FAB): Calcd for compound **8** [M + H]$^+$, 1184.5792; found 1184.5794.

Synthesis of MMPM-protected thiouracil SNA monomer

Synthesis of compound 10: Compound **9** (2.03 g, 12.8 mmol) was dissolved in EtOH (32 mL) and then NaBH$_4$ was added. The mixture was stirred at room temperature for 5 min. After the reaction was completed, H$_2$O (240 mL) was added into the solution. pH of the solution was adjusted to 4 using 4 N HCl, then organic layer was extracted with diethyl ether three times and dried over MgSO$_4$. The solvent was dried *in vacuo*, and the obtained crude product (compound **10**) was used in the next step without further purification (quantitative yield).

^1H NMR [CDCl$_3$, 500 MHz] δ= 7.22-7.20 (d, 1H), 6.74-6.69 (m, 2H), 4.60 (s, 2H), 3.78 (s, 3H), 2.35 (s, 3H), 1.66 (s, 1H). $^{13}C\{^1H\}$ NMR [CDCl$_3$, 125 MHz] δ= 158.82, 137.70, 131.14, 129.17, 115.91, 110.47, 62.41, 54.94, 18.66. HRMS (FAB): Calcd for compound **10** [M + H]$^+$, 152.08373; found 152.0837.

Synthesis of compound 12: Compound **10** (1.93 g, 12.7 mmol) was dissolved in dry CH$_2$Cl$_2$ under nitrogen atmosphere. PBr$_3$ was added into the solution stepwise at 0 °C over a 2.5 h period, and then the solution was stirred for 15 min. Cold NaHCO$_3$ and ice were mixed with the reaction solution. The organic layer was extracted with diethyl ether three times, and the pooled organic layers were dried

over MgSO₄, and the solvent was removed *in vacuo*. The obtained crude product (compound **11**) was used in the next step without further purification (quantitative yield).

2-Thiouracil (833 mg, 6.50 mmol) was dissolved in EtOH (8 mL). An aliquot of 1 N KOH solution (8 mL) was added into the solution and incubated at 45 °C then cooled to room temperature. Compound **11** dissolved in EtOH (5 mL) was added into the solution stepwise and stirred at room temperature overnight. After the reaction was completed, the reaction solution was mixed with saturated NaHCO₃ solution (15 mL). The precipitate was collected by filtration and washed with H₂O, EtOH, EtOAc, and Et₂O, then dried *in vacuo* to yield 1.24 g (4.71 mmol) of compound **12** (yield 72%).

^{1}H NMR [CDCl₃, 500 MHz] δ= δ= 7.91 (s, 1H), 7.30-7.27 (d, 1H), 6.79-6.77 (d, 1H), 6.72-6.69 (m, 1H), 6.12 (s, 1H), 4.35 (s, 2H), 3.71 (s, 3H), 2.31 (s, 3H). ^{13}C{^{1}H} NMR [CDCl₃, 125 MHz] δ= 158.76, 138.18, 131.24, 125.91, 115.83, 111.32, 55.01, 31.88, 19.04. HRMS (FAB): Calcd for compound **12** [M + H]⁺, 263.0849; found 263.0844.

Synthesis of compound 13: Compound **12** (1.24 g, 4.71 mmol) was dissolved in dry EtOH, and then NaOEt (2.0 eq., 20% in EtOH) was added. The solution was refluxed and mixed with BrCH₂CO₂Et (2.0 eq.) at 90 °C. The solution was refluxed at 90 °C for 2 h. After cooling to room temperature, EtOH was removed by evaporation, then saturated NaHCO₃ solution (30 mL) was added. The solution was extracted with CH₂Cl₂ and MeOH (3:1) three times, and the pooled organic layers were dried over MgSO₄, and the solvent was removed *in vacuo*. The crude mixture was subjected to silica gel column chromatography (hexane/AcOEt, 5:1 to 1:1, AcOEt, AcOEt/MeOH, 9:1) to afford 0.63 g (1.81 mmol) of compound **13** (yield 38%).

^{1}H NMR [CDCl₃, 500 MHz] δ= 7.27-7.24 (m, 2H), 6.73-6.71 (m, 1H), 6.70-6.67 (m, 1H), 6.078-6.05 (d, 1H), 4.56 (s, 2H), 4.46 (s, 2H), 4.24-4.22 (dd, 2H), 3.77 (s, 3H), 2.34 (s, 3H), 1.27-1.24 (t, 3H). ^{13}C{^{1}H} NMR [CDCl₃, 125 MHz] δ= 167.91, 166.03, 163.40, 159.54, 144.06, 138.89, 131.83,

124.27, 116.24, 111.44, 109.88, 62.63, 55.21, 52.83, 34.87, 19.51, 14.01. HRMS (FAB): Calcd for compound **13** [M + H]$^+$, 349.1217; found 349.1233.

Synthesis of compound 14: Compound **13** (0.63 g, 1.81 mmol) was dissolved with MeOH (4.7 mL), THF (11.1 mL), 2 N LiOH (1.6 mL) and stirred at room temperature for 10 min. The solvent was removed by evaporation, and the precipitate was collected by filtration. The crude product was washed with AcOEt and Et$_2$O. The crude product (compound **14**) was used in the next step without further purification (quantitative yield).

^{1}H NMR [CDCl$_3$, 500 MHz] δ= 7.52-7.51 (d, 1H), 7.45-7.43 (d, 1H), 7.31-7.28 (d, 1H), 6.78-6.76 (d ,1H), 6.72-6.68 (m, 1H), 5.82- 5.80 (d,1H), 5.72-5.69 (d, 1H), 4.28 (s, 2H), 4.10 (s, 2H), 4.05 (s, 1H), 3.79 (s 2H), 3.71 (s, 2H), 2.31 (s, 3H), 1.66 (s, 3H). ^{13}C{^{1}H} NMR [CDCl$_3$, 125 MHz] δ=175.82, 170.59, 168.50, 167.28, 167.90, 162.26, 158.81, 156.59, 146.39, 145.05, 138.36, 131.43, 125.71, 115.82, 111.34, 107.70, 106.63, 55.78, 55.05, 54.78, 53.26, 32.85, 25.22, 19.13. HRMS (FAB): Calcd for compound **14** [M + Li]$^+$, 327.09853; found 327.0988.

Synthesis of compound 15: Compound **14** (0.57g, 1.67 mmol) was dissolved in DMF and then coupled with 0.64 g (1.6 eq) of compound **6** (2.59 mmol, dissolved in DMF) in the presence of Et$_3$N (3.0 eq) and DMT-MM (1.8 eq). After the reaction, the mixture was diluted with CHCl$_3$, and the organic layer was washed with saturated NaHCO$_3$. The mixture was dried over MgSO$_4$. The solvent was removed, and the residue was subjected to silica gel column chromatography (CHCl$_3$/MeOH, 20:1 to 10:1 including 2 % Et$_3$N) to afford 0.65 g (0.93 mmol) of compound **15** (yield 56%).

^{1}H NMR [CDCl$_3$, 500 MHz] δ= 7.37-7.35 (m, 2H), 7.27-7.00 (m, 10H), 6.79-6.76 (m 4H), 6.66-6.64 (d, 1H), 6.58-6.55 (m, 1H), 5.98-5.96 (d, H), 4.47-4.40 (dd, 2H), 4.35-4.20 (dd, 2H), 4.14 (m, 1H), 3.78-3.73 (m, 10H), 3.69-3.65 (m, 1H), 3.29-3.19 (m, 2H), 2.20 (s, 3H). ^{13}C{^{1}H} NMR [CDCl$_3$, 125 MHz] δ=168.53, 164.87, 163.95, 159.59, 158.69, 158.67, 144.76, 144.68, 138.97, 135.83, 135.72, 131.92, 130.14, 130.05, 128.12, 128.03, 127.04, 124.32, 116.35, 113.34, 111.51, 109.71, 86.51,

62.71, 55.34, 54.44, 52.05, 46.13, 34.99, 19.55. HRMS (FAB): Calcd for compound **15** $[M + H]^+$, 696.2738; found 696.2768.

Synthesis of compound 16: Compound **15** (0.92 g, 1.32 mmol) was dissolved in dry CH_2Cl_2 (5 mL) and Et_3N (0.9 mL) and cooled on ice under nitrogen. Then 0.44 mL (1.98 mmol) of 2-cyanoethyl *N,N*-diisopropylchlorophosphoramidite was added dropwise. The crude mixture was subjected to silica gel column chromatography ($CHCl_3$/acetone, 4:1 to 2:1 including 3 % Et_3N) to afford 0.78 g (0.87 mmol) of compound **16** (yield 66 %).

[^1]H NMR [$CDCl_3$, 500 MHz] δ=7.40-7.38 (m, 2H), 7.30-7.18 (m, 9H), 7.11-7.07 (d, 1H), 6.81-6.78 (m, 4H), 6.69-6.66 (m, 1H), 6.65-6.59 (m, 1H), 6.43-6.38 (m, 1H), 6.03-6.036(m, 1H), 4.51-4.29 (m, 5H), 3.93-3.85 (m, 1H), 3.77 (m, 10H), 3.56-3.45 (m, 3H), 3.35-3.25 (m, 1H), 3.18-3.12 (m, 1H), 2.52-2.35 (m, 2H), 2.26-2.25 (m, 3H), 1.15-1.05 (m, 12H). [^13]C{[^1]H} NMR [$CDCl_3$, 125 MHz] δ= 164.77, 158.58, 154.41, 152.05, 150.84, 150.03, 146.58, 146.48, 144.73, 144.63, 135.91, 135.83, 135.75, 130.13, 130.09, 130.07, 130.04, 128.16, 128.11, 127.93, 126.94, 126.80, 118.59, 118.48, 113.23, 113.20, 86.29, 86.27, 83.73, 83.72, 83.28, 83.24, 65.86, 61.45, 58.54, 58.44, 58.40, 58.29, 50.43, 50.37, 45.55, 45.46, 43.18, 43.08, 30.95, 27.82, 27.71, 24.68, 24.62, 20.62, 20.60, 20.56, 15.31. [^31]P NMR [$CDCl_3$, 202 MHz] δ= 148.03, 147.76. HRMS (FAB): Calcd for compound **16** $[M + H]^+$, 896.3817; found 896.3824.

Syntheses of bisPac-protected D-SNA/L-*a*TNA phosphoramidite monomers

Synthesis of compound 17. 2,6-Diaminopurine (compound **1**; 6.00 g, 40.0 mmol) and phenoxyacetic anhydride (TCI, 25.0 g, 87.3 mmol) were dissolved in pyridine (250 ml) under a N_2 atmosphere. The mixture was stirred at 90 °C overnight. After cooling to 4 °C, the mixture filtered and washed with pyridine, EtOH, and Et_2O, then dried *in vacuo* to yield compound **17** as a white solid (13.5 g, 32.2 mmol, 80%). [^1]H NMR [DMSO-*d*6, 500 MHz] δ 12.36 (br s, 1H), 11.12 (br s, 1H), 10.48 (s, 1H), 8.33 (s, 1H), 7.30 (m, 4H), 6.99-6.93 (m, 6H), 5.08 (s, 2H), 5.04 (s, 2H). [^13]C{[^1]H}

NMR [DMSO-$d6$, 125 MHz] δ 168.6, 167.7, 158.0, 157.8, 151.4, 129.5, 129.4, 121.1, 120.9, 114.54, 114.48, 67.4, 66.8. HRMS (FAB): Calcd for $C_{21}H_{19}N_6O_4$ [M + H]$^+$, 419.1462; found, 419.1474.

Synthesis of compound 18. Compound **17** (13.5 g, 32.2 mmol) and K_2CO_3 (4.90 g, 35.4 mmol) were suspended in dry DMF (150 mL) under a N_2 atmosphere. *Tert*-butyl bromoacetate was added to the suspension at room temperature, and then the mixture was stirred at 50 °C overnight. The reaction solution was co-evaporated with toluene   and suspended in EtOH (100 ml) at 4 °C. The precipitate was collected by filtration and washed with H_2O, EtOH, and Et_2O which had been cooled to 4 °C, then dried *in vacuo* to yield compound **18** as a white solid (12.8 g, 24.0 mmol, 75%). ^{1}H NMR [DMSO-$d6$, 500 MHz] δ 10.93 (s, 1H), 10.70 (s, 1H), 8.32 (s, 1H), 7.26 (m, 4H), 6.97-6.92 (m, 6H), 5.23 (s, 2H), 5.11 (s, 2H), 5.01 (s, 2H), 1.41 (s, 9H). ^{13}C{^{1}H} NMR [DMSO-$d6$, 125 MHz] δ 168.2, 166.6, 158.01, 157.95, 152.8, 151.8, 148.9, 144.1, 129.4, 120.9, 120.8, 118.1, 114.6, 114.5, 82.4, 67.9, 67.6, 44.8, 27.6. HRMS (FAB): Calcd for $C_{27}H_{29}N_6O_6$ [M + H]$^+$, 533.2143; found, 533.2128.

Synthesis of compound 19. Compound **18** (12.8 g, 24.0 mmol) was dissolved in CH_2Cl_2 (90 ml) and trifluoroacetic acid (180 ml). The mixture was stirred at room temperature for 2 h and then evaporated to dryness under reduced pressure. The resultant solid was suspended in Et_2O (200 ml). The product was collected by filtration and then dried *in vacuo* to yield compound **19** as a white solid (12.7 g, quant.). ^{1}H NMR [DMSO-$d6$, 500 MHz] δ 13.44 (br s, 1H), 10.98 (s, 1H), 10.76 (s, 1H), 8.35 (s, 1H), 7.29-7.25 (m, 4H), 6.98-6.92 (m, 6H), 5.24 (s, 2H), 5.10 (s, 2H), 5.04 (s, 2H). ^{13}C{^{1}H} NMR [DMSO-$d6$, 125 MHz] δ 169.0, 168.5, 168.1, 158.0, 157.9, 152.9, 151.8, 148.8, 144.2, 129.4, 120.9, 120.8, 118.1, 114.6, 114.5, 67.8, 67.5, 44.3. HRMS (FAB): Calcd for $C_{23}H_{21}N_6O_6$ [M + H]$^+$, 477.1517; found, 477.1551.

Synthesis of compound 21. Compound **19** (3.14 g, 6.60 mmol) was suspended in DMF (40 ml) and then coupled with compound **6** (2.35 g, 6.00 mmol) in the presence of *N*-methylmorpholine (NMM) (1.98 ml, 18.0 mmol) and (4-(4,6-dimethoxy-1,3,5-triazin-2-yl)-4-methyl-morpholinium chloride

(DMT-MM) *n*-hydrate (10.8 mmol, 1.8 eq). After the reaction was complete, H_2O (200 ml) was added, the mixture was filtered, and the precipitate was washed with H_2O. The residue was diluted in $CHCl_3$, co-evaporated with MeCN, and then purified by silica gel column chromatography ($CHCl_3$:MeOH, 30:1 (v/v), then $CHCl_3$:MeOH, 20:1 (v/v) pretreated with 2% Et_3N) to afford compound **21** as a white solid (4.72 g, 5.54 mmol, 92%). ^{1}H NMR [DMSO-*d*6, 500 MHz] δ 10.96 (s, 1H), 10.65 (s, 1H), 8.34 (d, 1H), 8.28 (s, 1H), 7.38 (d, 2H), 7.31-7.19 (m, 11H), 6.98-6.86 (m, 10H), 5.24 (s, 2H), 5.08 (s, 2H), 4.94 (s, 2H), 4.78 (s, 1H), 4.03 (m, 1H), 3.73 (s, 6H), 3.55 (s, 2H), 3.02 (m, 2H). ^{13}C{^{1}H} NMR [DMSO-*d*6, 125 MHz] δ 168.4, 168.2, 165.8, 158.02, 157.97, 153.0, 151.7, 148.7, 145.0, 144.7, 135.7, 129.7, 129.42, 129.37, 127.8, 127.7, 126.6, 120.9, 120.7, 118.1, 114.6, 114.5, 113.2, 85.3, 67.9, 67.5, 62.3, 60.5, 55.0, 51.4, 45.1. HRMS (FAB): Calcd for $C_{47}H_{46}N_7O_9$ [M + H]$^+$, 852.3352; found, 852.3346.

Synthesis of compound 22. Compound **19** (1.60 g, 3.35 mmol) was suspended in DMF (40 ml) and then coupled with compound **20** (1.24 g, 3.05 mmol) in the presence of NMM (1.01 ml, 9.15 mmol) and DMT-MM *n*-hydrate (5.49 mmol, 1.8 eq). After the reaction was complete, H_2O (200 ml) was added, the mixture was filtered, and the precipitate was washed with H_2O. The residue was dissolved in $CHCl_3$, co-evaporated with MeCN, and then purified by silica gel column chromatography ($CHCl_3$:MeOH, 30:1 (v/v), then $CHCl_3$:MeOH, 20:1 (v/v) pretreated with 2% Et_3N) to afford compound **22** as a white solid (2.45 g, 2.83 mmol, 93 %). ^{1}H NMR [DMSO-*d*6, 500 MHz] δ 10.95 (s, 1H), 10.67 (s, 1H), 8.31 (s, 1H), 8.20 (d, 1H), 7.46 (d, 2H), 7.34-7.23 (m, 11H), 7.23 (t, 1H), 6.98-6.85 (m, 10H), 5.23 (s, 2H), 5.11 (s, 2H), 5.01 (s, 2H), 4.53 (s, 1H), 3.80 (m, 1H), 3.73 (s, 6H), 3.64-3.59 (m, 1H), 3.53-3.47 (m, 2H), 0.64 (d, 3H). ^{13}C{^{1}H} NMR [DMSO-*d*6, 125 MHz] δ 168.5, 168.1, 166.2, 158.02, 157.97, 153.0, 151.7, 148.7, 146.6, 144.8, 136.8, 136.7, 130.1, 129.42, 129.38, 127.9, 127.6, 126.5, 120.9, 120.7, 118.2, 114.6, 114.5, 113.0, 85.5, 68.8, 67.8, 67.5, 60.3, 56.0, 55.0, 45.1, 17.4. HRMS (FAB): Calcd for $C_{48}H_{48}N_7O_9$ [M + H]$^+$, 866.3508; found, 866.3514.

Synthesis of compound 23. 2-Cyanoethyl-*N*,*N*-diisopropylphosphoramidochloridite (Fujifilm Wako Pure Chemical Industries, Ltd. >80%, 0.85 ml, 3.63 mmol, 1.5 eq) was added to a solution of compound **21** (2.06 g, 2.42 mmol) and triethylamine (1.34 ml, 9.68 mmol, 4.0 eq) in dry chloroform (40 ml) at 0 °C under a N_2 atmosphere. After stirring at room temperature for 30 min, the mixture was concentrated, and the residue was purified using silica gel column chromatography (CHCl$_3$:AcOEt, 2:1 (v/v), then CHCl$_3$:AcOEt, 1:1 (v/v)   including 2% Et$_3$N) to afford compound **23** as a white solid (2.10 g, 2.00 mmol, 83%). ^{1}H NMR [DMSO-*d*6, 500 MHz] δ 10.93 (s, 1H), 10.61 (s, 1H), 8.41-8.39 (m, 1H), 8.26 (d, 1H), 7.38-7.35 (m, 2H), 7.31-7.19 (m, 11H), 6.97-6.85 (m, 10H), 5.22 (s, 2H), 5.07 (s, 2H), 4.96-4.88 (m, 2H), 4.20-4.10 (m, 1H), 3.76-3.55 (m, 10H), 3.53-3.44 (m, 2H), 3.11-3.00 (m, 2H), 2.96-2.65 (m, 2H), 1.10 (dd, 6H), 1.03 (dd, 6H). ^{13}C{^{1}H} NMR [DMSO-*d*6, 125 MHz] δ 168.4, 165.9, 158.1, 157.97, 157.96, 152.9, 151.7, 148.8, 144.9, 144.6, 135.5, 129.72, 129.68, 129.42, 129.35, 127.8, 127.6, 126.7, 120.9, 120.7, 118.9, 118.1, 114.6, 114.4, 113.1, 85.38, 85.37, 67.8, 67.5, 61.9, 61.8, 61.7, 58.4, 58.33, 58.29, 58.2, 55.0, 50.2, 45.1, 42.5, 42.4, 24.3, 19.9, 19.8. ^{31}P NMR [DMSO-*d*6, 202 MHz] δ 146.9, 146.6. HRMS (FAB): Calcd for $C_{56}H_{63}N_9O_{10}P$ [M + H]$^+$, 1052.4430; found, 1052.4473.

Synthesis of compound 24. 2-Cyanoethyl-*N*,*N*-diisopropylphosphoramidochloridite (Fujifilm Wako Pure Chemical Industries, Ltd. >80%, 1.00 ml, 4.07 mmol, 1.5 eq) was added to a solution of compound **22** (2.35 g, 2.71 mmol) and triethylamine (1.50 ml, 10.8 mmol, 4.0 eq) in dry chloroform (40 ml) at 0 °C under a N2 atmosphere. After stirring at room temperature for 30 min, the mixture was concentrated, and the residue was purified using silica gel column chromatography (CHCl$_3$:AcOEt, 2:1 (v/v), then CHCl$_3$:AcOEt, 1:1 (v/v) including 2% Et$_3$N) to afford compound **24** as a white solid (1.65 g, 1.56 mmol, 57%). ^{1}H NMR [DMSO-*d*6, 500 MHz] δ 10.93 (s, 1H), 10.63 (s, 1H), 8.32 (dd, 2H), 7.46 (dd, 2H), 7.36-7.24 (m, 10H), 7.12 (t, 1H), 6.98-6.85 (m, 10H), 5.23 (s, 2H), 5.12 (s, 2H), 5.02 (dd, 2H), 3.97-3.88 (m, 1H), 3.74-3.59 (m, 10H), 3.55-3.42 (m, 3H), 2.67 (dt, 2H), 1.12 (dd, 6H), 1.04 (dd, 6H), 0.70 (dd, 3H). ^{13}C{^{1}H} NMR [DMSO-*d*6, 125 MHz] δ 168.6, 166.7,

166.6, 158.5, 158.5, 158.4, 153.4, 152.1, 149.2, 147.0, 146.8, 145.2, 137.0, 136.9, 136.9, 130.54, 130.48, 129.9, 129.8, 128.3, 128.0, 127.02, 126.97, 121.3, 121.2, 119.4, 118.6, 115.0, 114.9, 113.4, 86.1, 86.0, 69.3, 68.9, 68.3, 68.0, 59.0, 58.9, 58.7, 55.5, 42.93, 42.90, 42.84, 42.80, 24.83, 24.78, 24.7, 20.3, 20.3, 18.1, 17.9. ^{31}P NMR [DMSO-d6, 202 MHz] δ 147.0, 146.9. HRMS (FAB): Calcd for $C_{57}H_{65}N_9O_{10}P$ [M + H]$^+$, 1066.4587; found, 1066.4605.

Syntheses of Aob-protected sU-SNA/L-*a*TNA phosphoramidite monomers

Synthesis of compound 26. 4-Hydroxybenzaldehyde (compound 25; 12.2 g, 100 mmol) was dissolved in CH_2Cl_2 (200 ml) and triethylamine (41.9 ml, 300 mmol, 3.0 eq). Acetyl chloride (10.7 ml, 150 mmol, 1.5 eq) were added stepwise to the solution of compound **25** at 0 ºC under a N_2 atmosphere. After the mixture was stirred for 2 h, 1 N HCl aq. (50 ml) was added to the mixture and stirred for 20 min. The organic phase was washed twice with 1 N HCl aq. (50 ml), dried over $MgSO_4$, concentrated, and then dried *in vacuo* to yield compound **26** as a brown oil (21.6 g, quant.). ^{1}H NMR [CDCl$_3$, 500 MHz] δ 9.99 (s, 1H), 7.92 (d, 2H), 7.28 (d, 2H), 2.34 (s, 3H). ^{13}C{^{1}H} NMR [CDCl$_3$, 125 MHz] δ 191.0, 168.8, 155.5, 134.2, 131.4, 122.5, 21.3. HRMS (FAB): Calcd for $C_9H_9O_3$ [M + H]$^+$, 165.0546; found, 165.0570.

Synthesis of compound 27. NaBH$_4$ (5.67 g, 150 mmol) was added to compound **26** (100 mmol) dissolved in THF (150 ml) at 0 ºC. After stirring at 0 ºC for 1.5 h, EtOAc (150 ml) and satd. aq. NH$_4$Cl (100 ml) were added stepwise to the mixture. The organic phase was washed with satd. aq. NH$_4$Cl (100 ml) and was dried over $MgSO_4$. After removal of $MgSO_4$ by filtration, the solution was evaporated and dried *in vacuo* to yield compound **27** as a yellow oil (16.0 g, 96 mmol, 96%). ^{1}H NMR [CDCl$_3$, 500 MHz] δ 7.37 (d, 2H), 7.07 (m, 2H), 4.67 (s, 2H), 2.30 (s, 3H). ^{13}C{^{1}H} NMR [CDCl$_3$, 125 MHz] δ 169.7, 150.2, 138.7, 128.2, 121.8, 64.9, 21.2. HRMS (FAB): Calcd for $C_9H_{11}O_3$ [M + H]$^+$, 167.0703; found, 167.0679.

Synthesis of compound 29. Compound **27** (16.0 g, 96.3 mmol) was dissolved in dry toluene (100 ml) with dry pyridine (0.1 ml) under a N_2 atmosphere. The mixture was heated to 80 $^{\circ}$C with stirring, followed by the addition of $SOCl_2$ (12.0 ml, 164 mmol, 1.7 eq), and the solution was stirred at 80 $^{\circ}$C for 1 h. After cooling to 0 $^{\circ}$C, satd. aq. $NaHCO_3$ (200 ml) and crashed ice were added to the reaction solution. The organic phase was washed twice with H_2O (100 ml), dried over $MgSO_4$, filtered, and then evaporated under reduced pressure. The obtained crude compound **28** (17.7 g, 95.8 mmol, 99%) was used in the next step without further purification. 2-Thiouracil (6.34 g, 49.4 mmol) was suspended in EtOH (60 ml). KOH (>85%, 3.61 g, 54.7 mmol) in H_2O (60 ml) was added to the solution and incubated at 45 $^{\circ}$C to dissolve 2-thiouracil, then cooled to room temperature. Compound **28** was added dropwise to the 2-thiouracil solution and stirred at room temperature overnight. The reaction solution was then evaporated under reduced pressure and satd. aq. $NaHCO_3$ (50 ml) and H_2O (100 ml) were added. The precipitate was collected by filtration and washed with H_2O, EtOH, EtOAc, and Et_2O, then dried *in vacuo* to yield compound **29** as a white powder (10.5 g, 38.1 mmol, 77%). ^{1}H NMR [DMSO-*d*6, 500 MHz] δ 12.71 (br s, 1H), 7.91 (d, 1H), 7.44 (m, 2H), 7.07 (m, 2H), 6.14 (d, 1H), 4.41 (s, 2H), 2.25 (s, 3H). ^{13}C{^{1}H} NMR [DMSO-*d*6, 125 MHz] δ 169.2, 149.6, 134.8, 130.1, 121.8, 33.0, 20.8. HRMS (FAB): Calcd for $C_{13}H_{13}N_2O_3S$ $[M + H]^+$, 277.0641; found, 277.0615.

Synthesis of compound 30. Compound **29** (10.5 g, 38.1 mmol) was suspended in dry CH_2Cl_2 (20 ml) and *N,N*-diisopropylethylamine (7.12 ml, 41.9 mmol, 1.1 eq). *Tert*-butyl bromoacetate (6.15 ml, 41.9 mmol, 1.1 eq) was added to the solution at 0 $^{\circ}$C and stirred for 16 h at room temperature. After the stirring, H_2O (140 ml) was added to the mixture, and the mixture was stirred for 10 min. The organic phase was washed with H_2O and brine, dried over $MgSO_4$, filtered, and then evaporated under reduced pressure. The residue was purified using silica gel column chromatography ($CHCl_3$:MeOH, 30:1 (v/v) then $CHCl_3$:MeOH, 20:1 (v/v)) to afford compound **30** as a white solid (10.0 g, 25.6 mmol, 67%). ^{1}H NMR [CDCl$_3$, 500 MHz] δ 7.41 (d, 2H), 7.06 (d, 2H), 7.03 (m, 2H),

6.11 (d, 1H), 4.51 (s, 2H), 4.38 (s, 2H), 2.29 (s, 3H), 1.45 (s, 9H). ^{13}C{^{1}H} NMR [CDCl$_3$, 125 MHz] δ 169.6, 167.8, 164.9, 162.8, 150.4, 143.9, 133.2, 130.7, 122.0, 110.3, 84.7, 53.8, 35.8, 28.0, 21.3. HRMS (FAB): Calcd for C$_{19}$H$_{23}$N$_2$O$_5$S [M + H]$^+$, 391.1322; found, 391.1367.

Synthesis of compound 31. Compound **30** (10.0 g, 25.6 mmol) was dissolved in CH$_2$Cl$_2$ (90 ml) and trifluoroacetic acid (180 ml). The mixture was stirred at room temperature for 2 h, and then the solvent was evaporated under reduced pressure. The resultant solid was suspended in Et$_2$O (200 ml). The product was collected by filtration and then dried *in vacuo* to yield compound **31** as a white solid (10.0 g, quant.). ^{1}H NMR [DMSO-*d*6, 500 MHz] δ 13.57 (br s, 1H), 7.68 (d, 1H), 7.45 (d, 2H), 7.07 (d, 2H), 5.93 (d, 1H), 4.69 (s, 2H), 4.42 (s, 2H), 2.25 (s, 3H). ^{13}C{^{1}H} NMR [DMSO-*d*6, 125 MHz] δ 169.2, 168.4, 166.5, 162.1, 149.8, 145.7, 134.1, 130.3, 121.9, 108.6, 52.6, 33.9, 20.8. HRMS (FAB): Calcd for C$_{15}$H$_{15}$N$_2$O$_5$S [M + H]$^+$, 335.0696; found, 335.0686.

Synthesis of compound 32. Compound **31** (2.94 g, 8.80 mmol, 1.1 eq) was suspended in DMF (40 ml) and then coupled with compound **6** (3.15 g, 8.00 mmol) in the presence of NMM (2.64 ml, 24 mmol, 3.00 eq) and DMT-MM *n*-hydrate (14.4 mmol, 1.8 eq). After the reaction, H$_2$O (200 ml) was added to the mixture, and solid was collected by filtration and was further washed with H$_2$O. The residue was dissolved in CHCl$_3$, co-evaporated with MeCN, and then purified using silica gel column chromatography (CHCl$_3$:MeOH, 30:1 (v/v), then CHCl$_3$:MeOH, 20:1 (v/v) including with 2% Et$_3$N) to afford compound **32** as a white solid (4.51 g, 6.35 mmol, 79%). ^{1}H NMR [CDCl$_3$, 500 MHz] δ 7.38 (d, 2H), 7.28-7.23 (m, 10H), 7.17 (q, 2H), 7.09 (d, 1H), 6.91 (d, 2H), 6.79 (d, 4H), 5.93 (d, 1H), 4.37 (q, 2H), 4.32 (q, 2H), 4.15 (m, 1H), 3.78-3.74 (m, 7H), 3.65 (dd, 1H), 3.27 (m, 2H), 2.25 (s, 3H). ^{13}C{^{1}H} NMR [CDCl$_3$, 125 MHz] δ 169.9, 168.5, 164.8, 163.2, 158.7, 150.3, 144.9, 144.7, 135.81, 135.79, 133.2, 130.6, 130.14, 130.11, 128.2, 128.0, 127.1, 122.0, 113.3, 109.9, 86.5, 62.7, 62.6, 55.4, 54.4, 45.8, 35.7, 21.2. HRMS (FAB): Calcd for C$_{39}$H$_{40}$N$_3$O$_8$S [M + H]$^+$, 710.2531; found, 710.2513.

Synthesis of compound 33. Compound **19** (3.42 g, 10.2 mmol, 1.1 eq) was suspended in DMF (50 ml) and then coupled with compound **20** (3.79 g, 9.30 mmol) in the presence of NMM (3.07 ml, 27.9 mmol, 3.0 eq) and DMT-MM n-hydrate (16.7 mmol, 1.8 eq). After the reaction was complete, H_2O (250 ml) was added to the mixture, and the precipitate was collected by filtration and was washed with H_2O. The residue was dissolved in $CHCl_3$, co-evaporated with MeCN, and then purified using silica gel column chromatography ($CHCl_3$:MeOH, 20:1 (v/v), then $CHCl_3$:MeOH, 10:1 (v/v) including with 2% Et_3N) to afford compound **33** as a white solid (6.60 g, 9.12 mmol, 98%). ^1H NMR [$CDCl_3$, 500 MHz] δ 7.42 (d, 2H), 7.35-7.28 (m, 6H), 7.23-7.13 (m, 5H), 6.95 (q, 2H), 6.79 (m, 2H), 6.00 (d, 1H), 4.48 (q, 2H), 4.39 (q, 2H), 3.89-3.82 (m, 1H), 3.76 (d, 6H), 3.62 (dd, 2H), 3.56 (m, 1H), 3.51 (dd, 1H), 2.26 (s, 3H), 0.89 (d, 3H). $^{13}C\{^1H\}$ NMR [$CDCl_3$, 125 MHz] δ 169.8, 168.4, 165.4, 163.1, 158.73, 158.71, 150.3, 146.1, 145.0, 136.8, 136.4, 133.1, 130.6, 130.5, 130.3, 128.2, 127.0, 122.0, 113.3, 113.2, 109.9, 86.7, 69.7, 63.1, 56.8, 55.3, 54.5, 35.8, 21.2, 19.0. HRMS (FAB): Calcd for $C_{40}H_{42}N_3O_8S$ $[M + H]^+$, 724.2687; found, 724.2681.

Synthesis of compound 34. 2-Cyanoethyl-N,N-diisopropylphosphoramidochloridite (Fujifilm Wako Pure Chemical Industries, Ltd. >80%, 2.13 ml, 9.53 mmol, 1.5 eq) was added to a solution of compound **32** (4.51 g, 6.35 mmol) and triethylamine (3.54 ml, 25.4 mmol, 4.0) in dry CH_2Cl_2 (30 ml) at 0 °C under a N_2 atmosphere. After stirring at room temperature for 30 min, the mixture was concentrated, and the residue was purified using silica gel column chromatography ($CHCl_3$:$(CH_3)_2CO$, 6:1 (v/v), then $CHCl_3$:$(CH_3)_2CO$, 4:1 (v/v) including with 2% Et_3N) to afford compound **34** as a white solid (3.45 g, 3.79 mmol, 60%). ^1H NMR [$CDCl_3$, 500 MHz] δ 7.40 (d, 2H), 7.31-7.25 (m, 8H), 7.22-7.18 (m, 1H), 7.13 (dd, 1H), 6.98-6.95 (m, 2H), 6.84-6.80 (m, 4H), 6.44 (dd, 1H), 6.05 (dd, 1H), 4.45-4.29 (m, 5H), 3.92-3.45 (m, 12H), 3.36-3.28 (m, 1H), 3.19-3.15 (m, 1H), 2.54-2.36 (m, 2H), 2.28 (d, 3H), 1.17-1.06 (m, 12H). $^{13}C\{^1H\}$ NMR [$CDCl_3$, 125 MHz] δ 169.54, 169.51, 167.9, 164.4, 164.3, 162.81, 162.77, 158.7, 150.3, 144.8, 144.7, 144.3, 144.2, 135.94, 135.86, 135.8, 133.0, 133.0, 130.7, 130.21, 130.17, 128.2, 128.02, 128.00, 127.0, 123.0, 122.0,

118.9, 113.3, 110.1, 86.3, 62.6, 62.5, 61.8, 61.7, 58.6, 58.5, 58.43, 58.36, 55.38, 55.37, 54.3, 54.2, 50.63, 50.57, 50.5, 43.2, 43.1, 35.9, 24.8, 24.7, 21.3 20.80, 20.76, 20.73, 20.69. ^{31}P NMR [CDCl$_3$, 202 MHz] δ 147.9, 147.6. HRMS (FAB): Calcd for C$_{48}$H$_{57}$N$_5$O$_9$PS [M + H]$^+$ 910.3609; found, 910.3628.

Synthesis of compound 35. 2-Cyanoethyl-*N*,*N*-diisopropylphosphoramidochloridite (Fujifilm Wako Pure Chemical Industries, Ltd. >80%, 3.06 ml, 13.7 mmol) was added to a solution of compound **33** (6.60 g, 9.12 mmol) and triethylamine (5.06 ml, 36.5 mmol, 4.0 eq) in dry CH$_2$Cl$_2$ (30 ml) at 0 ºC under a N$_2$ atmosphere. After stirring at room temperature for 30 min, the mixture was concentrated, and the residue was purified using silica gel column chromatography (CHCl$_3$:(CH$_3$)$_2$CO, 6:1 (v/v), then CHCl$_3$:(CH$_3$)$_2$CO, 4:1 (v/v) including 2% Et$_3$N) to afford compound **35** as a white solid (7.01 g, 7.59 mmol, 83%). ^{1}H NMR [CDCl$_3$, 500 MHz] δ 7.44 (d, 2H), 7.36-7.30 (m, 6H), 7.22 (m, 2H), 7.18-7.12 (m, 2H), 6.97 (d, 2H), 6.82-6.73 (m, 5H), 6.04 (dd, 1H), 4.50-4.37 (m, 4H), 4.02-3.95 (m, 1H), 3.80-3.57 (m, 11H), 3.54-3.44 (m, 3H), 2.52-2.45 (m, 2H), 2.26 (s, 3H), 1.13 (dd, 6H), 1.06 (dd, 6H), 0.91 (dd, 3H). ^{13}C{^{1}H} NMR [CDCl$_3$, 125 MHz] δ 169.4, 167.9, 164.6, 164.5, 162.7, 158.52, 158.49, 150.2, 146.3, 146.2, 144.54, 144.50, 136.8, 136.5, 132.8, 130.5, 130.42, 130.40, 130.3, 128.13, 128.11, 127.7, 126.8, 121.9, 121.8, 118.5, 113.04, 113.01, 109.9, 109.8, 86.3, 69.0, 68.9, 62.8, 62.63, 62.56, 62.45, 58.4, 58.34, 58.26, 58.2, 55.50, 55.45, 55.2, 54.3, 54.2, 43.0, 42.9, 35.8, 24.61, 24.59, 24.55, 21.1, 20.52, 20.48, 20.45, 18.7, 18.6. ^{31}P NMR [CDCl$_3$, 202 MHz] δ 147.9, 147.3. HRMS (FAB): Calcd for C$_{49}$H$_{59}$N$_5$O$_9$PS [M + H]$^+$, 924.3766; found, 924.3797.

3-6 References

[1] H. Kashida, K. Murayama, T. Toda, and H. Asanuma, *Angew. Chem., Int. Ed.*, **2011**, *50*, 1285-1288.

[2] K. Murayama, H. Kashida, and H. Asanuma, *Chem. Commun.*, **2015**, *51*, 6500-6503.

[3] F. B. Howard, H. T. Miles, *Biochemistry*, **1984**, *23*, 6723-6732.

[4] Y. Lebedev, N. Akopyants, T. Azhikina, Y. Shevchenko, V. D. Potapov, B. E. Stecenko, D. Berg, E. Sverdlov, *Genet. Anal. Biomol. Eng.*, **1996**, *13*, 15-21.

[5] B. A. Connolly, and P. C. Newman, *Nucleic Acids Res.*, **1989**, *17*, 4957-4974.

[6] P. C. Newman, V. U. Nwosu, D. M. Williams, R. Cosstick, F. Seela, and B. A. Connolly, *Biochemistry*, **1990**, *29*, 9891-9901,

[7] R. G. Kuimelis and K. P. Nambiar, *Nucleic Acids Res.*, **1994**, *22*, 1429-1436.

[8] F. Seela and K. Mersmann, *Helv. Chim. Acta*, **1993**, *76*, 1435-1449.

[9] I. V. Kutyavin, *et al.*, *Nucleic Acids Res.*, **2002**, *30*, 4952-4959.

[10] M. R. Dunn, A. C. Larsen, W. J. Zahurancik, N. E. Fahmi, M. Meyers, Z. Suo and J. C. Chaput, *J. Am. Chem. Soc.*, **2015**, *137*, 4014-4017.

[11] T. Hara, T. Kodama, Y. Takegaki, K. Morihiro, K. R. Ito and S. Obika, *J. Org. Chem.*, **2017**, *82*, 25-36.

[12] H. Mei, J. Y. Liao, R. M. Jimenez, Y. Wang, S. Bala, C. McCloskey, C. Switzer and J. C. Chaput, *J. Am. Chem. Soc.*, **2018**, *140*, 5706-5713.

[13] D. R. Mills and F. R. Kramer, *Proc. Natl. Acad. Sci. U. S. A.*, **1979**, *76* , 2232-2235.

[14] H. B. Gamper, Jr., A. Gewirtz, J. Edwards and Y. M. Hou, *Biochemistry*, **2004**, *43*, 10224-10236.

[15] M. Hibino, Y. Aiba, and O.Shoji, *Chem. Commun.*, **2020**, *56*, 2546-2549.

[16] R. K. Kumar and D. R. Davis, *J. Org. Chem.*, **1995**, *60*, 7726-7727.

[17] I. Okamoto, K. Seio, M. Sekine, *Tetrahedron Lett.*, **2006**, *47*, 583-585.

[18] A. P. Guzaev, *Tetrahedron Lett.*, **2011**, *52*, 434-437.

[19] D. Ackermann and M. Famulok, *Nucleic Acids Res.*, **2013**, *41*, 4729-4739.

[20] T. Sugiyama, G. Hasegawa, C. Niikura, K. Kuwata, Y. Imamura, Y. Demizu, M. Kurihara, and A. Kittaka, *Bioorg. Med. Chem. Lett.*, **2017**, *27*, 3337-3341.

[21] H. Kashida*, *et al.*, *J. Am. Chem. Soc.*, **2018**, *140*, 8456-8462.

[22] E. Sochacka, P. Bartos, K. Kraszewska, B. Nawrot, *Bioorg. Med. Chem. Lett.*, **2013**, *23*, 5803-5805.

[23] F. Sobott, H. Hernandez, M. G. McCammon, M. A. Tito, C. V. Robinson, *Anal. Chem.*, **2002**, *74*, 1402-1407.

[24] M. Nishio, *et al.*, *Proc. Natl. Acad. Sci. U.S.A.*, **2010**, *107*, 4034-4039.

[25] C. Gemmell, G. Janairo, J. Kilburn, H. Ueck, A. Underhill, *J. Chem. Soc.*, *Perkin Trans. 1*, **1994**, 2715-2720.

[26] L. D. Taylor, J. M. Grasshoff, M. Pluhar, *J. Org. Chem.*, **1978**, *43*, 1197-1200,

[27] J. C. Schulhof, D. Molko, and R. Teoule, *Nucleic Acids Res.*, **1987**, *15*, 397-416.

Chapter 4 Anti miRNA oligonucleotides composed of SNA or L-*a*TNA and artificial nucleobases

4-1 abstracts

As shown in chapter 2, SNA-based Anti miR-21 has no miR-21 inhibitory activity because it preferentially forms self-duplex rather than hetero duplex with miR-21. In this chapter, incorporating artificial nucleobases, we suppressed forming SNA-AMO homo duplex and improved its activity.

We designed several AMOs with different numbers of artificial nucleobases. First, we investigated effect of D-sU base pairs to formation of its self-duplex. By measuring melting temperature and Native-PAGE analysis, D-sU base-pair introduction decreased self-association of SNA. Second, we evaluated miR-21 inhibitory activities of AMOs by Luciferase assay

4-2 Introduction

Our group developed functional *acyclic* nucleic acids which can form hetero-duplexes with natural nucleic acids, Serinol nucleic acid(SNA)[1], *acyclic* L-threoninol nucleic acid (L-*a*TNA).[2] SNA and L-*a*TNA are useful for bioapplications through formation of hetero duplexes, such as Moleculer Beacon (MB), and nucleic acid therapeutics.[3~9] Especially, SNA and L-*a*TNA which don't have similar structures with natural nucleic acids have strong nuclease-enzyme resistance,[9] which is important element for activities of nucleic acid drugs. Our group have been reported siRNA and antisense oligonucleotides partially or perfectly composed of SNA or L-*a*TNA.[8~11] As explained in general chapter 1 and chapter 2, we have been trying to develop antisense oligonucleotide against miR-21 composed of SNA or L-*a*TNA.[9] They have a big problem that their stable formation of higher-order structures inhibits to hybridization to miR-21. We mentioned that decrease self-association of SNA and L-*a*TNA improve their miR-21 inhibitory activities and D-sU base pair

introduction would realize it. According to the hypothesis in chapter 3, for phosphoramidite based solid-phase synthesis, we attempted to apply some protecting groups for D and sU to phosphoramidite monomers. As a result, we utilized Pac group to D and Aob, *p*-acetoxybenzyl, group to sU and demonstrated that syntheses and purification of oligomer bearing D and sU through conventional phosphoramidite method modified slightly are done. We expected that D-sU introduction into SNA or L-*a*TNA based anti miR-21 oligonucleotides improve their miR-21 inhibitory activities. In this chapter, we aimed to design optimal SNA or L-*a*TNA based anti miR-21 oligonucleotides bearing D and sU residues *in vitro* and demonstrate their activity *in vivo* study. First, we evaluated miR-21 inhibitory activities of various anti miR-21 bearing D and sU residues by dual luciferase assay, RT-qPCR, and western bloting. Next, we tried to evaluate anti-tumor activities in syngeneic mice.

4-3 Results and discussions

Evaluation of D-sU effects directly

As described in chapter 1, while SNA based anti miR-122 has good activity, SNA based anti miR-21 has no activity. Anti miR-21 oligonucleotides have corresponding self-complementary sequence to the self-complementary sequence of miR-21 and can form homo-duplexes potentially. First, to examine that suppression of self-association of SNA based anti miR-21 improve its activity, we designed SNA based anti miR-21 oligonucleotides having D and sU residues in the self-complementary region (figure 4-1 A). Then, we performed Native-PAGE analysis (figure 4-1 B). S-cD3, AMO having only D residues in self-complementary region, is designed as the model that form stable homo-duplex. S-sU2D3 and S-sU3D3 were done as the model that were suppressed homo-duplex formation. For Native-PAGE analyses, all oligonucleotides were dissolved in incubated at 1 mM phosphate 100 mM NaCl buffer and anneled 95 °C to 4 °C for 1 h. As shown Native-PAGE, in

the case of SNA and S-cD3 without miR-21 sequence, band intensity of homo-duplexes are strong. In contrast, the band intensity decreased depending on the number of D-sU base pairs. In addition, the band intensity of single strand increased with the D-sU base pairs. These data means homo-duplex formation of SNA-based anti miR-21 oligonucleotide was suppressed by D-sU base pair introduction. Therefore, we evaluated miR-21 inhibitory activities (figure 4-1 C)

Figure 4-1 (A) Sequences of miR-21 and SNA based anti miR-21 oligonucleotides. (B) Native-PAGE analysis of SNA based anti miR-21 oligonucleotides in the presence or absence with miR-21. 20 μM oligonucleotidess in 10 mM phosphate buffer (pH 7.0) containing 100 mM NaCl was heated to 95 °C and then cooled to 4 °C. Loading buffer without bromophenol blue was mixed with the sample and the mixture was analyzed using 20 % native PAGE containing 10% glycerol at 750 CV for 2 h. The temperature of electrophoresis apparatus was kept at 5 ~ 10 °C during the electrophoresis. The gels were stained with Fast Blast™ DNA stain (Biorad). The gel image was captured by FLA9500 (GE healthcare). (C) miRNA inhibitory activities in HeLa cells cotransfected 40 nM AMOs and miR-21 reporter plasmid by Lipofectamine 2000. After incubation for 24 h, relative luciferase activity (firefly/Renilla) was evaluated. Luciferase activity in the presence of pmir-GLO, which has no miRNA target region, and oligonucleotide with scramble sequence is set 1.0.

Comparing to S-RD2SD2 and S-sU3D4, introduction of only sU residues into self-complementary region of SNA based anti miR-21 oligonucleotide didn't affect its miR-21 inhibitory activity. S-cD3 has no activity, which is because S-sD3 form stable homo-duplex. On the other hand, introduction of the sets of D and sU dramatically improved their miR-21 inhibitory activity according to the number of D-sU. Moreover, while the number of D residues in S-sU3D3 is smaller the that in S-RD2SD2, S-sU3D3 that is suppressed formation of homo-duplex by D-sU base pairs has higher miR-21 inhibitory activity than S-RD2SD2. These data indicate inhibition of SNA based anti miR-21 oligonucleotide's homo-duplex formation by D-sU directly contributes improvement of their activities. As shown above, we confirmed D-sU effects to self-association of SNA based anti miR-21 oligonucleotides.

Design of SNA or L-*a*TNA based anti miR-21 oligonucleotides involving D-sU base-pairs

Therefore, based on S-D7 sequence, we designed SNA based anti miR-21 oligonucleotides, S-sU1D7, S-sU2D7, and S-sU3D7, which were introduced sU residues into self-complementary region of S-D7. We evaluated their miR-21 inhibitory activities and compared their activities to them of 2'-OMe or tiny-LNA based anti miR-21 oligonucleotides. (figure 4-2)
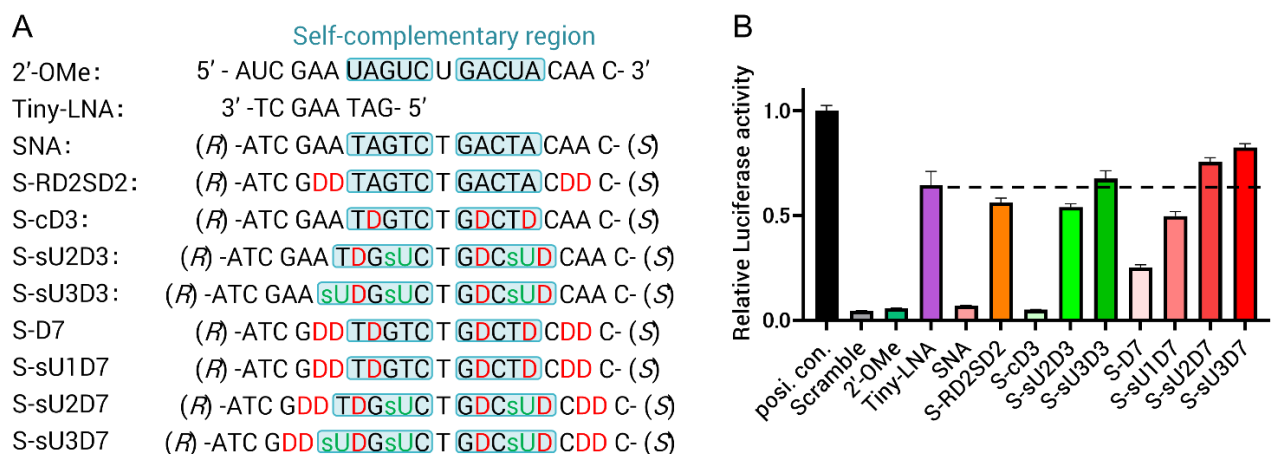
Figure 4-2 (A) Sequences of anti miR-21 oligonucleotides. (B) miRNA inhibitory activities in HeLa cells cotransfected 40 nM AMOs and miR-21 reporter plasmid by Lipofectamine 2000. After incubation for 24 h, relative luciferase activity (firefly/Renilla) was evaluated. Luciferase activity in the presence of pmir-GLO, which has no miRNA target region, and oligonucleotide with scramble sequence is set 1.0.

Like the series of SNA based anti miR-21 oligonucleotides bearing D and/or sU residues, S-D7 based anti miR-21 oligonucleotides, S-sU1D7, S-sU2D7, and S-sU3D7, having sU residues in the self-complementary region dramatically improve their activities in proportion to the number of sU. In addition, S-sU3D7 that has the highest activity in SNA based anti miR-21 oligonucleotides has higher activity than Tiny-LNA. Then, we evaluated the L-*a*TNA based anti miR-21 oligonucleotide, T-sU3D7, having same sequence to S-sU3D7 (figure 4-3). As we described in chapter 1, L-*a*TNA based anti miR-21 oligonucleotide bearing no D and sU also has no activity. T-sU3D7 shows higher activity than S-sU3D7. In summary, D-sU introduction into self-complementary region of SNA or L-*a*TNA based anti miR-21 oligonucleotides suppressed homo-duplex formation and improved dramatically their activities. Both of SNA and L-*a*TNA based anti miR-21 oligonucleotides show superior activity over Tiny-LNA. Moreover, the activity of L-*a*TNA based anti miR-21 is higher than the one of SNA based. *In vitro* study, we successfully designed SNA or L-*a*TNA based anti miR-21 oligonucleotides by introducing D and sU residues.
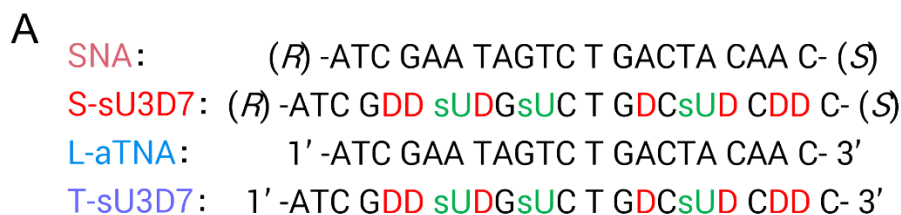
A

SNA: (*R*)-ATC GAA TAGTC T GACTA CAA C- (*S*)

S-sU3D7: (*R*)-ATC GDD sUDGsUC T GDCsUD CDD C- (*S*)

L-aTNA: 1′-ATC GAA TAGTC T GACTA CAA C- 3′

T-sU3D7: 1′-ATC GDD sUDGsUC T GDCsUD CDD C- 3′

B
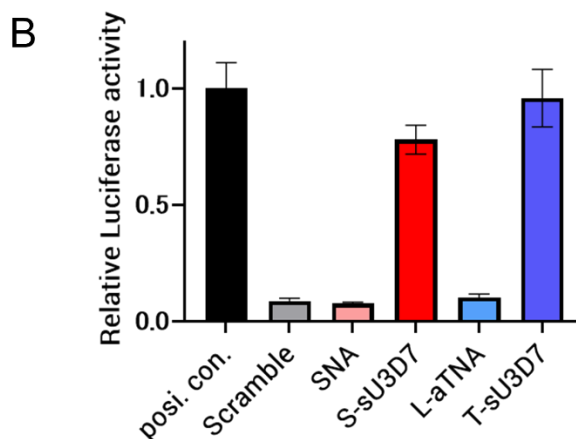
Figure 4-3 (A) Sequences of SNA or L-*a*TNA based anti miR-21 oligonucleotides. (B) miRNA inhibitory activities in B16 cells reverse transfected 0.2 nM AMOs and miR-21 reporter plasmid by Lipofectamine 2000. After incubation for 24 h, relative luciferase activity (firefly/Renilla) was evaluated. Luciferase activity in the presence of pmir-GLO, which has no miRNA target region, and oligonucleotide with scramble sequence is set 1.0.

Evaluation of miR-21 inhibitory activities by RT-qPCR, Western Boltting

So far, we evaluated miR-21 inhibitory activities by only dual luciferase assay. We thought that we should proof SNA or L-*a*TNA based anti miR-21 oligonucleotides effect internal target mRNAs because dual luciferase assay is an exogenous target mRNA. Therefore, we performed the evaluation of their miR-21 inhibitory activities by RT-qPCR, western blotting in various cancer cells derived from human breast cancers, mice breast cancers, mice melanoma cells, and human squamous cell carcinoma cells. Through their assay, we will briefly mention the differences of mRNA and protein expressions which are regulated by anti miR-21 oligonucleotides.

ANKRD46 and DDAH1 are known as target mRNA regulated by miR-21 directly. Ankyrin domains regulated protein-protein interactions in a variety of cellular processes, but the detail isn't

revealed. DDAH1, dimethylarginine dimethylaminohydrorase 1, metabolizes ADMA and L-NMMA, which inhibit nitric oxide synthase (NOS) and promotes NO synthesis. ADMA and LNMMA causes vascular endothelial disorder by suppressing NO synthesis. MiR-21 regulates tumor suppressor genes. SPRY2, PTEN, RECK, TIMP3, BCL2, and PDCD4 are the most famous for proteins regulated by miR-21 (figure 4-4).[12] RHOB is known as tumor suppressor and its knockdown is associated with high aggressive tumors by regulating changes in cell shape, migration, and adhesion.[13]
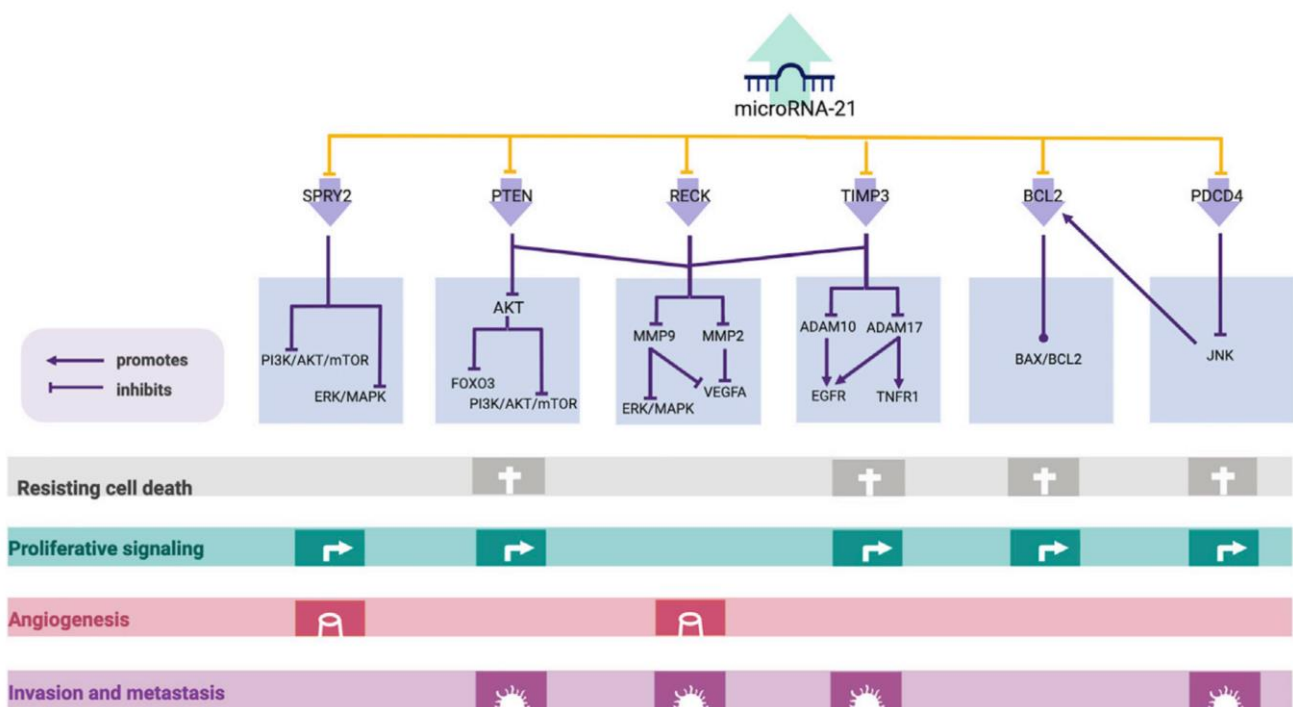
Figure 4-4 miR-21 Targets and Pathways Associated with the Hallmarks of Cancer[12]

In these target proteins, we analyzed mRNA expressions of ANKRD46, RECK, PDCD4, and RHOB for RT-qPCR. Others are not affected by miR-21 expression levels. In addition, we also analyzed miR-21 expression levels by stem loop RT-PCR method.[14, 15] First, we evaluated the activities of SNA based anti miR-21 oligonucleotides with or without D-sU pairs, SNA-AMO or S-sU3D7. In two cancer cells with different degrees of malignancy, MCF-7 and MDA-MB-231 cells, we confirmed that knockdown of miR-21, and remarkable up-regulation of ANKRD46, DDAH1, and

RHOB. In only MCF-7 cells, PDCD4, apoptosis-inducing protein, was upregulated remarkably (figure 4-5). While miR-21 was remarkably down-regulated by S-sU3D7 in both of cells, PDCD4 mRNA expression level didn't change, which may be related to malignancy. In cells, many miRNAs regulate cell functions. Commonly, less than dozens of miRNAs have a role to regulate the expression of a protein. In the case of PDCD4, miR-21-5p, miR-17-5p, etc. are related to the regulation(from Target Scan 8.0). There is a possibility that only miR-21 knockdown is insufficient for up-regulating PDCD4. We consumed miRNAs expression level are controlled depending on tumor malignancy and cell types. Then, we evaluated the miR-21 inhibitory activities of SNA or L-*a*TNA based anti miR-21oligonucleotides in the same cells by measuring RNA expression levels of miR-21, PDCD4, RHOB, ANKRD46, DDAH1 (figure 4-6). As shown in figure 4-6, we confirmed the activity of T-sU3D7 as well as S-sU3D7.
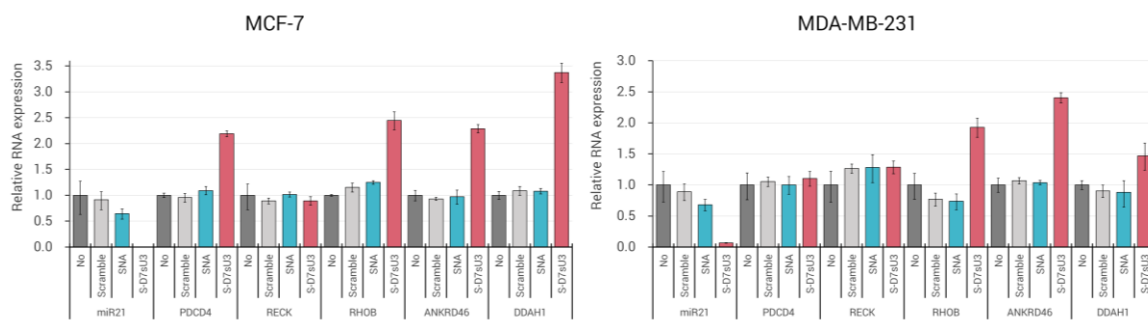
Figure 4-5 Relative RNA expressions of miR-21 target proteins in MCF-7 transfected 50 nM SNA based anti miR-21 oligonucleotieds and MDA-MB-231 cells transfected 25 nM SNA based anti miR-21 oligonucleotides by Lipofectamine® 3000.
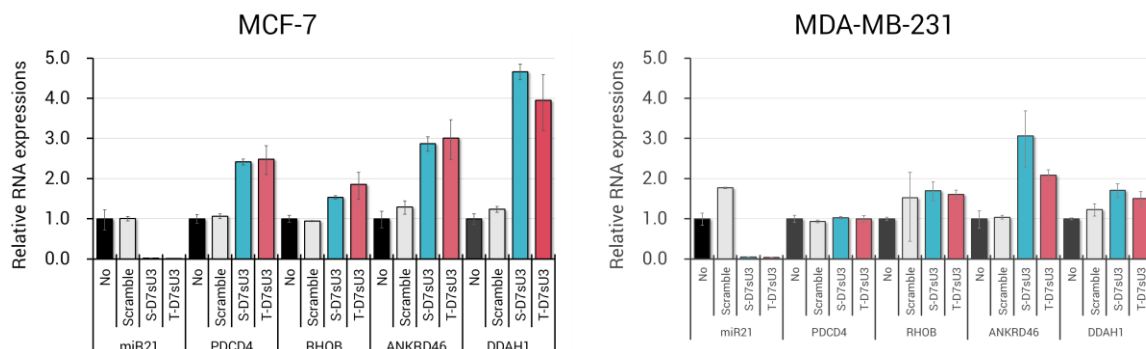
Figure 4-6 Relative RNA expressions of miR-21 target proteins in MCF-7 and MDA-MB-231 cells transfected 50 nM anti miR-21 oligonucleotieds by Lipofectamine® 3000.

71

Moreover, we performed the same analysis in breast cancer cells from mice, 4T1 (figure 4-7). In mice cells, ANKRD46 is not targeted by miR-21. We excepted ANKRD46.
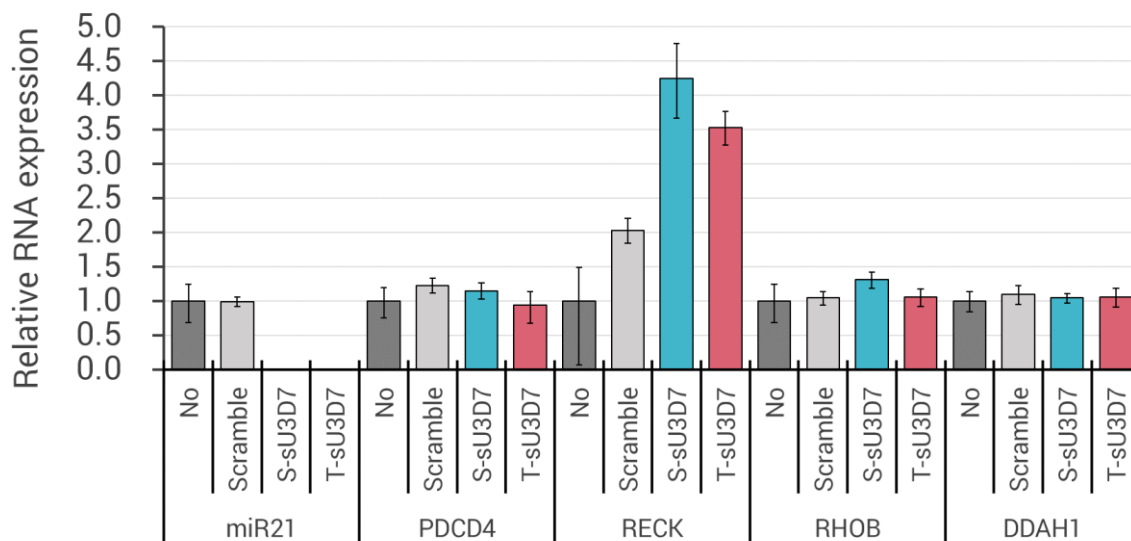

Figure 4-7 Relative RNA expressions of miR-21 target proteins in 4T1 cells transfected 20 nM anti miR-21 oligonucleotieds by Lipofectamine® RNAiMAX.

While 4T1 is from breast cancer which is the same type of MCF-7 and MDA-MB-231 cells, PDCD4, RHOB, and DDAH1 were not affected, but RECK is remarkably up-regulated in 4T1 cells by anti miR-21 oligonucleotides. The slightly lower activity of L-*a*TNA than SNA may show the difference of transfection efficiency.

Then, we evaluated protein expression levels of PDCD4 in MCF-7 cells. As shown in figure 4-8, in both of SNA based anti miR-21 oligonucleotides and L-*a*TNA based anti miR-21 oligonucleotides, PDCD4 was up-regulated to 2-fold from Non treat and Scramble treated groups. Also, we evaluated PDCD4 expression levels in MDA-MB-231 and 4T1 cells, but we couldn't observe the upregulation (data is not shown). Moreover, we tried to observe upregulation of ANKRD46 and RHOB, but we couldn't do them because their band intensities were very weak in western blotting analysis.
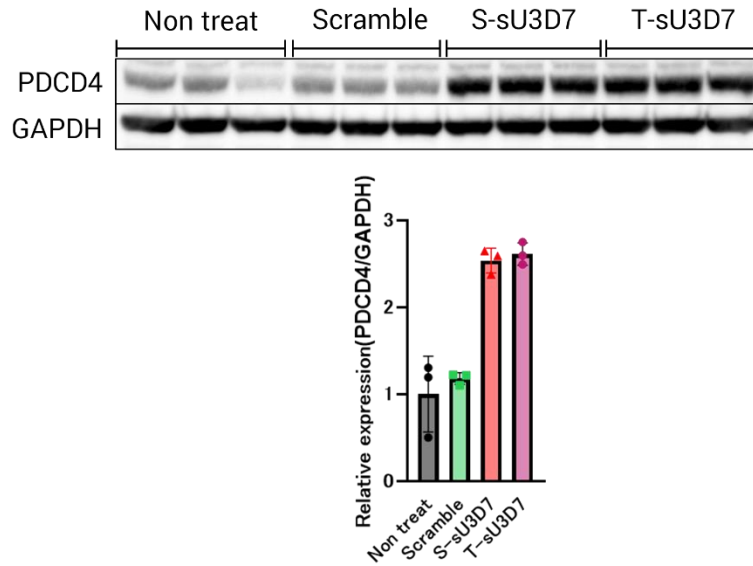
Figure 4-8 Relative PDCD4 expressions of MCF-7 cells treated scramble and S-sU3D7. MCF-7 cells were treated with 50 nM Scramble and S-sU3D7 with Lipofectamine® 3000 for 72 h. Western blot analyses were performed by using 30 μg total protein/well. Data were expressed relative to GAPDH. n = 3. Protein expressions of MCF-7 cells without oligos were set to 1.0.

In vivo **study**

As shown above, *in vitro* study, SNA or L-aTNA based anti miR-21 oligonucleotides bearing D-sU base pairs, S-sU3D7 or T-sU3D7 showed excellent miR-21 inhibitory activities in dual luciferase assay, RT-qPCR, and Western Blotting analyses. Therefore, we tried to evaluate anti-tumor activity. First, we evaluated phosphorothioate modified S-sU3D7, S-sU3D7(PS) in syngeneic mice which were inoculated 4T1 cells in the fourth mammary mice pad. To vivo study, we subcutaneously injected 1.0 x 10^5 4T1 cells in RPMI-1640 (-FBS, -P&S) under the fourth nipple with 26G syringe. After 5 days from cell inoculation, we peritumorally injected 50 mg/kg S-sU3D7(PS) every 3 days (figure 4-9).
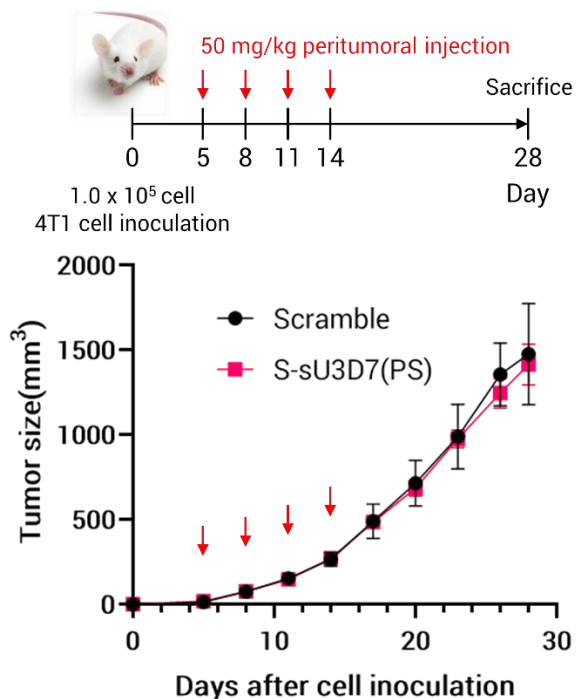
Figure 4-9 Tumor growth curves of 4T1-bearing mice monitored for 28 days after tumor inoculation following treatment with

Scramble and S-sU3D7(PS). ($n = 3$ per group)

Unfortunately, S-sU3D7(PS) didn't suppress tumor growth even though the amount of S-sU3D7(PS) injection was high. So, we analyzed the reason why S-sU3D7(PS) has no anti-tumor activity. Possible reasons are decrease of RNA affinity by introduction of phosphorothioate linkages, insufficient endosomal escape efficiency, and insufficient accumulation to tumor. In general, RNA affinity of oligonucleotides with PS linkages are lower than without PS linkages. Sometimes, the presence or absence of PS modification greatly influences them activity, which is changed depending on the balance of nuclease resistance of oligonucleotides with PS linkages and decrease of them RNA affinity. Then, we evaluated T_m values (Table 4-1) and miR-21 inhibitory activities by dual luciferase assay (figure 4-10).

Table 4-1 Tm values of S-sU3D7 with or without PS linkages.

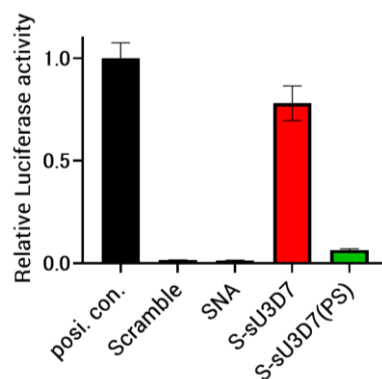|	T_{m} (°C)
S-sU3D7	77.6
S-sU3D7(PS)	64.8

Figure 4-10 miRNA inhibitory activities in MCF-7 cells reverse transfected 4 nM AMOs and miR-21 reporter plasmid by

Lipofectamine 2000. After incubation for 24 h, relative luciferase activity (firefly/Renilla) was evaluated. Luciferase activity in the

presence of pmir-GLO, which has no miRNA target region, and oligonucleotide with scramble sequence is set 1.0.

As shown in table 4-1, the T_{m} value of S-sU3D7 without PS linkages is 77.6 °C. On the other hand, the T_{m} value of fully phophorothiate modified S-sU3D7 is 64.8 °C, which is much lower than that without PS linkages. As described in figure 4-10, S-sU3D7 without PS linkages also showed high miR-21 inhibitory activity, however S-sU3D7, which is phosphorothioate modified, did as low activity as SNA. These data means that PS linkages, which is need for vivo study to improve internalization efficiency of nucleic acid drug into cells, decrease the RNA affinity, resulting in decrease of miR-21 inhibitory activity for SNA. For improving SNA based anti miR-21 inhibitory activity, ensuring cell internalization by another method, or DDS, and reduction of the number of PS linkages as much as possible is better. Basically, SNA and L-aTNA is strong resistance to nuclease resistance without PS linkages, if cell internalization of SNA and L-aTNA is ensured, PS linkages

may not be need. In addition, we performed comparing miR-21 inhibitory activity of T-sU3D7 and phosphorothioate T-sU3D7 (figure 4-10).
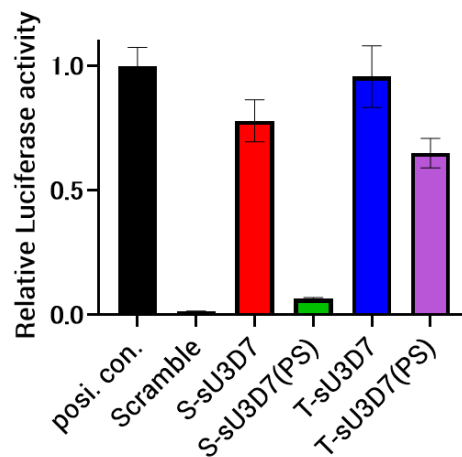

Figure 4-10 miR-21 inhibitory activity of SNA based or L-*a*TNA based anti miR-21 with or without PS linkages.

In the case of L-*a*TNA, the activity did not decrease significantly as SNA due to PS modification, but a decrease in activity was still observed. That means that even in the case of L-*a*TNA, it is better to reduce PS modification.

Second, we mentioned insufficient endosomal escape efficiency and insufficient accumulation to tumor of SNA based anti miR-21 oligonucleotides. Endosomal escape efficiency of any nucleic acid drugs is a few percent to total amount of injection, and even though oligonucleotides with PS linkages are peritumoral injected, most of them accumulate mainly in the liver and kidneys, and to a small extent throughout the body.[16] So, we checked tumor accumulation *ex vivo* imaging. We prepared disulfoCy5 modified S-sU3D7(PS) and injected Balb/c mice peritumorally or intravenously. After a week from injection, *ex vivo* imaging was performed (figure 4-11).
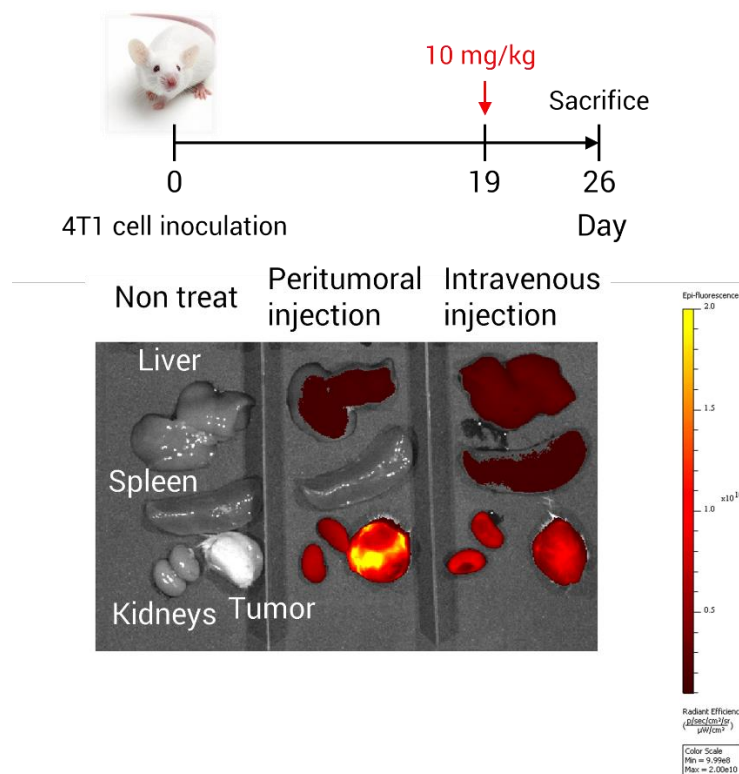
Figure 4-11 *Ex vivo* images of representative tissues from mice after a week of administration.

In *ex vivo* images, both of peritumoral injection and intravenous injection, strong fluorescence was observed in the kidneys and the tumor. So, we judged tumor accumulation efficiency of S-sU3D7(PS) is sufficient and endosomal escape efficiency is not sufficient. Therefore, we tried to use invivojet® PEI *in vivo* study using syngeneic mice. Invivojet® PEI is polyethyleneimine(M.W. 23000Da), which is a cationic polymer, and realizes systemic delivery of oligonucleotides. PEI/oligonucleotides complexes are internalized through endocytic pathway and promotes endosomal escape of oligonucleotides by proton sponge effects. We thought if we use invivojet® PEI for evaluation of anti-tumor activity, we can realize reduction of PS linkages and improvement endosomal escape of SNA based anti miR-21 oligonucleotides. According to manufacture protocols, we intravenously injected 2 mg/kg/2 days S-sU3D7 without PS linkages into syngeneic mice implanted 1.0×10^5 4T1 cells in the fourth mammary pad (figure 4-12).
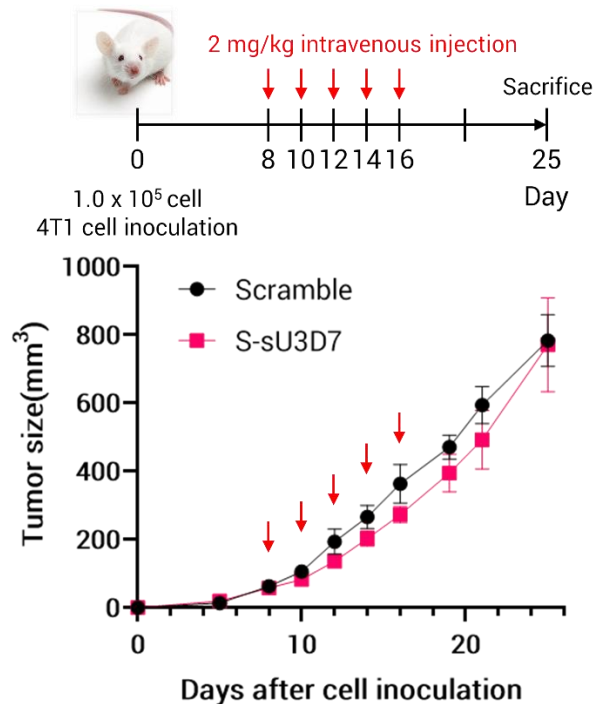
Figure 4-12 Tumor growth curves of 4T1-bearing mice monitored for 25 days after tumor inoculation following treatment with

Scramble and S-sU3D7. (n = 6 per group)

As shown in figure 4-12, S-sU3D7 without PS linkages slightly suppressed tumor growth during treatment, which means that reduction of PS linkages and/or improvement of oligonucleotide endosomal escape is important factor for suppressing tumor growth by anti miR-21 oligonucleotides. However, we thought there is room for improvement in activity because in the above study, invivojet® PEI realize systemic delivery but don't do tumor specific delivery. We will try to use tumor-targeting lipid nanoparticles (LNPs) in the future.

4-4 Conclusion

We analyzed effects of D-sU introduction into self-complementary region of SNA or L-aTNA based anti miR-21 oligonucleotides and could improve dramatically their miR-21 inhibitory activity. In RT-qPCR, some mRNA of proteins targeted by miR-21 were up-regulated remarkably by transfection of

anti miR-21 oligonucleotides. Also, we confirmed upregulation of PDCD4 protein. Then, we evaluated anti-tumor activity of phosphorothioate S-sU3D7, however S-sU3D7(PS) didn't show any activities. From T_m measurement, dual luciferase assay, and *in vivo* study with invivojet® PEI, we revealed the reasons why S-sU3D7(PS) has no activity, decrease of RNA affinity by PS linkages, insufficient endosomal escape of oligonucleotides. We succeeded to suppress tumor growth by injection of S-sU3D7 with PEI. For improving anti-tumor activity, we thought high RNA affinity by reduction of PS linkages, and efficient endosomal escape of oligonucleotides, and tumor-specific accumulation of oligonucleotides are need. In the future, we will try to utilize lipid nanoparticles (LNPs), which realizes their three factors. We concluded that we developed chemical modifications of SNA and L-*a*TNA which overcome their problem, formation of stable higher-order structures, and established basic technology for nucleic acid medicine. For treatment to diseases, we should develop drug delivery system for SNA and L-*a*TNA.

4-5 Experimental Section

Materials

For Luciferase assay, all anti miR-21 oligonucleotides were purchased from FASMAC, or Genedesign, Inc., or Hokkaido system science Co., Ltd. We prepared the pmirGLO-miR21, by inserting the miR-21 binding sequence (5′-CAACA TCAGT CTGAT AAGCT A-3′) between the XhoI and SalI sites in the 3′-UTR region of the gene encoding the firefly luciferase.

Dual luciferase assay

  Cotransfections of HeLa, MCF-7, MDA-MB-231, and B16 cells with AMO and 100 ng/well vector plasmids (100 ng) were performed by using Lipofectamine® 2000 (Invitrogen) in 96-well plates according to the manufacturer's instructions. After 24 h incubation, we removed 75 µl culture

medium and added Dual-Glo regent (75 µL, Promega) to the medium of HeLa cells in 96 well-plates. We measured Firefly luciferase luminescence by using Multi-label Plate Reader (EnSpire, PerkinElmer). Subsequently, we adeed Dual-Glo Stop & Glo reagent (75 µL, Promega), and measured Renilla luciferase luminescence.

Melting-temperature measurements

Oligonucleotides of SNA or L-aTNA with or without RNA (2 µM) were dissolved in 10 mM sodium phosphate buffer (pH 7.0) with 100 mM NaCl. The melting curves were obtained with a Shimazu UV-1800 by measuring the change in absorbance at 260 nm versus temperature. Temperature ramp was 0.5 oC min-1. Tm values were determined from the maximum in the first derivative of the melting curve.

RT-qPCR

After transfection of oligonucleotides, total RNA was isolated using Direct-zol RNA MiniPrep Kit, with TRI-Reagent(ZYMO research) according to the manufacturer's protocol. Total RNA was extracted from tumor cells after 48 h. The level of miR-21 was measured using stem-loop RT qPCR technology (45, 46). Complementary DNA (cDNA) synthesis was performed using ReverTra Ace® qPCR RT Master Mix (TOYOBO) with 0.05 µM RT-qPCR primer for miR-21 and U6 snRNA (for control of miR-21). PCR amplification was carried out by LightCycler® 96 Instrument (Roche) with FastStart Essential DNA Green Master Mix (Roche) according to the manufacturer's protocol. The obtained qPCR data were analyzed by Light Cycler® 96 SW1.1 software. Each protein expression levels were calibrated by β-actin, GAPDH, or U6 snRNA.

Western Boltting

After transfection of oligonucleotides, cells were trypsinyzed and collected tubes, then were washed by PBS once. The cells were homogenized in RIPA(Radio-Immunoprecipitation Assay) Buffer. Protein concentrations were measured by Pierce™ BCA Protein Assay Kits. 30 µg protein/each sample were applied to Bullet PAGE One Precast Gel and performed electrophoresis according to manufacturer' protocols. The proteins were transferred membranes by TransBlot TurboBlotting system (Bio-rad). Membranes were blocked for 1 h in Blocking one. Washes were done at each steps by Tris-buffered saline with Tween (TBS-T; Takarabio), then probed overnight at 4°C with the following primary antibodies respectively: PDCD4 (1：500 dilution, Abcam), GAPDH (1：2000 dilution, Wako). Membranes were then incubated with secondary anti-rabbit and anti-mouse horseradish peroxidase (HRP)-conjugated IgGs at room temperature for 1 h. Clarity Western ECL Substrate (Bio-Rad) was added to the membrane, and signals were detected by using a ImageQuant LAS 4000mini (GE Healthcare). PDCD4 expression levels were normalized by GAPDH levels. The PDCD4/GAPDH intensity of non-treat cells was set to 1.0.

Anti-tumor activity evaluation

4~6 weeks old female Balb/c mice were purchased from Japan SLC, Inc. and were bred in light-dark cycle, each 12 h. Mice could access food and water freely. Mice breast cancer cells, 4T1, were initiated in Balb/c female mice by subcutaneous (s.c.) injection as 1.0 x 10^6 cells/ml in 0.1 mL in RPMI-1640 into the fourth mammary pad by 26G needle. After few days, all mice that having palpable tumor were randomized. At day 7~8 after transplantation, each mouse was injected any oligonucleotides diluted in PBS or deionized water with invivojet® PEI according to manufacturer's protocols. . The tumor volumes were calculated as V = (1/2 × length × width^2). Each length was measured using calipers.

Biodistribution

10 mg/kg disulfoCy5 modified SNA based anti miR-21 oligonucleotides were injected peritumorally or intravenously. After a week, *ex vivo* images were captured by IVIS Lumina III. Ex. and Em. wavelengths were default for Cy5 fluorescence measurement.

4-6 References

[1] H. Kashida, K. Murayama, T. Toda, and H. Asanuma, *Angew. Chem., Int. Ed.*, **2011**, *50*, 1285-1288.

[2] K. Murayama, H. Kashida, and H. Asanuma, *Chem. Commun.*, **2015**, *51*, 6500-6503.

[3] Y. Chen, R. Nagao, K. Murayama, H. Asanuma, *J. Am. Chem. Soc.*, **2022**, *144*, 5887-5892.

[4] K. Makino, E. Susaki, M. Endo, H. Asanuma, and H. Kashida, *J. Am. Chem. Soc.*, **2022**, *144*, 1572-1579.

[5] K. Murayama, Y. Yamano, and H. Asanuma, *J. Am. Chem. Soc.*, **2019**, *141*, 9485-9489.

[6] K. Murayama and H. Asanuma, *ChemBioChem*, **2020**, *21*, 120-128.

[7] Y. Chen, K. Murayama, and H. Asanuma, *Chem. Lett.*, **2022**, *51*, 330-333.

[8] B. T. Le, K. Murayama, F. Shabanpoor, H. Asanuma, and R. N. Veedu, *RSC Advances*, **2017**, *7*, 34049-34052.

[9] Y. Kamiya, Y. Donoshita, H. Kamimoto, K. Murayama, J. Ariyoshi, and H. Asanuma, *ChemBioChem*, **2017**, *18*, 1917-1922.

[10] Y. Kamiya, J. Takai, H. Ito, K. Murayama, H. Kashida, and Hiroyuki Asanuma, *ChemBioChem*, **2014**, *15*, 2549-2555.

[11] Y. Kamiya, K. Iishiba, T. Doi, K. Tsuda, H. Kashida, and H. Asanuma, *Biomater. Sci.*, **2015**, *3*, 1534-1538.

[12] Diana Bautista-Sánchez, *et al*, *Molecular Therapy - Nucleic Acids*, **2020**, *20*, 409-420.

[13] E. C. Connolly, K. V. Doorslaer, L. E. Rogler, and C. E. Rogler, *Mol Cancer Res*, **2010**, *8* 691-700.

[14] C. Chen *et al.*, *Nucleic Acids Res.*, **2005**, *33*, e179.

[15] E. Varkonyi-Gasic and R. P. Hellens, *Methods Mol. Biol.*, **2011**, *744*, 145-157.

[16] R. S. Geary, D. Norris, R.Yu, and C. F. Bennett, *Advanced Drug Delivery Reviews,* **2015**, *87*, 46-51.

LIST OF PUBLICATIONS

1. "Incorporation of Pseudo-complementary Bases 2,6-Diaminopurine and 2-Thiouracil into Serinol Nucleic Acid (SNA) to Promote SNA/RNA Hybridization"

   Kamiya, Y.; Sato, F.; Murayama, K.; Kodama, A.; Uchiyama, S.; Asanuma, H.

   Chem. Asian J., **2020**, *15*, 1266-1271.

2. "Syntheses of base-labile pseudo-complementary SNA and L-*a*TNA phosphoramidite monomers"

   Sato, F.; Kamiya, Y.; Asanuma, H.

   J. Org. Chem., **2023**, *88*, 796-804.

LIST OF PRESENTATIONS

International Conference

Poster

1. Sato F., Kamiya Y., Asanuma H., "Development of anti miR-21 oligonucleotide consisting of only SNA, an *acyclic* artificial nucleic acid"

   Oligonucleotide Therapeutics Society 19th Annual meeting(2023), October 22-25, Palau de Congressos de Barcelona, Spain

Internal Conference

18 presentations. Omitted.

Lists of Awards

1. 「日本化学会東海支部長賞」　日本化学会東海支部（修論発表会）　2021 Mar.

2. 「博士学術賞」名大鏡友会 2023, Oct.

ACKNOWLEDGEMENTS